Drying of fine coal using warm air in a dense medium fluidised bed

MJ van Rensburg

21089906

Dissertation submitted in fulfilment of the requirements for the degree *Magister* in Chemical Engineering at the Potchefstroom Campus of the North-West University

Supervisor: Dr M le Roux

Co-supervisor: Prof QP Campbell

November 2014

OVERVIEW OF DOCUMENT

This document presents a dissertation for a Masters Research project that was completed at the North-West University, Potchefstroom Campus. The title of the research project is "Drying of fine coal using warm air in a dense medium fluidised bed"

General information of candidate

Candidate	M.J. van Rensburg
Student number	21089906
Highest qualification	B.Eng. Chemical
Year	2011
Curriculum code	I103P
Project title	Drying of fine coal using warm air in a dense medium fluidised bed
Level of study	M. Eng. in Chemical Engineering
Curriculum code	I871P
Institution	North-West University, Potchefstroom Campus
Department	Department of Chemical and Mineral Engineering
	Coal research group
Study leaders	Dr. M. le Roux
	Prof. Q.P. Campbell

DELIVERABLES FROM THIS STUDY

1. Articles

The following articles were completed and submitted during the course of this study.

1.1. International published article

Le Roux, M., Campbell, Q.P. & Van Rensburg, M.J. 2013. Fine coal dewatering using high airflow. International Journal of Coal Preparation and Utilization (In press). http://dx.doi.org/10.1080/19392699.2014.869939

1.2. International article (Awaiting approval)

Submitted for the ***XXVII International Mineral Processing Conference (IMPC). Santiago, Chile. 20-24 October 2014.***

Le Roux, M., Campbell, Q.P. & Van Rensburg, M.J. 2013. Drying of fine coal using air in a fluidized bed.

2. Conferences

The following work was presented at conferences during the course of this study.

2.1. Local conference (Presentation)

Fossil Fuel Foundation Conference. 18th Southern African Coal Science and Technology Indaba: Latest Research and Development at Universities and Industry. Parys, South Africa. 13- 14 November 2013.

Van Rensburg, M.J., Le Roux, M. & Campbell Q.P. Drying of fine coal using warm air in a fluidised dense medium bed.

2.2. Local conference (Presentation)

SAMMRI Workshop. Cape Town, South Africa. 5 August 2013.

Van Rensburg, M.J., Le Roux, M. & Campbell Q.P. Drying of fine coal using warm air in a fluidised dense medium bed.

2.3. Local conference (Presentation)

Minproc 2013 Southern Africa Mineral Beneficiation and Metallurgy Conference. Cape Town, South Africa. 7-8 August 2013.

Van Rensburg, M.J., Le Roux, M. & Campbell Q.P. Drying of fine coal using warm air in a fluidised dense medium bed.

2.4. International conference (Presentation)

Paper presented at the ***17th International Coal Preparation Congress (ICPC 2013). Turkey, Istanbul. 1-6 October 2013.***

Le Roux, M., Campbell, Q.P. & Van Rensburg, M.J. Fine coal dewatering using high air flow.

2.5. International conference (Awaiting approval)

Paper to be presented at the ***XXVII International Mineral Processing Conference (IMPC). Santiago, Chile. 20-24 October 2014.***

Le Roux, M., Campbell, Q.P. & Van Rensburg, M.J. 2013. Drying of fine coal using air in a fluidized bed.

DECLARATION

I, **Jana van Rensburg**, hereby declare that the dissertation entitled: **Drying of fine coal using warm air in a dense medium fluidised bed**, which is done for the completion of the degree Magister in Engineering, is my own work and has not been submitted to any other institution.

_____

Jana van Rensburg

_____

Date

ACKNOWLEDGEMENTS

I hereby want to thank the following people and institutions for their assistance and contributions made in the completion of this project:

- Firstly I want to thank my heavenly Father for giving me love, support and guidance throughout the whole process. All the work that was completed wouldn't be possible without the encouragement of my God and my provider. Daniel 2: *"Praise the name of God forever and ever, for he has all wisdom and power. He gives wisdom to the wise and knowledge to the scholars."*
- Thanks are due to my study leaders and Dr. Marco le Roux and Prof. Quentin Campbell for their guidance and help throughout the project. Without their input and ideas this project wouldn't have been possible.
- A special thanks to Mr. Adrian Brock for his help with building the experimental setup and for technical assistance throughout the course of the project. All his hard work and efforts are truly appreciated.
- I would also like to thank the personnel of the North-West University, School of Chemical and Minerals engineering, for all their support, help and ideas.
- A special thanks to my friends and family for moral support and encouragement.
- I would also like to thank Coaltech, SAMMRI and the NRF for making funding and resources available to pursue this research. The work presented in this paper is based on the research supported by the South African Research Chairs Initiative of the Department of Science and Technology and National Research Foundation of South Africa (Coal Research Chair Grant No. 86880). Any opinion, finding or conclusion or recommendation expressed in this material is that of the author(s) and the NRF does not accept any liability in this regard.

ABSTRACT

Fluidised bed drying is currently receiving much attention as a dewatering option after the beneficiation of fine coal (defined in this study as between 1mm and 2mm particles). The aim of this study was to investigate the removal of moisture from fine coal by using air at relatively low temperatures of between 25°C and 60°C within a controlled environment by lowering of the relative humidity of air. The first part of the experimental work was completed in a controlled climate chamber with the coal samples in a static non-fluidised state. Drying in the second part was carried out using a fluidised bed with conditioned air as the fluidising medium.

Introduction of airflow to the system led to a lower moisture content in the coal samples and it also proved to have the ability to increase the drying rate. It was determined that the airflow had the ability to remove more free moisture from the filter cake. In addition more inherent moisture could also be removed by using upward flowing air, resulting in a lower equilibrium moisture content. It was proven that the airflow rate and relative humidity of the drying air contributed to faster drying rates. The effect of temperature was not as significant as expected, but higher temperatures did increase the drying rate at higher airflow and lower humidity conditions. The larger surface areas of particles create surface and capillary forces that prevent the moisture from leaving the finer coal particles. It was found that the rate of drying is independent of the moisture content in the coal sample. Just in terms of the fastest drying time and drying rate in the fluidised bed, it was concluded that the most efficient conditions is airflow above minimum fluidisation point causing vigorous mixing and maximum contact with the drying air. In addition to the high airflow it was concluded that 30% relative humidity and 55°C resulted in the fastest drying time.

All the drying processes at all the airflow rates, temperature and relative humidity conditions were energy efficient. This process was shown to be energy positive, resulting in an overall energy gain. The overall energy consumption for the fluidised bed is lower than for all the dryer systems compared to and it compared favourably with other thermal drying technologies. It was therefore shown that this is a viable technology for the dewatering of fine coal.

Keywords: Dewatering; Drying; Fine coal; Fluidised bed; Warm air

TABLE OF CONTENTS

Appendix B

LIST OF FIGURES

Chapter 1

Chapter 2

Chapter 3

Chapter 4

Chapter 5

LIST OF TABLES

Chapter 3

Chapter 4

Chapter 5

.

LIST OF SYMBOLS AND ABBREVIATIONS

Symbol	Description	Unit
$\widehat{H}$	Enthalpy at saturation	kJ/kg dry air
k	Drying coefficient	% moisture/minute
m_{DA}	mass of dry air	kg
P	Partial pressure	bar
P_{sat}	Saturation pressure of water	bar
Q	Energy	kJ
r	Drying rate	% moisture/minute
t	Time	minutes
V	Volume	m^3
$\widehat{V}_H$	Humid volume	m^3/kg dry air
W	Power	Watt or J/s

Symbol or abbreviation	Description
Δ	Delta
b	blower
c	climate chamber
CV	Calorific value
DA	Dry air
i	internal
RH	Relative humidity
S	Standard deviation
w	water or moisture
wt	Weight
$\bar{x}$	Average

TERMINOLOGY

Fine coal: In this study fine coal is described as coal fractions between 1mm and 2mm.

Ultra-fine coal: Refers to coal fractions smaller than 1mm.

Warm air: The term warm air is used for slightly elevated temperatures between 25°C and 60°C.

Relative humidity: This term gives an indication of the water content in the air. Relative humidity is the percentage of the moisture relative to saturation.

Vitrinite and inertinite rich coal: These terms are used to label these two types of coal used in this study. The one sample contains more vitrinite and the other group of samples contained more inertinite. It doesn't necessarily mean that all vitrinite or inertinite a rich coal from other coal seams would have the same properties or dewatering abilities.

CHAPTER 1 - INTRODUCTION

1.1. Background and motivation

Coal is described as a solid sedimentary rock that formed as a result of altered plant and animal material. These fossil fuels are found within the crust of the earth that consists predominately of organic compounds and small fractions of mineral matter. According to Osborne (1988) coal is extracted commercially as it contains heating power and is utilised to provide for about 70% of the energy consumed in South Africa. South African coal resources contribute to a total of 93% of electricity generation and 30% of petroleum fuels in 2010 (Eberhard, 2011).

The economy will expand as the population grows and this will lead to an increased demand for energy (World Petroleum Coucil, 2011). The need for utilising coal will increase as coal is considered an abundant and cheap fossil fuel (Jangam *et al.*, 2011). According to the World Coal Association (2012) coal reserves will be available for more than 118 years if exploited and used constantly at the current rate. It is important to use coal sensibly as it is the primary energy resource for the South African economy. It is therefore, of utmost importance to improve all processes that contribute to the utilisation of coal, like mining, transport and beneficiation processes (Fourie *et al.*, 1980).

According to Reddick *et al.* (2007) coal fines (defined in this report as between 1mm and 2mm) are produced as a result of mechanised mining methods. It was estimated by Mangena *et al.* (2003) that about 12% of South African mined coal is classified as fines. Fine coal is difficult to dewater and can contain a total moisture content of higher than 25%$_{wt}$ even after filtration (Le Roux, 2003). This high moisture content causes problems in handling as well as a decrease in the calorific value of the coal. An added disadvantage of high moisture content is an increase in transportation and port costs. The difficulty in dewatering often leads to fines being discarded into discard dams. This is an unacceptable waste management procedure as the discarded fines contribute to a number of environmental problems, such as dust release and acid mine drainage. These fines also have the potential of combusting spontaneously if the waste isn't properly managed. Often fine coal is cleaned, dewatered and blended with the course beneficiated fraction. However the fines rarely reach a desirable quality and such a blend will reduce the quality of the final product by increasing the final product moisture (Reddick *et al.*, 2007).

The development of feasible fine coal beneficiation processes can result in potential revenue and, at the same time, reduce environmental problems (Reddick *et al*., 2007). Fluidisation is proving to be one such an option in beneficiating fine coal. Air dense medium fluidisation is a cheaper and effective alternative to beneficiate coal without using water, as wet beneficiating processes will only add water to the fines (Luo *et al.*, 2010). However research conducted at North-West University found that elevated moisture content in the feed decreases the efficiency of the process. It was found that a moisture content of larger than 5-7%$_{wt}$ caused the coal particles to stick to the sides of the fluidised vessel or agglomerate to block sufficient airflow, both preventing the system to reach fluidisation state (Terblanche, 2011).

There are several methods for reducing the moisture content in fine coal, for example pressure filtration, centrifuging and thermal drying. Thermal drying remains the most effective water reduction technique but the price of coal inhibits the use of thermal drying methods to dewater unbeneficiated and clean coal (Reddick *et al*., 2007). Mechanical dewatering is generally incapable of delivering the required moisture levels, especially for coal fines. Previous work on vacuum filtration by Le Roux & Campbell (2003) yielded an increase in the dewatering capabilities of the filter when the operational philosophy thereof was moved from a high-pressure differential that causes low airflow, to a low-pressure high airflow regime. It was decided to focus on fluidised bed drying as it causes a low pressure system with high airflow.

1.2. Scope of investigation

Fluidised bed drying is currently receiving much attention as a dewatering option after the beneficiation of fine coal. The aim of this study was to investigate the removal of moisture from fine coal by using air at relatively low temperatures of between 25°C and 60°C within a controlled environment by lowering of the relative humidity of air. Firstly, the drying performance at non-fluidised (static) conditions was studied to construct the desorption isotherms of coal samples. This was done to determine the ability of the fine coal to release moisture in various temperature and humidity conditions. The results were compared to drying in a fluidised bed using conditioned fluidised air as a drying medium. The optimum fluidised conditions were determined by evaluating drying rates and energy consumption of the process as well as the overall upgrading of the coal. This study would be the first stepping stone to investigate the possibility of drying within the fluidised bed.

1.3. Objectives of study

The following objectives were the driving force behind the study:

1) To construct and study the desorption isotherms of coal samples under controlled temperature and humidity conditions at non-fluidised (static) conditions. This information is of primary importance as it would give an understanding of the equilibrium moisture content and enable further analysis when samples will be dried within a fluidised bed.

2) To investigate the influence of temperature, relative humidity, coal characteristics and properties on the dewatering of coal, before introducing airflow within a fluidised bed.

3) The experimental work within the fluidised bed will focus on determining the optimum operating parameters for the fluidised bed drying operating with warm air as fluid. These variables will include temperature, relative humidity and airflow rate.

4) To investigate the drying performance of the fluidised bed and determine the drying rate at various conditions in order to determine the most efficient conditions.

5) To determine how well a model can predict the experimental data when drying within the fluidised bed.

6) To determine the effect of coal characterisation on the drying rate by investigating vitrinite as well as inertinite rich bituminous coal from the Waterberg coal field.

7) Variations in the initial moisture content of the filter cakes were made to determine its effect on the drying rate and the performance of the fluidised bed

8) To determine the energy required for the drying process at all the various temperature, relative humidity and airflow conditions.

9) To determine the extent to which the coal was upgraded by removing the moisture of coal samples dried in the fluidised bed.

10) To create a comparative study by completing energy balances to compare with other drying technologies and determine the most cost effective and efficient drying conditions.

1.4. Layout of dissertation

In order to meet the objectives of the study, a layout for the dissertation was determined. A schematic diagram containing the layout of the research approach and dissertation can be seen in Figure 1.1.

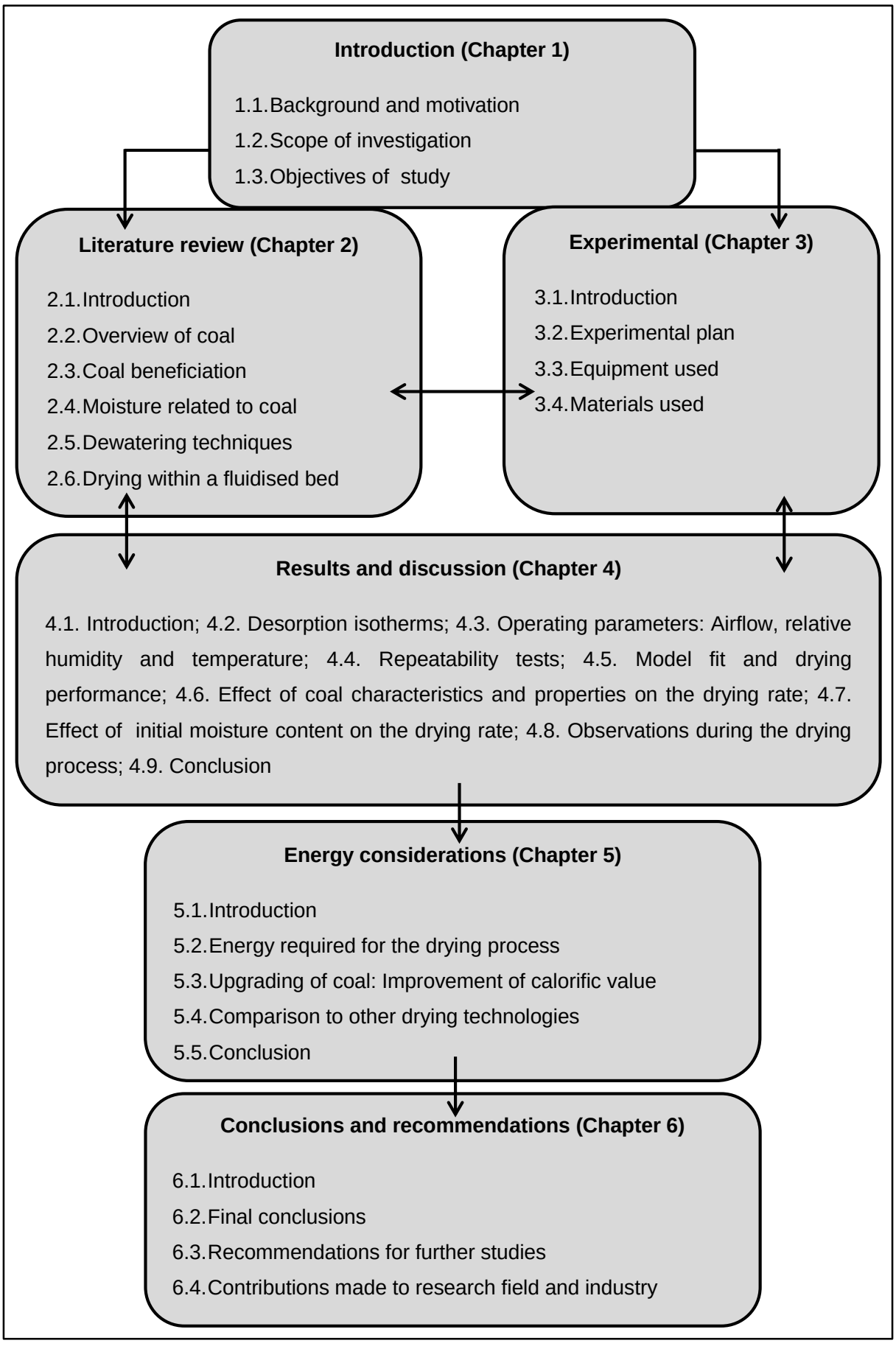

Figure 1.1. Layout of dissertation

CHAPTER 2 – LITERATURE REVIEW

2.1. Introduction

The literature survey will give an overview of coal as well as the importance of coal. Beneficiation and various existing technologies will be explained briefly and the review will specifically focus on fluidisation as a dry beneficiation method. The moisture content related to coal and specifically fine coal will be described. As warm fluidising air will be used to dry the fine coal in this study, the literature will also focus on describing the drying process.

2.2. Overview of coal

Coal is a solid sedimentary rock that formed as a result of altered plant and animal material. These fossil fuels are found within the crust of the earth that consists predominately of organic compounds and small fractions of mineral matter. Coal is a heterogeneous material and the properties and composition of the coal can vary due to the process of alteration throughout the years as well as the type of material it originated from (Osborne, 1988). The climate conditions, allocation of the coal seam and geological events in history contributed to the variation of coal across regions (Falcon & Ham, 1988). Section 2.2.1. through to Section 2.2.4. describes the main methods to classify coal.

2.2.1. Coal rank

The process by which coal is formed throughout years is generally referred to as coalification. Coal matures as a result of time, temperature as well as pressure within the crust of the earth where the coal is located (Falcon & Ham, 1988). The stages in coal maturity can be seen in Figure 2.1. Plant material from swamps changes into peat and then transforms into lignite, a brown and soft coal. Bituminous coal is the next rank of coalification, where the coal becomes harder and turns black. Further maturity brings forth anthracite which is a higher coal rank. Lower rank coals are more porous and have a higher moisture and volatile content. As the coal matures the physical and molecular structure also develops in order to form a structure with a higher organic content and less overall porosity (Falcon & Ham, 1988). Rong & Hitchins (1995) confirmed that lower rank coals have the tendency to contain larger moisture content and as the rank increases, the moisture content decreases.

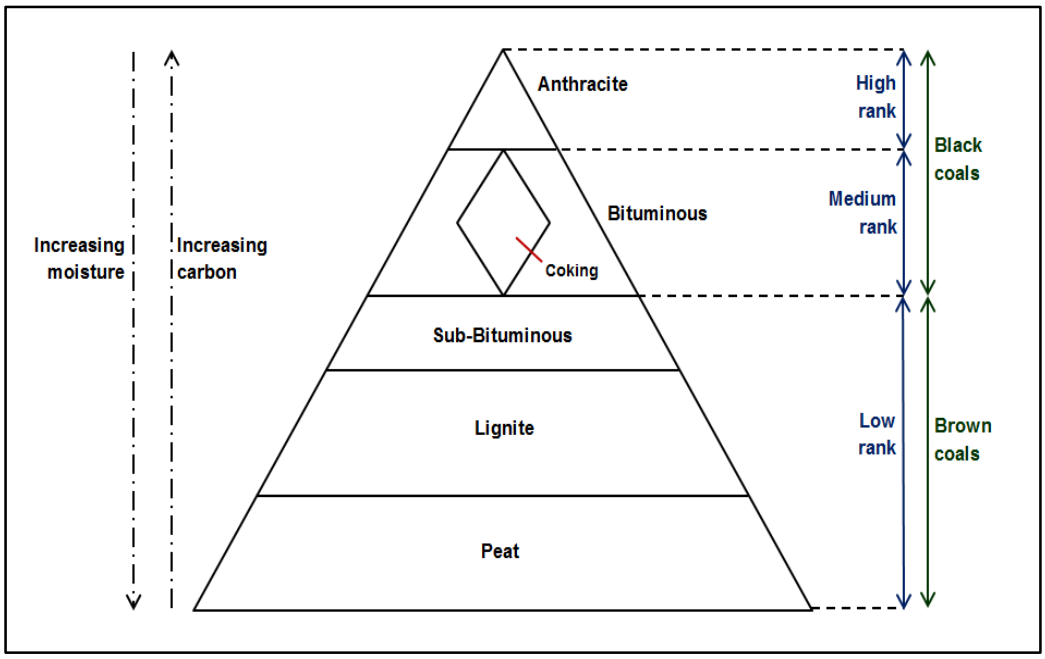

Figure 2.1. Coal formation; taken from Osborne (1988)

2.2.2. Macerals in coal

The term maceral refers to the organic material in a coal particle. The type of organic material gives an indication of the original plant and animal material that the coal developed from (Falcon & Ham, 1988). According to Osborne (1988) there are various macerals, but the three main types of macerals include:

i. *Inertinite:* This maceral can be in the form of the original plant structure or be unstructured. It is however easy to distinguish inertinite from other organic matter as it has a higher reflectance than vitrinite when observed in micrographs.
ii. *Vitrinite:* This maceral originates from the cell substances of plants and has a grey reflectance as can be seen in the petrographic scans in Appendix A. Vitrinite is also referred to as the maceral that is the most sought after compared to other macerals.
iii. *Liptinite:* This maceral is referred to as exinite and is furthermore reflective, yet not as highly as inertinite. Liptinite was formed from lipids and the waxy layers of plant material.

These maceral types are classified according to their molecular structure and physical properties, that can be seen within a coal sample, or by means of optical devices. The maceral groups are used mainly in order to classify a coal sample as reactive or unreactive. Vitrinite and liptinite rich coals tend to be reactive, while inertinite rich coal is generally defined as uncreative. Recent work has indicated that elements in the inertinite group are semi-reactive (Falcon & Ham, 1988).

2.2.3. Mineral matter content

The term mineral matter refers to the amount of this inorganic material in a coal sample and furthermore the content of this inorganic matter determines the grade of coal. The minerals can include silica, sulphides, carbonates and chlorides (Osborne, 1988). According to Rong & Hitchins (1995) typical types of mineral matter would include mostly a variety of kaolin, quartz and muscovite. The type of minerals and the arrangement of minerals in the organic molecular structure determine the hardness and abrasiveness of the coal sample. The type of mineral matter may also lead to different types of pollution released when coal is burned. Clays like kaolinite within the coal structure absorb more moisture than other minerals and leads to an increase in the overall coal moisture content. These inorganic materials ultimately decrease the calorific value of coal and therefore beneficiation processes are necessary to remove as much of the inorganic material as possible (Falcon & Ham, 1988).

2.2.4. Fine coal

Reddick *et al.* (2007) stated that coal fines are produced primarily as a result of mechanised mining methods. It was estimated by Mangena *et al.* (2003) that about 12% of South African mined coal is classified as fines. The coal fines mentioned in the study are coal particles below 1mm. However in comparison to coarse coal it is far more expensive to beneficiate fine coal as it entails extra capital costs and higher recovery costs which ultimately would lead to a poor return on investment. The large quantity of water associated with fine coal is the main contributor to the high processing costs (Firth & Swanson, 2002). This high moisture content causes difficulties in handling and also leads to a reduction in the calorific value of coal. This is the main reason why the South African mining industry disposes of coal fines by pumping it into dumps, underground areas or slurry dams (Mangena *et al.*, 2003).

Reddick *et al.* (2007) stated that the quality of the discarded fine coal is generally comparable to the quality of the rest of the mined coal, when beneficiated and dewatered. The loss of potential revenue from not utilising these fines can create an opportunity to improve fine coal beneficiation processes (Firth & Swanson, 2002). For drying to be a feasible process, the cost of beneficiation should not be higher than the value added to fine coal when reducing the moisture and cleaning the coal (Zhonghua & Mujumdar, 2011). Section 2.3. describes beneficiation of coal and specifically coal fines.

2.3. Coal beneficiation

Raw mined coal is beneficiated to retrieve the maximum amount of cleaner coal that can be utilised. The goal is specifically to clean the mined coal to meet the detailed requirements of industrial consumers, which usually includes the physical properties and characteristics of the mined coal (Dwari & Rao, 2007).

There are two types of beneficiation processes used currently, wet and dry beneficiation. Wet beneficiation processes are mostly used for coal cleaning, as water provides more efficient separation results than dry beneficiation processes. However large volumes of water are needed for density separation which makes it difficult to operate in dry or cold regions (Luo *et al.*, 2007). Extra water is added during wet beneficiation processes, which adds water to the already inherently wet coal particles (Karthikeyan *et al.*, 2009). Alternatively dry beneficiation methods do not require water and are mainly based on the physical properties, for example the density, size, friability and shape of the coal particles. Coal can also be sorted according to its appearance and colour. Screens are a method to separate coal by shape and size, while solid-gas systems are used to separate according to density (Dwari & Rao, 2007).

Dense medium fluidised beds are an example of a solid-gas or air dry beneficiation method. During the process the solid particles will separate in the fluidised bed according to density (Luo *et al.*, 2007). According to Terblanche (2011) and Willemse (2011) fine coal particles with high moisture contents, cleaves to the walls of the fluidised bed and blocks sufficient air flow to reach fluidisation state and ultimately density separation. This problem can be alleviated by drying the coal fines within the fluidised bed prior to density separation. This project would be the first stepping stone to investigate the possibility of drying within the fluidised bed.

2.3.1. Dense medium fluidised bed

A fluidised bed with conditioned air as the fluidising medium was used to dry coal samples. This section discusses the working of the fluidised bed. A fluidised bed is usually a cylindrical vessel that contains solid particles where gas or air is blown in an upward direction through the vessel. In this specific study air will be used and not gas. The air will percolate through the voids between the solid particles, but due to the low velocity of the air the solids will remain stationary. The stationary phase is referred to as a fixed bed or static bed as illustrated in Figure 2.2.a). A higher velocity of the air will cause the particles to vibrate and break away from one another. Some of the particles or clusters of particles will start to break away and get caught up in the air which flows in an upwards direction. No

fluidisation takes place at this stage; the height of the bed only expands. A further increase in the air velocity will cause the solid particles to behave like a fluid. At this point the particles will become suspended in the upward flowing air as shown in Figure 2.2.b) (Rhodes, 2008).

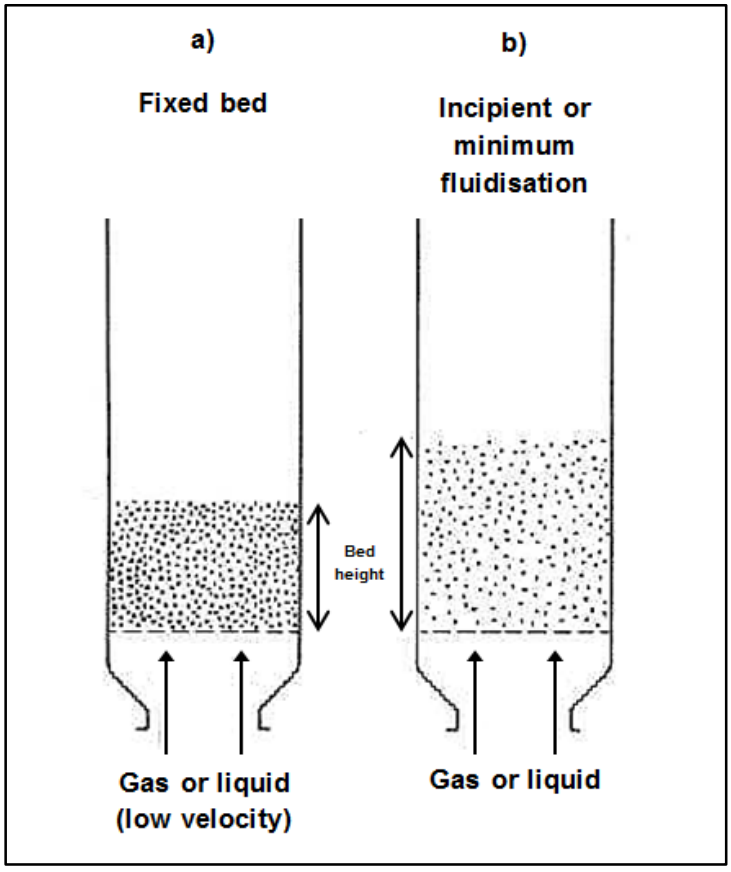

Figure 2.2. Fluidised bed; adapted from the University of Colorado at Boulder (2009)

When the particles are fluidised completely, micro bubbles will form in the bed and complete mixing will occur. When the process is stopped, the solid particles will separate in the fluidised bed according to density. The particles with a lower density will settle in the upper region of the fluidised bed. The higher density particles will settle in the lower sections, where the highest density will be at the bottom (Luo *et al.*, 2007).

There is a certain point where the airflow will cause perfect mixing to take place. However by increasing the flow rate beyond the minimum fluidisation point will result in a number of instabilities in the system. The high airflow rates will most likely lead to channelling of the airflow through the solid particles. Large bubbles can also form in the bed as a result of the high airflow rate, ultimately causing vigorous mixing as well as back mixing. At this stage uniform mixing will not take place and the particles will not separate as efficiently according to their density (Kunii & Levenspiel, 1991).

There are also a number of factors that may influence the system's ability to reach fluidisation state. The type and design of airflow distributor helps airflow to spread evenly across the fluidised cylinder and results in sufficient pressure drop across the bed. The heterogeneity of the solid particles affects the extent to which the fluidisation will be effective. Cohesion as well as non-spherical properties of particles will also inhibit effective fluidisation (Kunii & Levenspiel, 1991).

2.4. Moisture related to coal

During coalification as described in Section 2.2.1., plant material from swamps transforms into coal. These swamps contained large portions of water and during the coalification process the coal compacts under pressure and temperature, and the moisture is displaced. However the coal still contains portions of water after extraction from the ground. Additional water is needed during wet beneficiation of coal, which adds more water to the already inherently wet coal particles (Hatt, 2003).

According to Wakeman (1984) there are three types of moisture related to coal particles:

i. Surface moisture is found on the external surface of the coal particle and can also be captured between coal particles in a heap.
ii. Capillary moisture is held in the pore structure of a coal particle due to surface tension. The pore structures are the voids in the particle, as can be seen in Figure 2.3.
iii. Chemically bounded moisture forms part of the molecular structure of the coal particle.

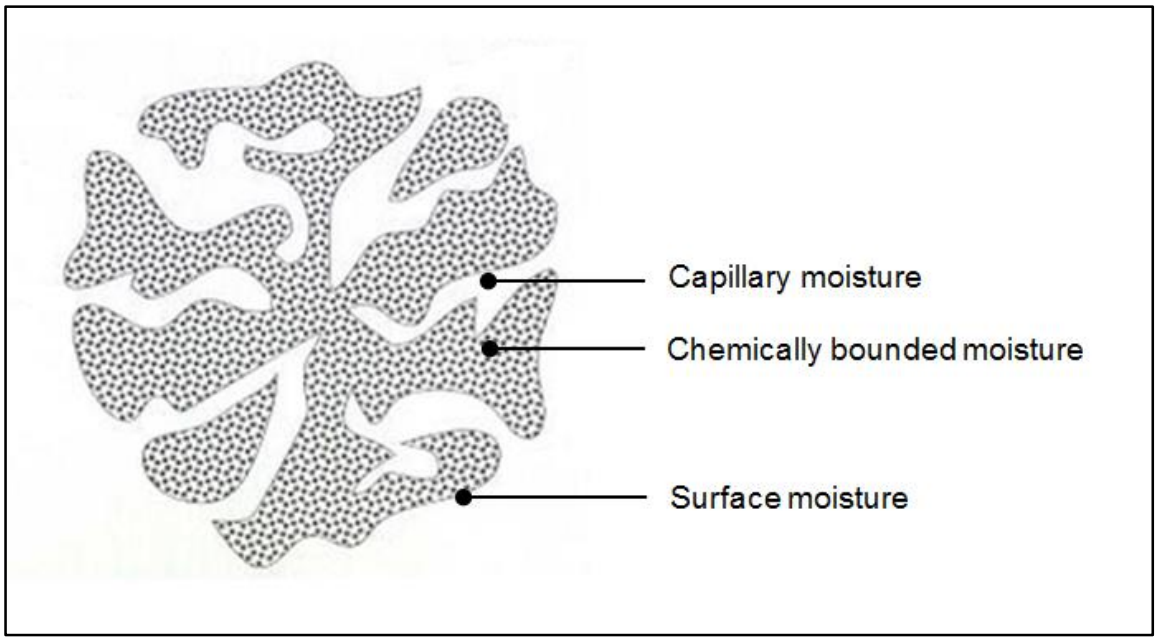

Figure 2.3. Porous coal particle; adapted from Lemley *et al.* (1995)

An overview of the types of moisture associated with coal is given in Figure 2.4. The surface moisture is also referred to as the free moisture as indicated in Figure 2.4. Surface moisture can be removed by means of mechanical dewatering technologies as the water is relatively free and able to move, specifically when external driving forces like pressure differentials are applied (Wakeman, 1984).

Equilibrium moisture is defined as the moisture content of coal subjected to a specific temperature and humidity (these conditions are defined as 30˚C and 96% relative humidity according to ISO 1080). This moisture reports as intra-particulate moisture and as films on the surface of the particles and cannot be removed by mechanical methods. It needs to be evaporated from the particle. The amount of equilibrium moisture changes according to the changes in atmospheric conditions (Rong & Hitchins, 1995).

According to Buckey & Nicol (1995) the chemically bounded moisture can only be removed by means of pyrolysis and not mechanical or thermal drying operations. Campbell (2006) also stated that the chemically bounded moisture is not considered part of the total measured moisture of a coal particle as it cannot be removed by dewatering technologies. Therefore the total moisture related to a coal particle that is going to be analysed in this study consists mainly of the residual moisture and the air dry loss free moisture.

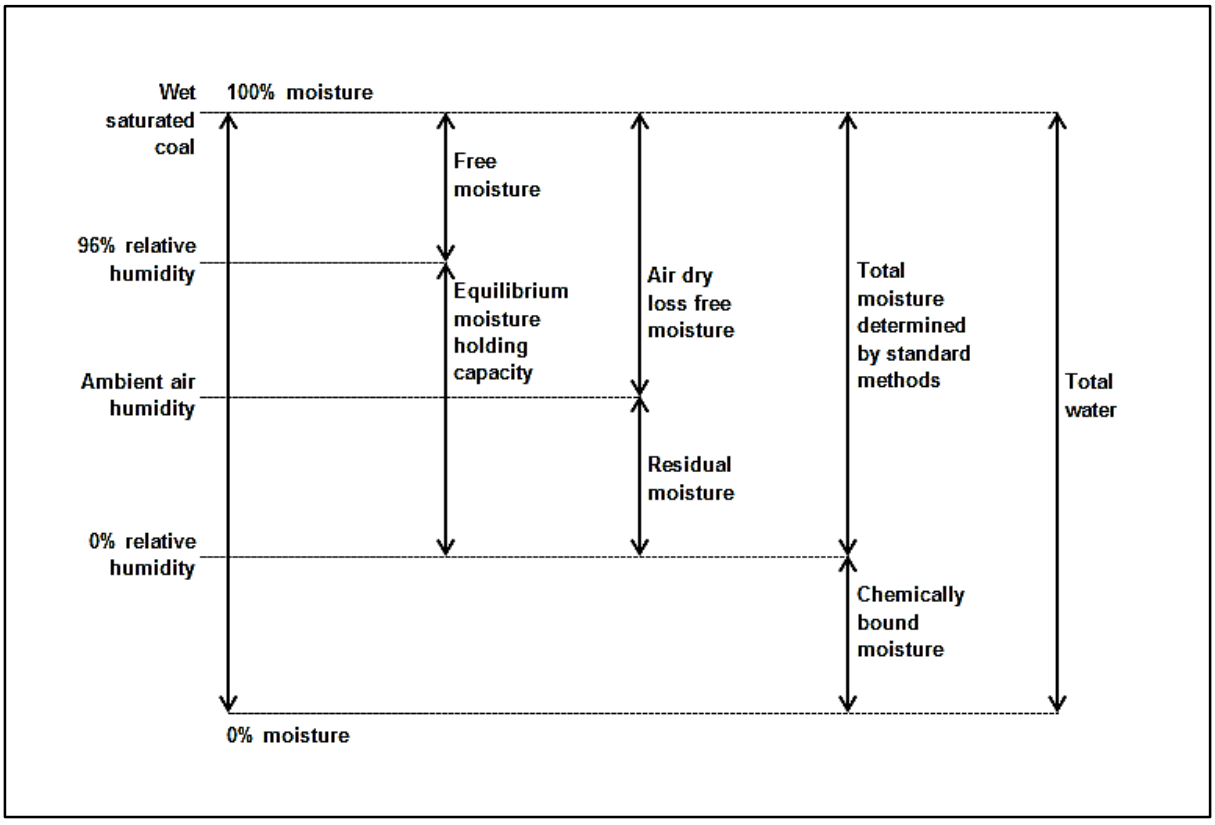

Figure 2.4. Moisture related to a coal particle; taken from Buckey & Nicol (1995)

2.4.1. Effects of coal properties on the moisture content

In order to improve dewatering technologies, it is very important to have an understanding of the influence that coal properties and characteristics have on the ability of coal particles to release moisture. The maceral type, total pore volume, mineral matter and total exposed particle surface of a coal sample will dictate its moisture content as well as the efficiency of dewatering. Coal is very heterogeneous as the size, shape, composition and porosity will differ from sample to sample. It is therefore important to determine the main coal properties and characteristics in order to get an understanding of the relationship between the coal particles and moisture content (Rong & Hitchins, 1995).

It was established by Rong & Hitchins (1995) that the moisture content of coal particles is not directly related to the maceral type. The organic matter has no effect on the dewatering potential of a coal sample. Work done by Unsworth *et al.* (1989) also showed that there was no correlation between the maceral type and the inherent moisture.

However the porosity in the maceral types may vary and that would influence the moisture uptake or release. Rong & Hitchins (1995) did a study on the dewatering of fine coal and found that the total pore volume as well as the specific surface area made it possible for more water to be absorbed or released from the coal. They concluded that an increase in porosity led to an increase in dewatering potential. According to (Mahajan & Walker, 1978) the pore volume and pore size distribution affects the magnitude and ease of diffusion through the coal particles.

Van der Merwe & Campbell (2002) observed that a higher mineral matter content in fine coal resulted in a higher moisture uptake as the mineral matter act as a hydrophilic site. The minerals can include silica, sulphides, carbonates and chlorides (Osborne, 1988). Work done by Rong & Hitchins (1995) as well as Du Preez (2012) proved that mineral matter and especially clay type minerals in coal is the main reason for a moisture absorption. Clay type minerals swell, which makes it easier for moisture uptake. Clays within the coal structure absorbs moisture and leads to an increase in the overall coal moisture content (Falcon & Ham, 1988).

Asmatulu & Yoon (2012) stated that finer particles are more difficult to dewater mainly because they have a larger surface area compared to coarser particles. The larger surface area creates more surface and capillary forces that prevent the moisture from leaving the finer coal particles. These forces are higher for finer particles compared to larger coal particles, which makes it hard to dewater. According to Van der Merwe & Campbell (2002) finer particles will not only absorb more moisture, but will also lead to a faster moisture uptake rate.

2.5. Dewatering techniques

There are several methods to reduce the moisture associated to coal. These methods are commonly divided into two groups; techniques to remove the surface moisture and then techniques used to remove the inherent moisture from the coal. The term inherent moisture refers to capillary and chemically bounded moisture. Figure 2.5. shows these drying techniques associated to particle size and moisture content.

Surface moisture can be removed by means of mechanical dewatering technologies as the water is relatively free and able to move when a pressure differential is applied across a bed of particles (Wakeman, 1984). The general mechanical dewatering technologies include screen-bowl centrifuges, belt filters, vacuum filters as well as plate and frame filter presses (Mohanty *et al*., 2012). These dewatering methods are only able to reduce the surface moisture from solid particles but not the inherent coal moisture (Wakeman, 1984). Mechanical dewatering is able to reduce the moisture content of fine coal (-0.5mm) to about 15%$_{wt}$ whereas the moisture content of ultra-fine coal (-0.1mm) is reduced to 25%$_{wt}$. These mechanical drying techniques are usually used as an initial process to reduce large volumes of surface moisture (De Korte & Mangena, 2004). Reddick *et al*. (2007) stated that mechanical dewatering is generally incapable of delivering the required moisture levels, especially for coal fines.

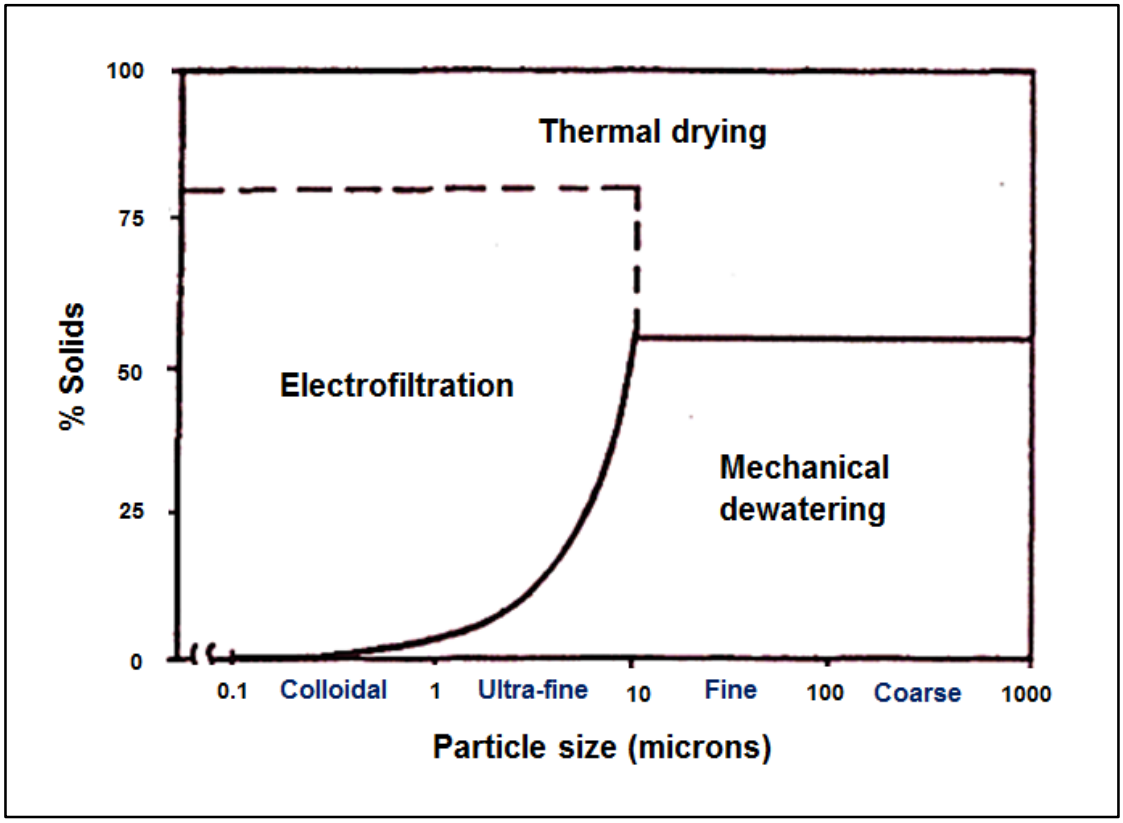

Figure 2.5. Drying techniques related to particle size; taken from Bourgeois *et al.* (2000)

According to (Campbell, 2006) and illustrated in Figure 2.5., large volumes of moisture can be more easily removed from coarse coal and fine coal by means of mechanical dewatering. It can be seen in Figure 2.5., that dewatering or drying becomes more difficult as the size of the particles decreases. Thermal drying is necessary to remove the remaining moisture as well as moisture particularly from smaller sized particles.

Thermal drying usually refers to a process where moisture is removed from wet solid particles by using a drying medium that is in the gaseous state. The moisture is then evaporated and carried away by the drying medium (Syahrul *et al.*, 2002).

There are various thermal drying techniques used, for example, rotary dryers, flash dryers, high temperature fluidised bed dryers as well as drying in chambers. These methods require high temperatures of the gasses or air used during drying. Thermal drying can take place by means of convection when the wet solid particles are in direct contact with the drying gas or air. It can however also occur when the wet particles are placed near a hot surface and drying takes place through indirect heating. The warm gas transfers energy to the wet solid particles to a point that the temperature of the solid particles will also increase and will lead to an increase in the vapour pressure of the moisture. The water will be evaporated from the solid particles when the vapour pressure of the water becomes higher than the partial pressure of the warm gas. The water vapour will be captured by the drying capacity of the warm gas or air and transferred away from the wet solid particles (De Korte & Mangena, 2004).

2.6. Drying within a fluidised bed using warm air

This section of work describes the drying process during fluidisation. It specifically focuses on how the moisture is transported from the coal particles to the drying capacity of the upward flowing air. To conclude this section of work, the drying rate is also discussed with an overview of a number of parameters that may cause changes in the drying rate.

Since slightly elevated temperatures below 60°C are used for drying within this project, the temperatures never reach the boiling point of water. Therefore the water does not reach a state where all the moisture gets evaporated and transported away from the wet sample. At these lower temperatures the moisture in the coal is mainly transferred to the drier air containing less moisture, as a result of the large concentration gradient between the wet coal and the dry air. The mass transfer during drying is called diffusion (Nellis & Klein, 2012).

A popular example to explain diffusion is by placing a glass of water in a room. The air in the room contains water vapour that is in the gaseous phase as indicated in Figure 2.6.

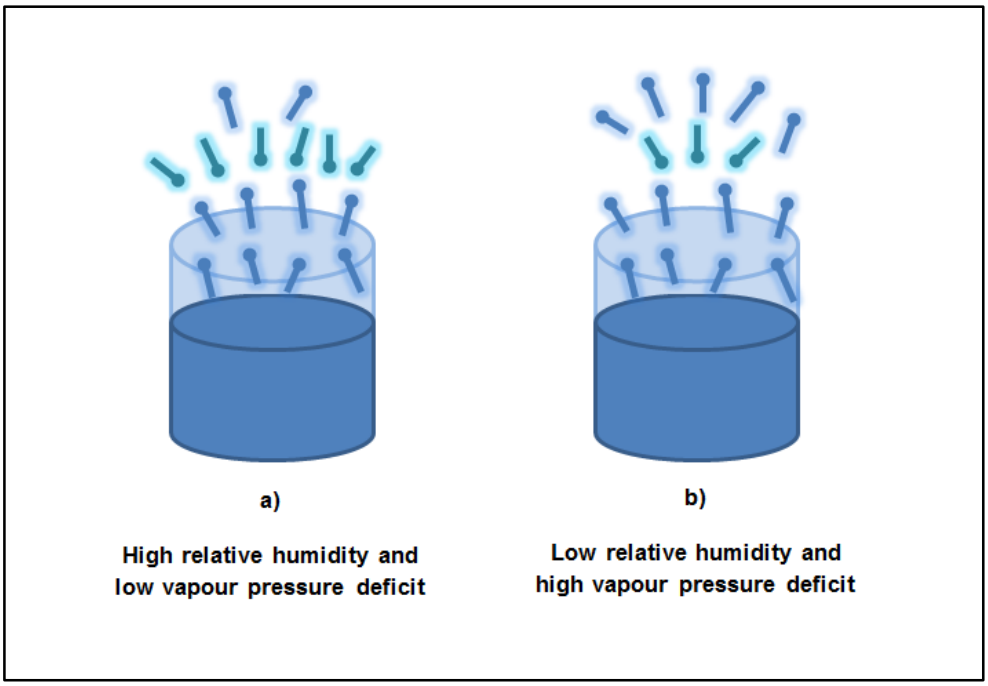

Figure 2.6. Vapour pressure deficit; taken from the University Corporation for Atmospheric research (2010)

Relative humidity is the moisture content relative to the saturation moisture content at the specified dry bulb temperature. The air near the open area of the glass of water is almost completely saturated with water vapour. The moment the water from the glass is transferred into the air, it transforms into a gaseous state called water vapour. The air further away from the glass contains less water vapour, thus a lower concentration. This phenomenon causes the water to be transferred from the air close to the water to the air further away. This process will continue until the water vapour in the whole room is equally distributed. If the relative humidity in the room is lower, there will be a larger mass concentration gradient and a higher vapour pressure deficit. This phenomenon can be seen in Figure 2.6. On the other hand a higher relative humidity will decrease the mass concentration gradient (Nellis & Klein, 2012).

Phase equilibrium between liquid water and water vapour is a state where the rate of diffusion from the liquid phase is the same as the rate of condensation of the vapour. Changes in the driving forces like temperature and partial pressure can disrupt the vapour-liquid equilibrium. Figure 2.7. illustrates how these driving forces lead to a change in the thermodynamic state of the pure substance.

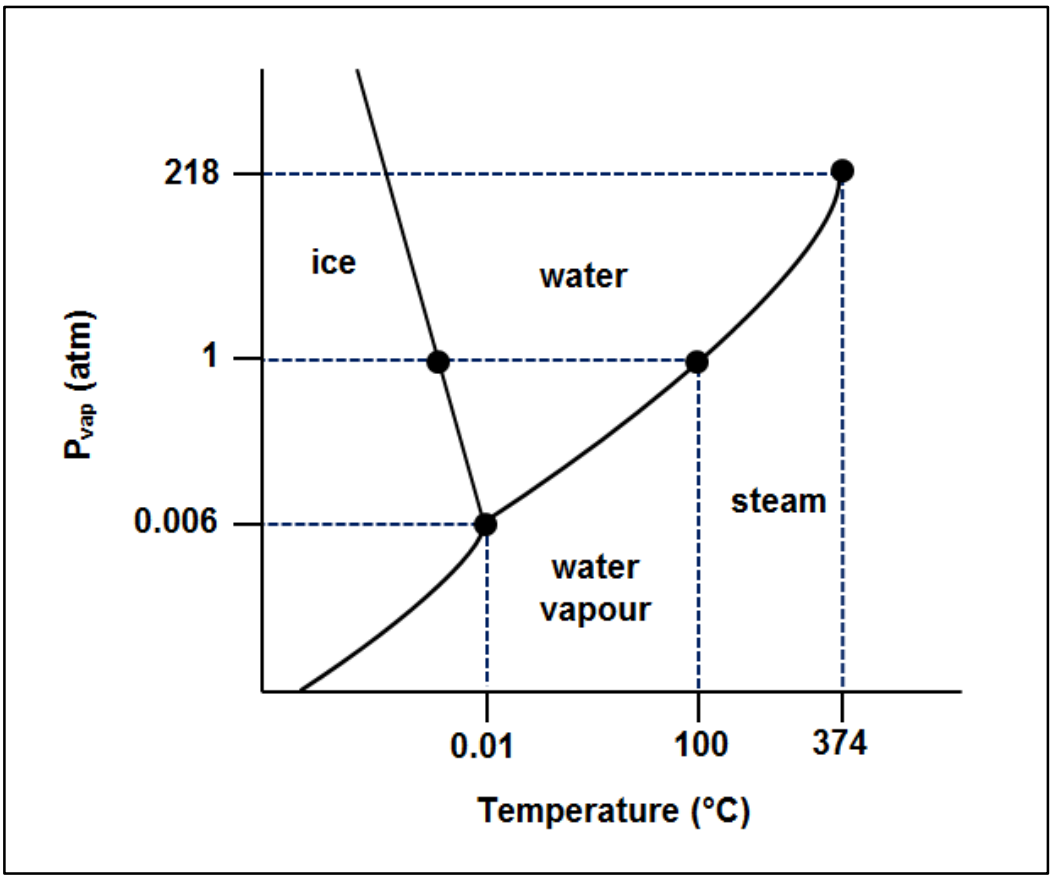

Figure 2.7. Phase diagram of water; taken from the University of Texas (2013)

Even slight changes in the temperature and/or relative humidity of the system, at constant pressure, may result in an equilibrium change between the liquid and the vapour, which will lead to the phase change of liquid to water vapour (Koretsky, 2004). By replacing the newly formed vapour with drier (less moist) air, the system equilibrium is again disturbed causing some of the remaining liquid to undergo a phase change to vapour. The system will move to a new equilibrium point where the liquid in the coal particle is in equilibrium with the vapour fraction of the dry air. This is defined as the irreducible equilibrium point of the specific water/air system.

Solid particles in a fluidised bed behave like a fluid when suspended in the upward flowing medium. Therefore drying in a fluidised bed is achieved by fluidising the solids by means of the drying medium, in this case, warm air. The water vapour is ultimately captured by the drying capacity of the upwards flowing warm air and continually transferred away from the wet solid particles (Syahrul *et al*., 2002). This sets in motion the process described in the paragraph above, constantly creating a larger concentration gradient.

When fluidising a wet bulk coal sample, the particles remain stationary. After a while the particles on the top layer of the sample can be fluidised, while the rest of the sample remains too wet to move. The air velocity through the fluidised bed will change constantly as the moisture decreases during the experimental run. This means that the pressure drop across the bed will decrease as well. An increase in the air velocity will bring forth a larger drag force on the particles and more of the particles will break loose from the wet sample to be fluidised. At a certain point during the experimental run, the air velocity will be sufficient to result in complete fluidisation of all the particles (Syahrul *et al*., 2002). The moisture content at this point correlates to the values found by Terblanche (2011) and Willemse (2011) and proved to be between 5-7%$_{wt}$.

2.6.1. Drying rate

The rate at which thermal drying can take place vary for each sample and can be represented by constructing a drying curve as illustrated in Figure 2.8. The factors that influence the drying rate can be investigated by studying these drying curves (De Korte & Mangena, 2004). It is suggested that drying using fluidised air at low temperatures will act similarly, but using different driving forces.

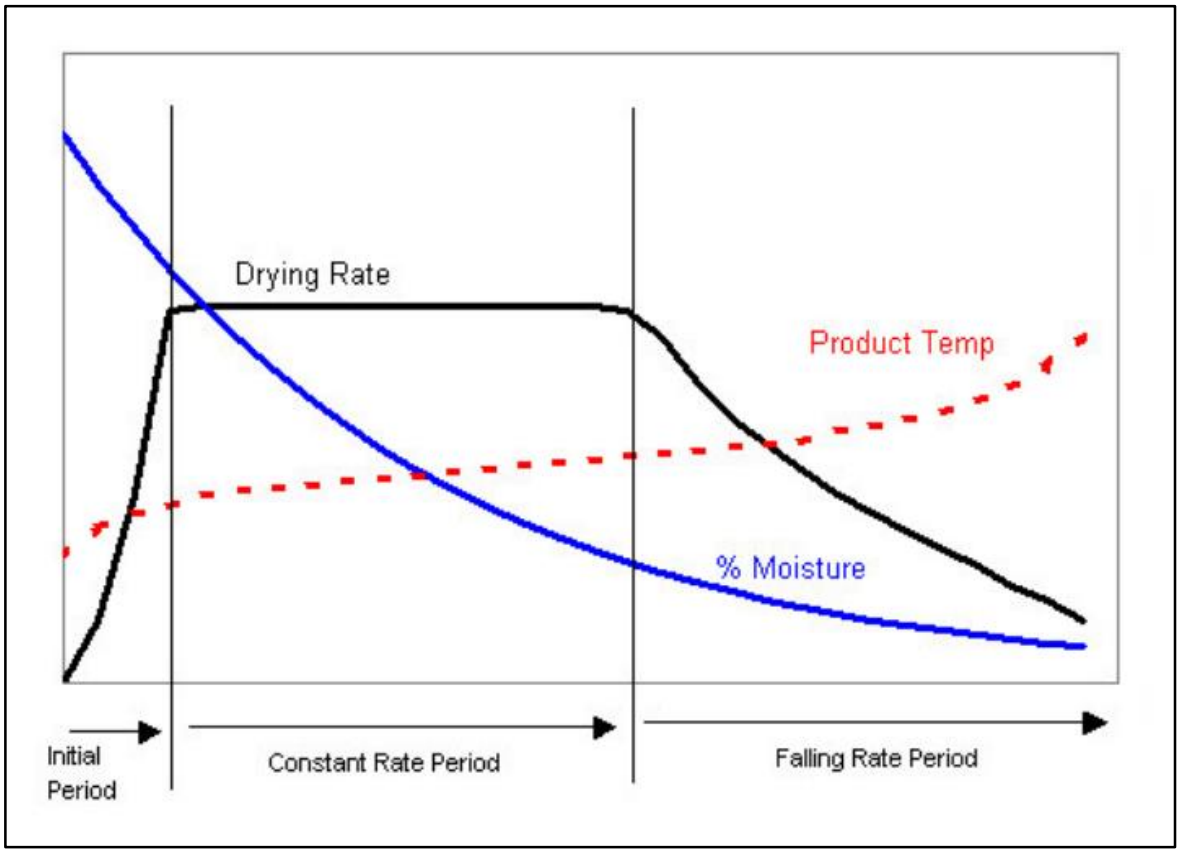

Figure 2.8. Typical drying curve; taken from De Korte & Mangena (2004)

According to (De Korte & Mangena, 2004) there are three phases during the drying process:

i. *Initial period:* During the first phase the coal fines are heated to reach the specified process temperature and humidity. The drying rate rapidly increases during the first phase. However this will depend mainly on how far the process conditions are from the initial temperature and relative humidity. At this stage the concentration gradient is large and a great deal of free moisture and surface moisture are removed.

ii. *Constant rate period:* During the second phase the moisture is still removed but at a constant rate. This means that the rate at which energy is transferred from the warm air to the wet coal fines is equal to the rate at which the moisture is removed. Surface moisture is removed during the constant rate period until the surface of the fine particles is dried. There are a number of factors that can influence the drying rate at this stage. The temperature of the drying air as well as the relative humidity or moisture content of the drying air will influence its ability to absorb water from the wet coal samples. The flow rate of the drying air will dictate its ability to hold the moisture and carry it away at a rate that would be sufficient to dry the coal efficiently. In addition the ability of the drying air to move effectively between the wet coal particles will also affect the drying rate.

iii. *Falling rate period:* It is more difficult to remove capillary moisture from particles and therefore the drying rate falls significantly during the third period. The moisture in the pores of the particle will need to be transferred to the surface before diffusion can take place. The physical properties and constitutes of the coal particle as described in Section 2.4.1. will play a definite role in the ability of the particle to release moisture.

2.6.2. Related case studies

Work done by (Chua & Chou, 2003) showed that fluidised bed dryers are a low cost drying system with low maintenance costs. Although there are a lot of fluidised bed dryers currently in operation, the majority of those fluidised beds use high temperatures for drying. According to (Chua & Chou, 2003) fluidised beds can operate with lower temperatures which would ultimately minimize operation costs as well as thermal related degradation. The use of airflow results in excellent air-particle contact, which leads to efficient mass and heat transfer rates. The airflow can percolate efficiently through all the particles in the bulk sample and in the end deliver a product that has evenly dried throughout. It has also been proved that the drying kinetics are improved using a fluidised bed causing shorter drying times. The added advantage is that the drying velocity can be changed to increase the drying rate as well. The

problem however is that if the airflow rate is too high, the air will pass around the particles' surfaces and won't be able to transfer moisture (Chua & Chou, 2003).

Fluidised bed dryers have been developed and used with great success throughout the world and the CSIR Division of Energy and Technology also tested a unit in 2003. The fluidised bed dryer could dry fine and ultra-fine coal at one ton per hour. Two particles sizes were used; one fraction smaller than 0.5mm containing a moisture content of 20% and another fraction of between 0.1mm and 1mm containing a moisture content of 22%. The fluidised bed dryer was able to reduce the moisture content to 1.2% for the fraction smaller than 0.5mm and to 2% for the fraction of between 0.1mm and 1mm. The advantage of the fluidised bed is that the air or gas flow is able to lift the wet particles in the sample to enhance the air and heat transfer to the coal particles and to ultimately transfer moisture. In addition the wet particles are also in direct contact with the heating source. Dust explosions are the major obstacle in drying fine coal in a fluidised bed and the problem was solved by working with air or gas with an oxygen content of lower than 5% and temperature lower than 120°C. It was also found that coal finer than 0.1mm couldn't be dried in the fluidised bed. Small particles are very cohesive and that leads to larger inter-particle forces that would be greater than the force that the drying medium can exert on the particles (De Korte & Mangena, 2004).

Levy *et al.* (2006) did a study on the drying of wet fine coal in a bubbling fluidised bed at temperatures ranging from 43°C to 60°C and a range of relative humidity conditions. Coal with a size distribution of between -4mm+0.3mm was used at high airflow conditions causing bubbling. The results showed that the drying rate in the bubbling fluidised bed was linear until it reached a point near the final moisture content. Furthermore it was shown that there is a linear correlation between the drying rate and an increase in the airflow. It has been proved that increasing the airflow rate resulted in a higher drying rate. Levy *et al.* (2006) found that the drying rate didn't depend mainly on the fluidised bed bubble behaviour. The drying rate rather depended on the airflow rate, the relative humidity of the inlet air and the equilibrium moisture content of the coal samples.

CHAPTER 3 – EXPERIMENTAL

3.1. Introduction

This chapter starts off by giving an overview of the experimental plan and the variables investigated in the experimental work. In addition the equipment and experimental procedures are also discussed. Furthermore it includes a detailed description of the coal samples used for the experimental work; this includes a maceral analysis, proximate analysis, maceral composition, size analysis as well as a porosity analysis. The sample preparation for the experimental work is also included.

3.2. Experimental plan

The experimental plan was divided into two sections according to the equipment used:

3.2.1. Static bed (non-fluidised state)

The first part of the experimental work was completed in a controlled climate chamber with the coal in a static non-fluidised state. The results made it possible to investigate the desorption isotherms at various temperatures and relative humidity conditions to get a better understanding of the equilibrium moisture content. By excluding the airflow rate in this part of the experimental work, it was possible to examine only the influence of temperature and relative humidity on the drying rate. The results yielded a better understanding of the influence of the coal characteristics and properties on the drying process as well.

3.2.2. Fluidised bed

The second part was carried out using a fluidised bed with conditioned air as the fluidising medium. The experimental work within the fluidised bed focused on determining the optimum operating parameters for different variables which included temperature, relative humidity and airflow rate. The results made it possible to study the drying performance of the fluidised bed and to determine the drying rate at various conditions. A number of variables were investigated to determine the effect thereof on the drying rate. Some of the variables included the airflow rate, initial moisture content and coal characterisation and properties. Section 3.2.3 gives a layout of all the experimental variables.

3.2.3. Variables

The following variables were investigated during the experimental work:

- ***Coal type:*** Waterberg vitrinite rich coal and Waterberg inertinite rich coal
- ***Initial moisture content:*** Bulk coal sample with an equilibrium moisture content of ±2.5%$_{wt}$, filter cakes with high moisture content of 20-25%$_{wt}$ and filter cakes with lower moisture content of ±15%$_{wt}$.
- ***Relative humidity of drying air:*** 70%, 50% and 30% RH
- ***Temperature of drying air:*** 25°C, 40°C and 55°C
- ***Airflow rate of drying air:*** Static non-fluidised conditions, minimum fluidisation velocity and above minimum fluidisation velocity resulting in vigorous mixing.

3.3. Equipment used

The first part of the experimental work was completed in a controlled climate chamber with the coal in a static non-fluidised state, while the second part was carried out using a fluidised bed with conditioned air as the fluidising medium. Samples with a weight of 100g were used for every experiment, both for the static non-fluidised and fluidised conditions. The climate chamber and fluidised bed consisted of a cylinder with a diameter of 10cm to hold the test samples.

3.3.1. Climate chamber

The climate chamber (C-40/100) was pre-programmed to keep the conditions within the chamber at specific temperatures and relative humidity conditions. The machine had an inlet at to back to draw air into the chamber for conditioning. Figure 3.1. is a schematic diagram of the experimental setup for the static bed tests. The prepared sample was placed in a cylinder with a diameter of 10cm and situated on top of a load cell. Changes in the mass of the coal were recorded on a computer in real time while the humidity and temperature inside the climate chamber were continually controlled to prescribed set points.

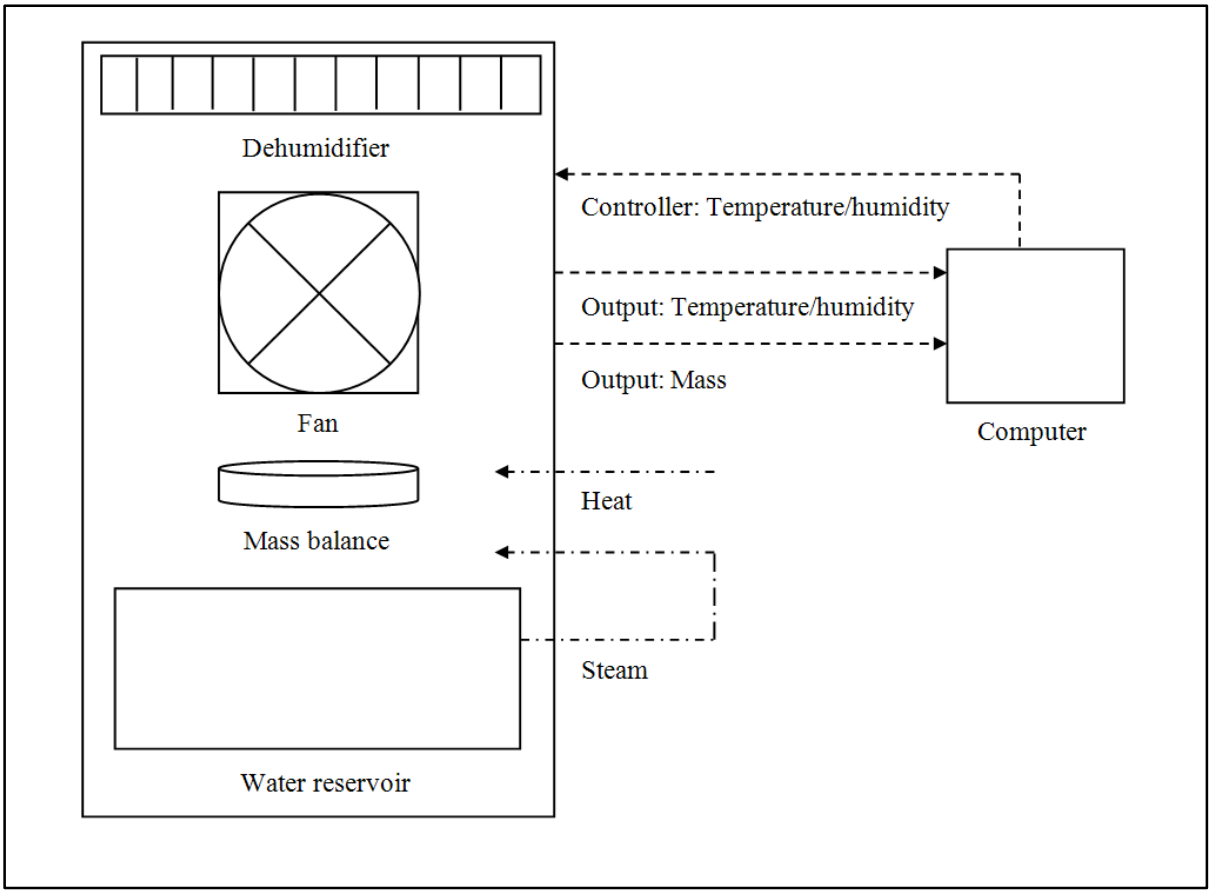

Figure 3.1. Diagram of experimental setup (climate chamber)

Figure 3.2. shows a photograph of the entire climate chamber, consisting of the actual chamber with conditioned air at the top section.

Figure 3.2. Photograph of the climate chamber

The temperature and humidity probe are placed on the plate at the back of the chamber as shown in Figure 3.3. The bottom section contains the heating coils, water reservoir and refrigeration gas to produce the conditioned air. The temperature was controlled with an error boundary of ±1°C and the humidity had a range of ±3%.

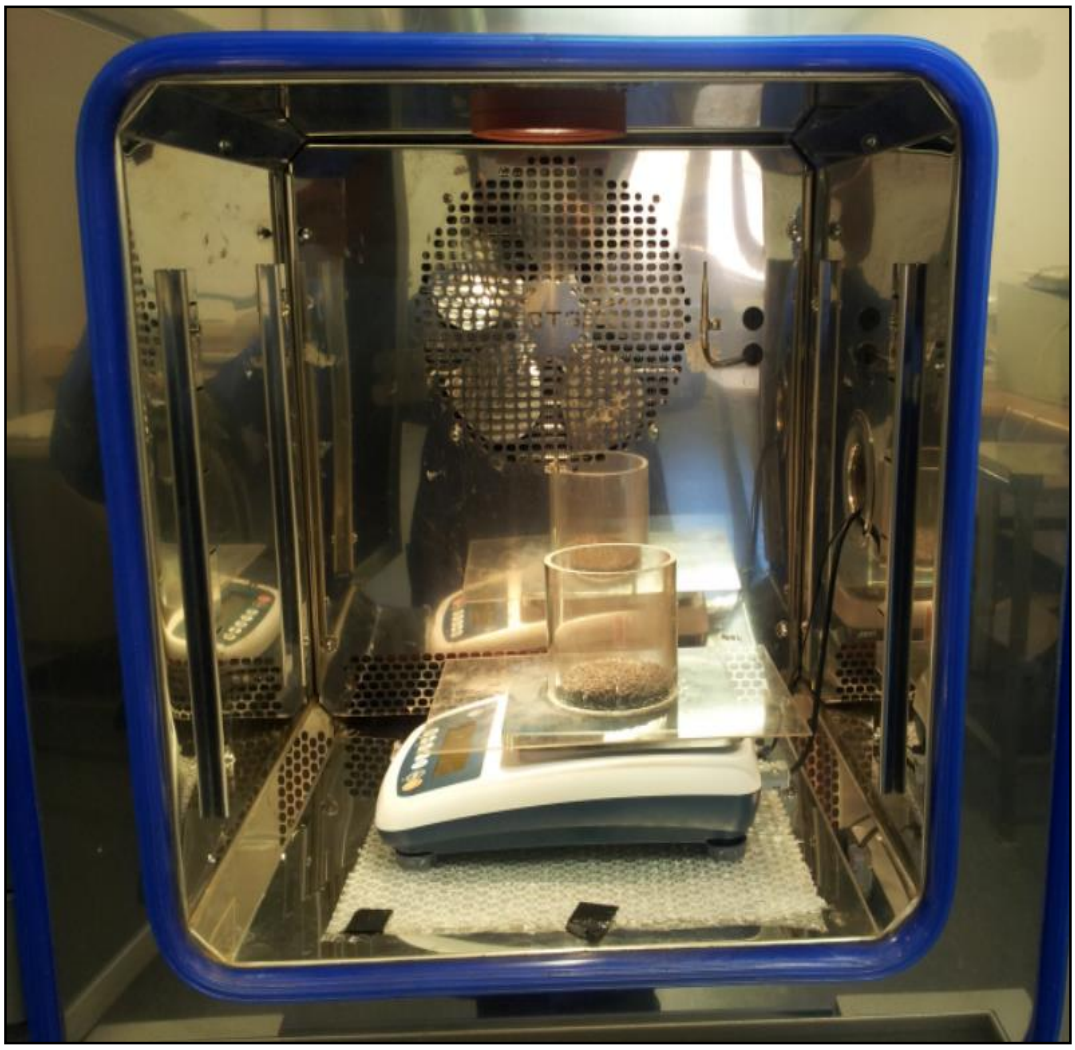

Figure 3.3. Photograph of the sample on the load cell inside the climate chamber

3.3.2. Fluidised bed

The fluidised bed test cell was attached to the side of the climate chamber and coupled with it in order for the blower to draw conditioned air from the chamber. The setup can be seen in the diagram in Figure 3.4. and the photograph in Figure 3.5.

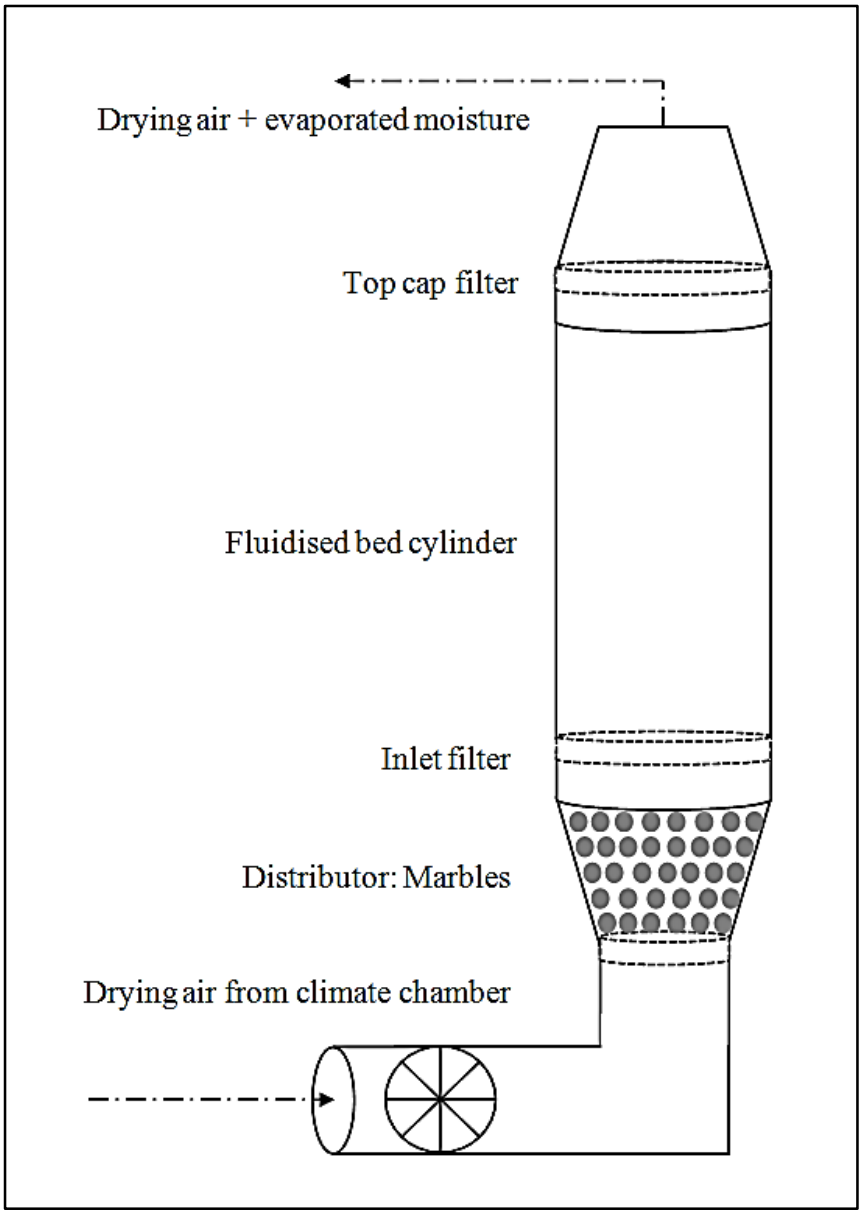

Figure 3.4. Diagram of experimental setup (fluidised bed)

A mesh cover was placed at the top and bottom of the fluidised bed cylinder to prevent fine particles from exiting. A fluidised vessel with a diameter of 10cm was used to correlate the results to the static bed test also did on a cylinder with the same diameter. A packed bed of small glass marbles was used to distribute the up flowing air evenly across the cylinder. Humidity detectors were used to observe the moisture loss or gain in the airflow and values were correlated by weighing the samples before, and at regular intervals during a test. The drying air and evaporated moisture was recycled back to the climate chamber to be conditioned again. The climate chamber was used to condition the fresh air before fluidisation as well as conditioning the recycled air throughout the experimental run.

Figure 3.5 Photograph of the fluidised bed and climate chamber setup

3.4. Materials used

Vitrinite and inertinite rich bituminous coal from the Waterberg coal field in the northern Limpopo province of South Africa was used in the study. Section 3.4.1. through to Section 3.4.6. provides results of analysis done on both the vitrinite and inertinite rich bituminous coal samples. All the analysis was done at Bureau Veritas, Advanced Coal Technology.

3.4.1. Sample acquisition

The vitrinite and inertinite rich coal samples were run off mine coal and used as is for the experimental work. The samples were visually sorted into a bright (vitrinite rich) and dull (inertinite rich) fractions. The samples were left in ambient air to dry, then crushed and sieved to a particle size range of -2mm+1mm and thereafter mixed and split into 100g sub-samples.

Figure 3.6. is a photograph of the coal samples used; the sample on the left is vitrinite rich coal with a high reflectance and the sample on the right is inertinite rich coal which appears duller as can be seen in Figure 3.6.

Figure 3.6. Photograph of coal samples, vitrinite rich coal left and inertinite rich coal right

3.4.2. Maceral analyses

Petrographic analyses were completed to confirm the maceral content of the visually sorted vitrinite and inertinite rich coal samples. The maceral analyses of the coal samples yielded the results listed in Table 3.1. The procedures and standards used to obtain the maceral composition as well as the micrographs can be seen in Appendix A.

Table 3.1. Maceral composition

Sample Identification ($\%_{wt}$)	Vitrinite rich coal ($\%_{wt}$)	Inertinite rich coal ($\%_{wt}$)
Vitrinite	40.1	9.2
Liptinite (Exinite)	4.6	3.5
Reactive Semifusinite	14.8	17.7
Inert Semifusinite	9.3	55
Fusinite and secretinite	1.7	1.1
Micrinite	0.2	0.7
Mineral matter	29.3	12.8

The vitrinite rich coal contained more mineral matter that the inertinite rich coal. The bright fraction of coal contained more vitrinite as speculated during the visual sorting and the dull fraction contained more inertinite. The inertinite rich coal (dull fraction) does contain higher values of reactive semifusinite and inert semifusinite compared to the vitrinite rich coal containing more mineral matter.

3.4.3. Proximate analysis

Proximate analysis was done in order to determine the fixed carbon, volatiles, ash and specifically the moisture content of the coal fines. The results of the proximate analysis can be seen in Table 3.2. In addition the sulphur content and calorific values of both samples were also determined to add to the data from the proximate analysis and is given in Table 3.3. The procedures and standards used to obtain the results can be seen in Appendix A.

Table 3.2. Proximate analysis results (Air-dried basis)

Sample identification ($\%_{wt}$)	Vitrinite rich coal ($\%_{wt}$)	Inertinite rich coal ($\%_{wt}$)
Inherent moisture content	1.2	1.4
Ash content	52.9	21.7
Volatile matter	20.5	21.2
Fixed carbon	25.4	55.7

Table 3.3. Sulphur content and calorific values (Air-dried basis)

Sample Identification	Vitrinite rich coal	Inertinite rich coal
Sulphur content ($\%_{wt}$)	1.11	3.18
Calorific value (MJ/kg)	13.36	24.46

The results of the proximate analysis show that the vitrinite rich coal sample had a very high mineral content. This is common for Waterberg run on mine coal due to the layered structure of the ore body (Jeffrey, 2004). The result of this high mineral content is a low calorific value, as indicated in Table 3.3.

3.4.4. Size analysis

The coal was crushed to the described particle distribution of -2mm+1mm. Figure 3.7. contains the data for the sieve analysis done prior to the experimental work.

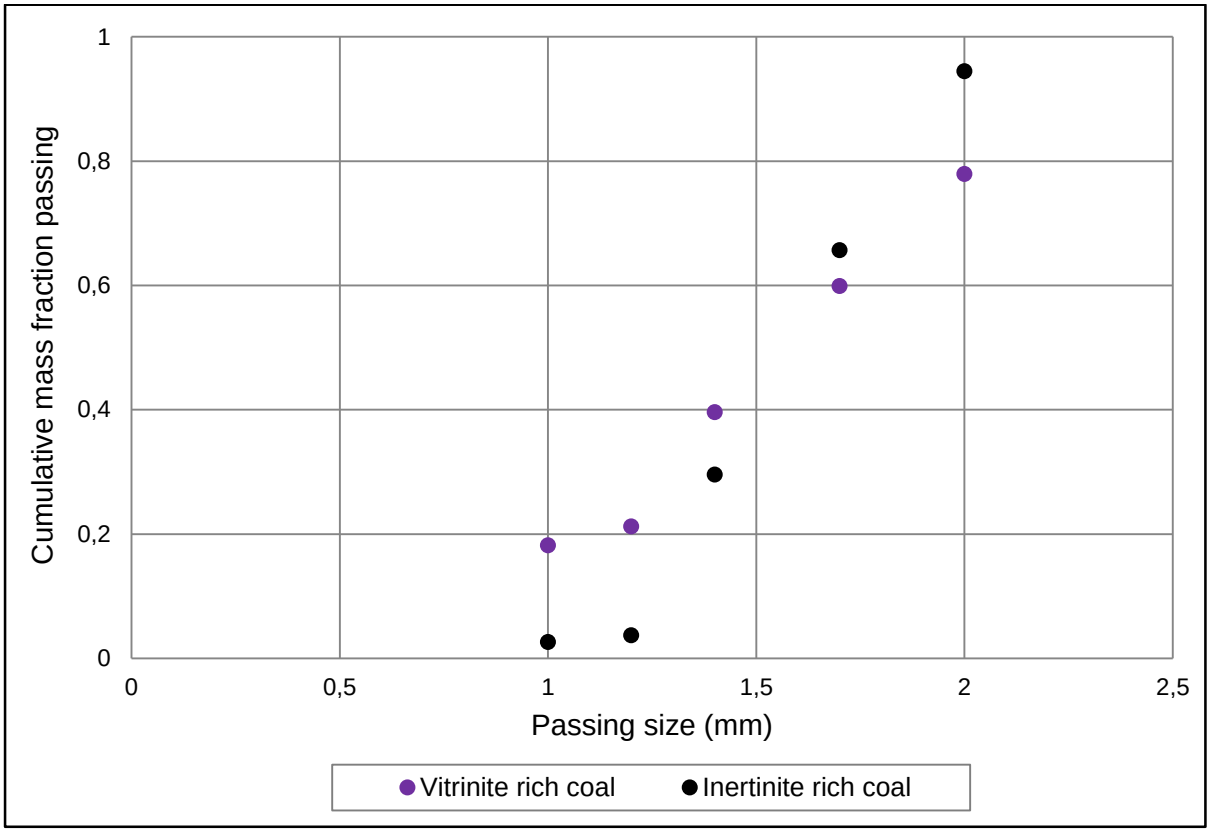

Figure 3.7. Screen analysis for vitrinite and inertinite rich coal samples

The particle size analysis of the two different coal samples yielded similar d_{50} values. The vitrinite rich sample has a d_{50} of 1.5mm while the d_{50} of the inertinite rich sample was calculated as 1.55mm. There was however a large difference between the coarse and fine particle fractions of the two coal samples, as can be seen in Figure 3.7. The vitrinite rich sample had more fine material than the inertinite rich coal sample. It is noted that this would possibly influence the dewatering characteristics of the two samples. The vitrinite rich coal contained more finer particles in the sample and it was observed to be a much more brittle coal. The vitrinite rich coal also showed to release more fine coal dust than the inertinite rich coal.

3.4.5. Porosity analysis

The porosity was determined by means of N_2 as well as CO_2 intrusion and the results can be seen in Table 3.4.

Table 3.4. Porosity of coal samples

Sample Identification	Vitrinite rich coal	Inertinite rich coal
Porosity (m^2/g) N_2 intrusion	2.5	6.2
Porosity (m^2/g) CO_2 intrusion	79.5	131.9

The porosity was determined as the open area per mass of the sample. The inertinite rich coal had a much higher porosity than the vitrinite rich coal. As described in Chapter 2.4.1., the difference in porosity contributes to a particle's ability to absorb or release moisture, making it possible for drying air to percolate through the pores (Rong & Hitchins, 1995).

3.4.6. Sample preparation for experimental work

The samples were firstly left in ambient air to dry and after that crushed and sieved to a particle size range of -2mm+1mm. A sample splitter was used to obtain uniform samples to obtain more accurate experimental data. Each sample consisted of 100g of coal with a particle size range of -2mm+1mm.

The sample either had an equilibrium moisture content or was a filter cake with a high moisture content. Before the experimental work, some samples were conditioned in the climate chamber at a temperature of 25°C and a relative humidity of 80% for two hours to reach its equilibrium moisture content at those conditions. Other samples were drenched in water and filtered to a total moisture content of about 15%$_{wt}$ as well as 20-25%$_{wt}$. The moisture of each sample was determined prior to the experimental run. A Metler Toledo Halogen Moisture analyser with an analysing standard according to SABS 924 was used to determine the total moisture related to the coal particle by evaporating the moisture at 105°C for 2 hours.

CHAPTER 4 – RESULTS AND DISCUSSION

4.1. Introduction

This chapter includes the results from the experimental work done in order to meet the objectives stipulated in Chapter 1.3. Firstly, the desorption isotherms were discussed to give a clear understanding of the equilibrium moisture content. Thereafter the operating parameters, that included the airflow, relative humidity and temperature, were investigated. The drying performance was studied and accompanied a number of factors that may have an influence on the drying performance of the fluidised bed.

Drying at non-fluidised (static) and fluidised conditions were investigated in order to get a thorough understanding of the drying process. Both vitrinite and inertinite rich coal was studied. The majority of the results discussed in this chapter are for the inertinite rich coal, as both coal samples showed similar trends. The complete set of results can be found in Appendix B. Selected experiments were repeated and with a confidence interval of 95%, the minimum error was 0.03% and the maximum error was 1.75%.

4.2. Desorption isotherms

A bulk coal sample was conditioned at 25°C and 80% relative humidity for about two hours to reach a moisture content of 2.20%$_{wt}$. The sample of 100g was put onto the mass balance inside the climate chamber, after which the relative humidity was reduced in a stepwise manner in percentage points of 10% from 70% down to 30%. This was done at a temperature of 40°C. The mass loss, and thus moisture content, was determined after equilibrium was reached at each step. The moisture analyser with an analysing standard according to SABS 924 was used to determine the total moisture related to the coal particle and the samples were also weight to correlate the results found. The relative humidity could be related to the partial pressure of water by Equation 4.1.

$$P = \frac{RH}{100} * P_{sat} \quad \textbf{(4.1)}$$

The Antoine equation presented in Equation 4.2., and coefficients according to Koretsky (2004) were used to determine the saturation pressure, P_{sat}, of water, which is a function of the process temperature.

$$In\,(P^{sat}[bar]) = A - \frac{B}{T[K]+C} \quad \textbf{(4.2)}$$

Figure 4.1 shows the desorption isotherm of the inertinite rich coal sample at partial pressures corresponding to progressive reduction in the relative humidity from 70% to 30% at 40°C.

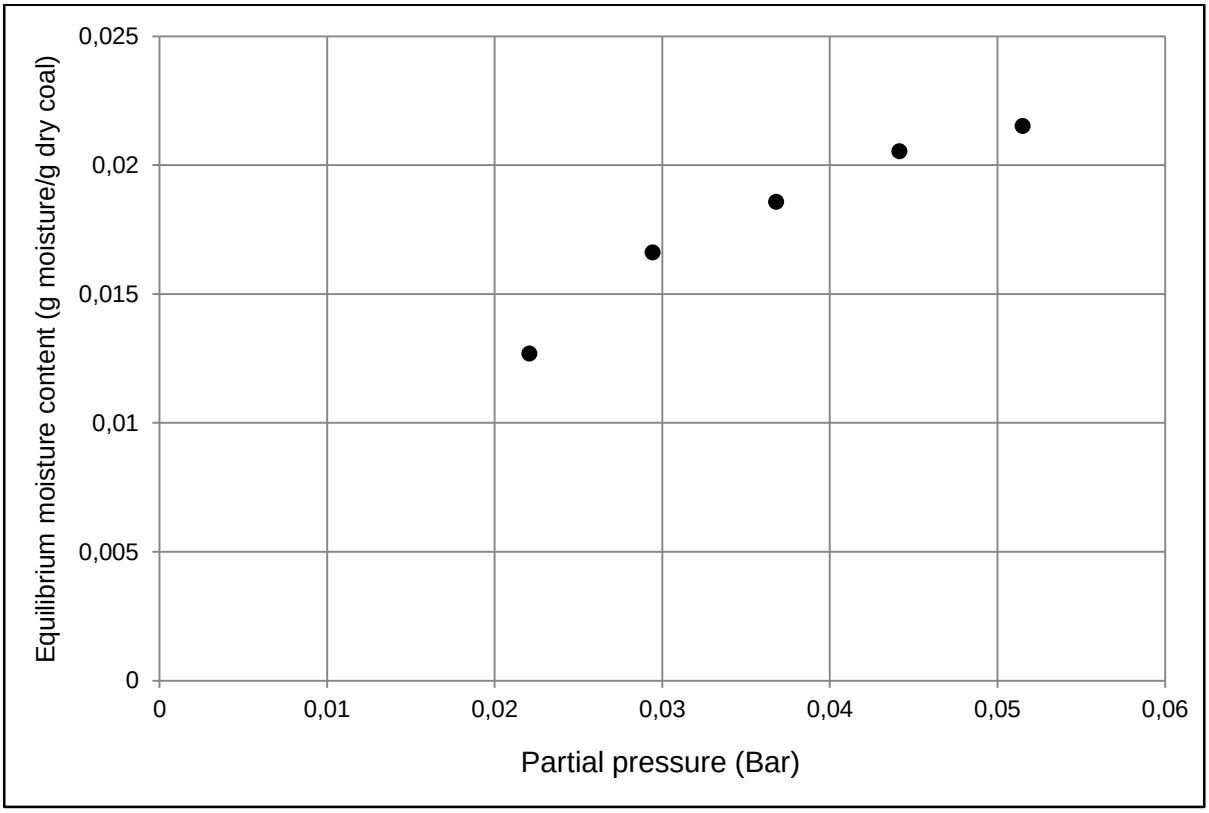

Figure 4.1. Desorption isotherm at 40°C and a humidity range of 70% to 30%

The sample reached an equilibrium moisture content at each of the relative humidity conditions and it was clear that a decrease in the relative humidity lead to a lower equilibrium moisture content. After each relative humidity step change, as shown in Figure 4.1., the system moved to a new equilibrium point where the moisture in the coal particle was in equilibrium to the vapour fraction of the dry air. The equilibrium moisture content also gives an indication of the open porosity of the bulk coal sample.

As stated in Chapter 2.4. and Chapter 2.6., the amount of equilibrium moisture changes to correspond to the changes in the atmospheric conditions (Rong & Hitchins, 1995). By lowering the partial pressure (moisture content) of the surrounding air, the system equilibrium is again disturbed causing some of the remaining liquid to again undergo a phase change to vapour. According to Koretsky (2004) the phase change is driven by an increase or decrease in the vapour pressure of the water surrounding the coal particles. The system will move to a new equilibrium point where the moisture in the coal particles is in equilibrium with the vapour fraction of the drying air.

4.2.1. Temperature effect on desorption isotherms

The same experiment was repeated at 25°C and 55°C in order to determine the effect of temperature on the desorption isotherms. Figure 4.2. shows the comparison between the amount of moisture that each coal sample contained at all three temperatures at various relative humidity conditions.

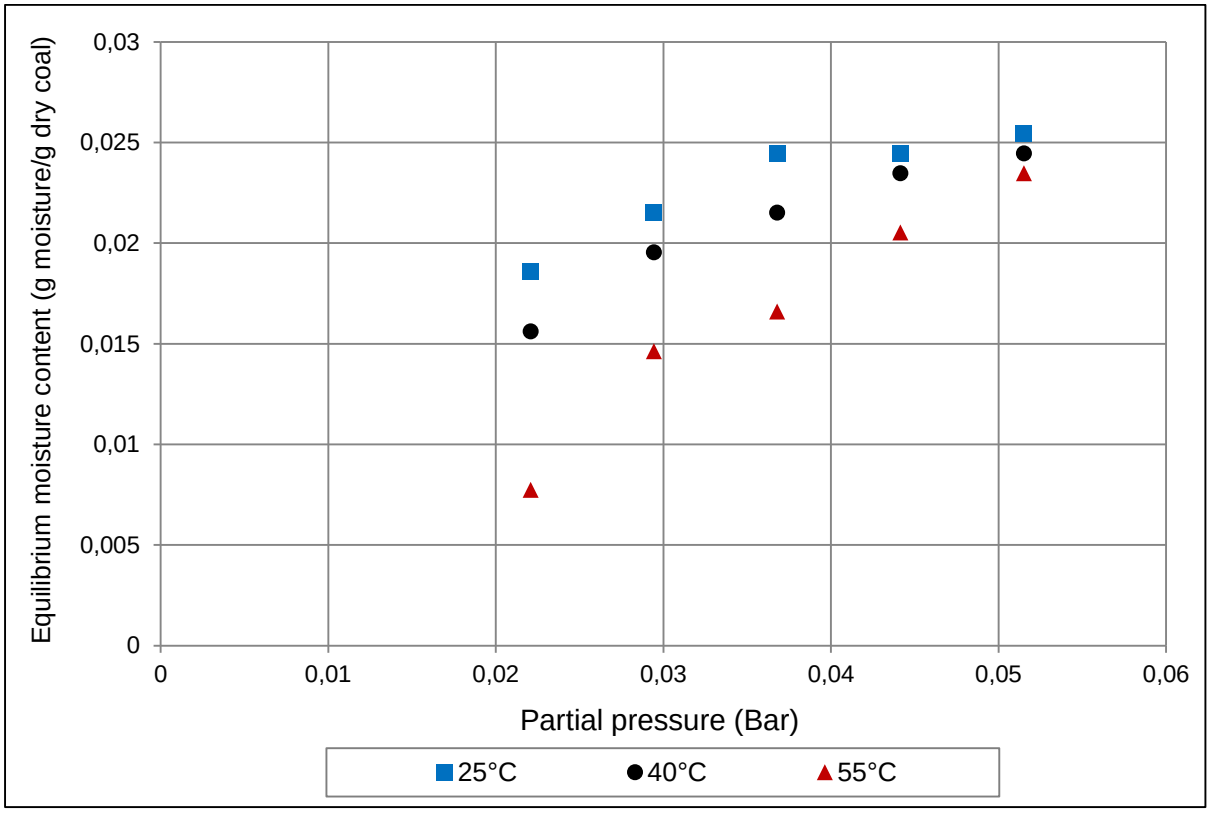

Figure 4.2. Desorption isotherm at 25°C, 40°C and 55°C and a humidity range of 70% to 30%

Similar trends in the desorption isotherms were found at temperatures, 25°C as well as 55°C. All three isotherms, as shown in Figure 4.2., show that a decrease in the relative humidity leads to a lower moisture content.

It was interesting to note that the coal sample reached a lower equilibrium moisture content at the high temperature of 55°C and a higher moisture content at a lower temperature of 25°C. The sample placed in drying air of 55°C showed a larger difference in the equilibrium moisture content compared to samples placed at 25° and 40°C. Du Preez (2012) also investigated the absorption and desorption isotherms of coal and found that higher temperatures lead to a lower equilibrium moisture content in the samples.

It can be seen in Figure 4.2. that the coal samples can only absorb a certain amount of moisture at the high partial pressures, resulting in similar moisture contents as it reaches a

saturation point. However lower partial pressures resulted in a larger difference in the equilibrium moisture content of the coal samples exposed to the different temperatures and indicated that the temperature of drying air is a driving force at these low partial pressures at static conditions. The results found by Du Preez (2012) confirmed this phenomenon and also indicated that temperature plays a greater role at lower relative humidity conditions.

Figure 2.4. in Chapter 2.4., shows that when the coal sample is exposed to a relative humidity below 96%, the moisture at equilibrium moisture holding capacity will be removed. As the relative humidity is lowered, the coal samples will contain less inherent moisture and a smaller volume of water. De Korte & Mangena (2004) stated that the physical properties and constitutes of the coal particle will play a more definite role in its ability to release the equilibrium moisture, when a coal sample containing less moisture is dried. Some of the equilibrium moisture needs to move through the pore network in the coal sample to the surface from where the moisture can be captured by the drying air. As mentioned in Chapter 2.6., it is more difficult to remove the inherent equilibrium moisture from the coal particles and therefore the drying rate falls significantly (De Korte & Mangena, 2004). According Lawluvl & Ayensu (1998) the external factors like higher temperatures will lead to more moisture released and transferred through the pores to the surface of the coal particle. This explains why higher temperatures of the drying air were able to reduce the equilibrium moisture content, especially when drying the coal samples containing less moisture at the lower relative humidity conditions.

4.3. Operating parameters

The experimental work completed for this section of work focussed on determining the optimum operating parameters for fluidised bed drying operating with warm air as fluid. These operating parameters included the airflow rate, temperature and relative humidity.

4.3.1. Introducing airflow

To determine the influence of airflow, the fluidised conditions were firstly compared to static bed conditions (without airflow). The coal samples of about 100g each were conditioned prior to the experiment, at 25°C and 80% relative humidity for about two hours to reach a moisture content of 2.20%$_{wt}$. One sample was tested again in a static bed, and the other in the fluidised bed cell, both subjected to air at 40°C and a relative humidity of 30%. The fluidisation velocity was adjusted above the minimum fluidisation level at 1.5-1.7m/s. Figure 4.3. shows the comparison in the drying performance between the static and fluidised bed.

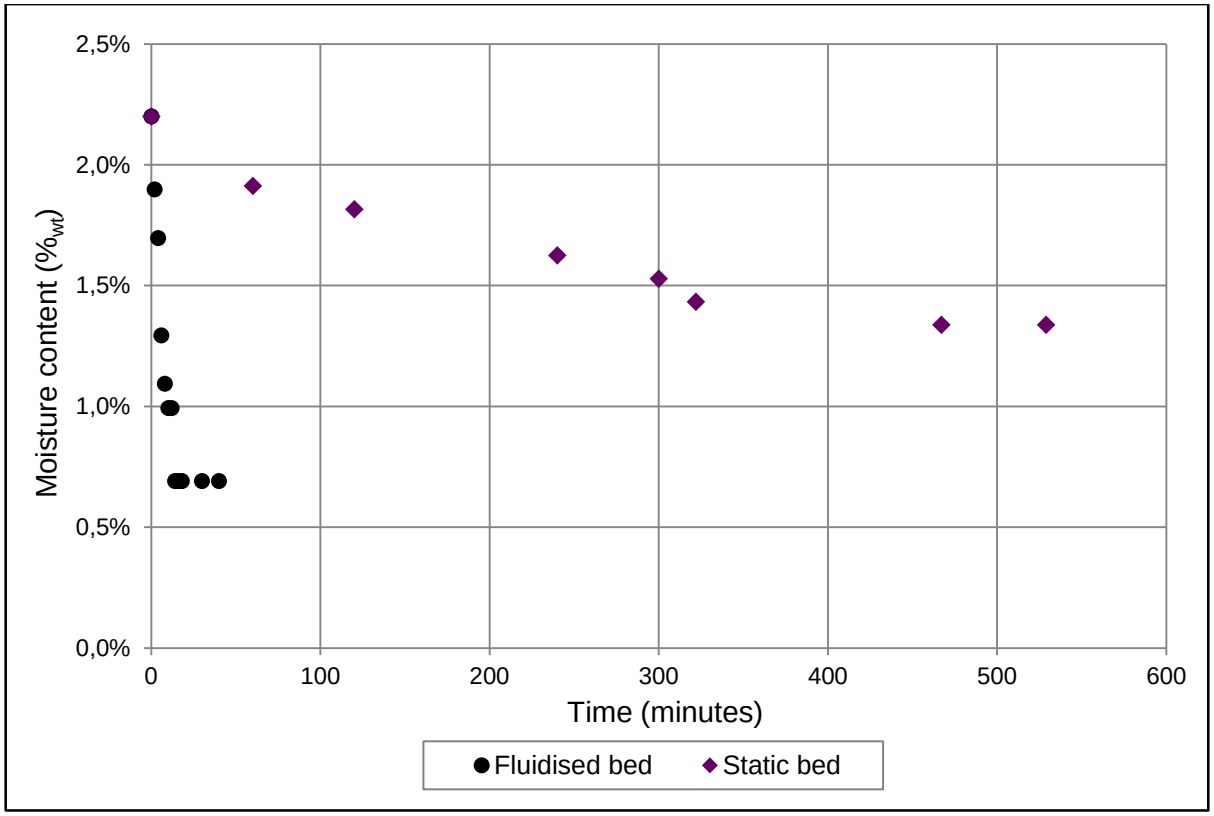

Figure 4.3. Comparison between static and fluidised bed to reduce equilibrium moisture content at 40°C and 30% RH

The coal sample placed at static conditions reached an equilibrium moisture content of 1.34%$_{wt}$ after almost six hours. On the other hand the coal sample placed in the fluidised bed took only 18 minutes before reaching equilibrium at 0.69%$_{wt}$. In addition the fluidising air also caused a lower final equilibrium moisture at a much faster rate, when compared to static conditions.

4.3.2. Airflow and relative humidity of drying air

Filtered fine coal cakes of 100g each and a moisture content of about 25%$_{wt}$ were placed in the climate chamber at 40°C and subjected to various humidity conditions at three levels: 30%, 50% and 70% at static conditions. The tests were run sufficiently long to allow the coal sample to reach its equilibrium moisture content at the chosen conditions. Figure 4.4. shows the influence of relative humidity at static conditions.

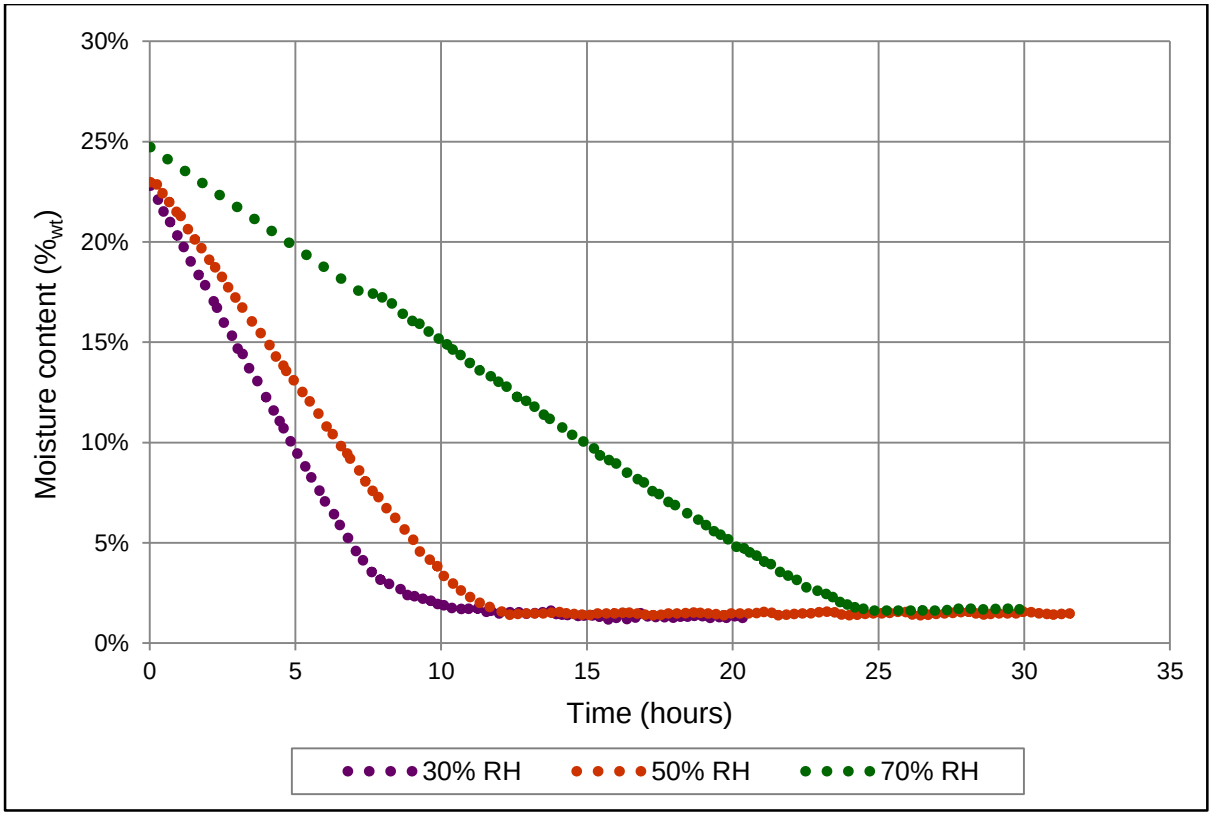

Figure 4.4. Static bed drying of filter cakes at 40°C and various relative humidity conditions

As shown in Figure 4.4, the relative humidity affected the drying rate of the coal quite significantly. Lower humidity conditions and therefore lower partial pressures of the drying air increased its ability to absorb moisture from the wet coal samples at a faster rate. The filter cake sample exposed to 30% relative humidity took about 10 hours to reach equilibrium, whilst the sample exposed to 70% relative humidity was only able to reach equilibrium after 24 hours. The difference between 30% and 50% had a surprisingly small influence on the total drying time. When the air is continually conditioned, the water concentration gradient will stay large enough for diffusion and evaporation. This process will continue until the moisture content is in equilibrium to the surrounding drying air and at that point the moisture content stays constant as shown in Figure 4.4. The final equilibrium moisture consequently correlates to the relative humidity or moisture content of the drying air.

Experimental runs at the same temperature and relative humidity conditions were repeated, but this time in the fluidised bed cell. Again filter cakes of 100g and a moisture content of about 25%$_{wt}$ were fed to the fluidised bed and dried with warm fluidising air at 1.5-1.7m/s and 40°C. The drying air humidifies as it captures moisture from the wet coal particles and therefore, the air entering the fluidised bed was continually conditioned to maintain the process relative humidity. Figure 4.5. shows the drying curves at these process conditions.

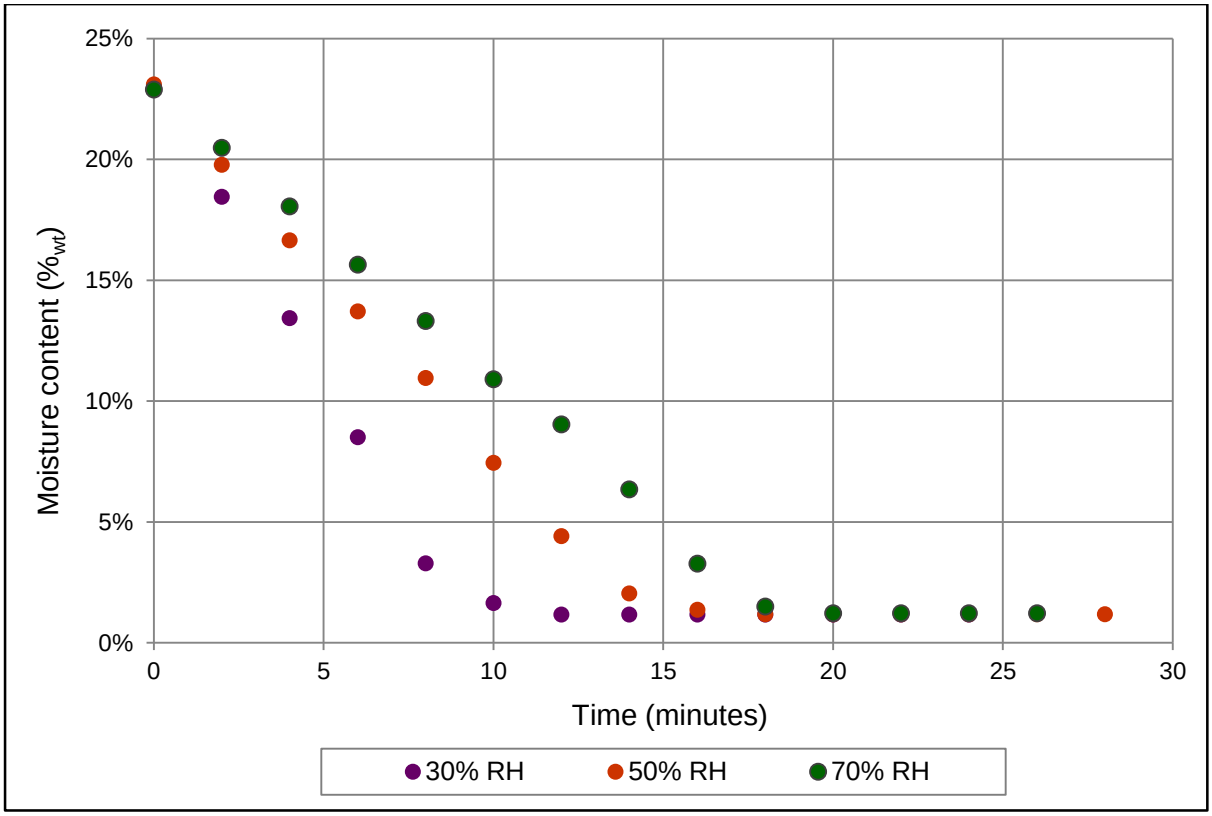

Figure 4.5. Drying of filter cakes in a fluidised bed at 40°C and various relative humidity conditions

Filter cakes dried at 30%, 50% and 70% relative humidity took about 10 minutes, 14 minutes and 18 minutes respectively to dry to its equilibrium moisture content. The drying performance just over minimum fluidisation velocity proved to be more efficient than static conditions without airflow as the drying time in a fluidised bed was 10 minutes to 18 minutes, while drying at static conditions took longer than 10 hours at best.

Introducing airflow to the system lead to a lower moisture content of the coal samples, but also proved to have the ability to increase the drying rate. It was determined that the airflow had the ability to remove more free moisture from the filter cake. In addition more inherent moisture could also be removed by using up flowing air, resulting in a lower equilibrium moisture content. The moisture is ultimately captured by the drying capacity of the upward flowing warm air and transferred away from the wet solid particles (Syahrul *et al*., 2002).

As described in Chapter 2.6., the airflow in the fluidised bed replaces the newly formed vapour with drier (less moist) air. The moisture in the coal is mainly transferred to the drier air containing less moisture, as a result of the large concentration gradient between the wet coal and the dry air. Once the system equilibrium is disturbed again, some of the remaining liquid will undergo a phase change to vapour. This process causes a constant moisture concentration gradient that ultimately leads to faster drying rates.

4.3.3. Airflow rate of drying air

The next set of experiments was completed to demonstrate the extent to which the drying rate was improved by a variation in airflow conditions. Two airflow rates were introduced; one slightly above the minimum fluidisation level at about 0.8-1.1m/s and the other above fluidisation velocity causing vigorous mixing at 1.5-1.7m/s. Wet filter cakes of 100g each and a moisture content of about 25%$_{wt}$ were fed to the fluidised bed operating with warm air at temperatures of 25°C, 40°C and 55°C. The air entering the fluidised bed was conditioned to maintain a relative humidity of 30%. Figure 4.6. shows the drying curves at these conditions. Note that the hollow data points were added for readability and represent the high airflow conditions.

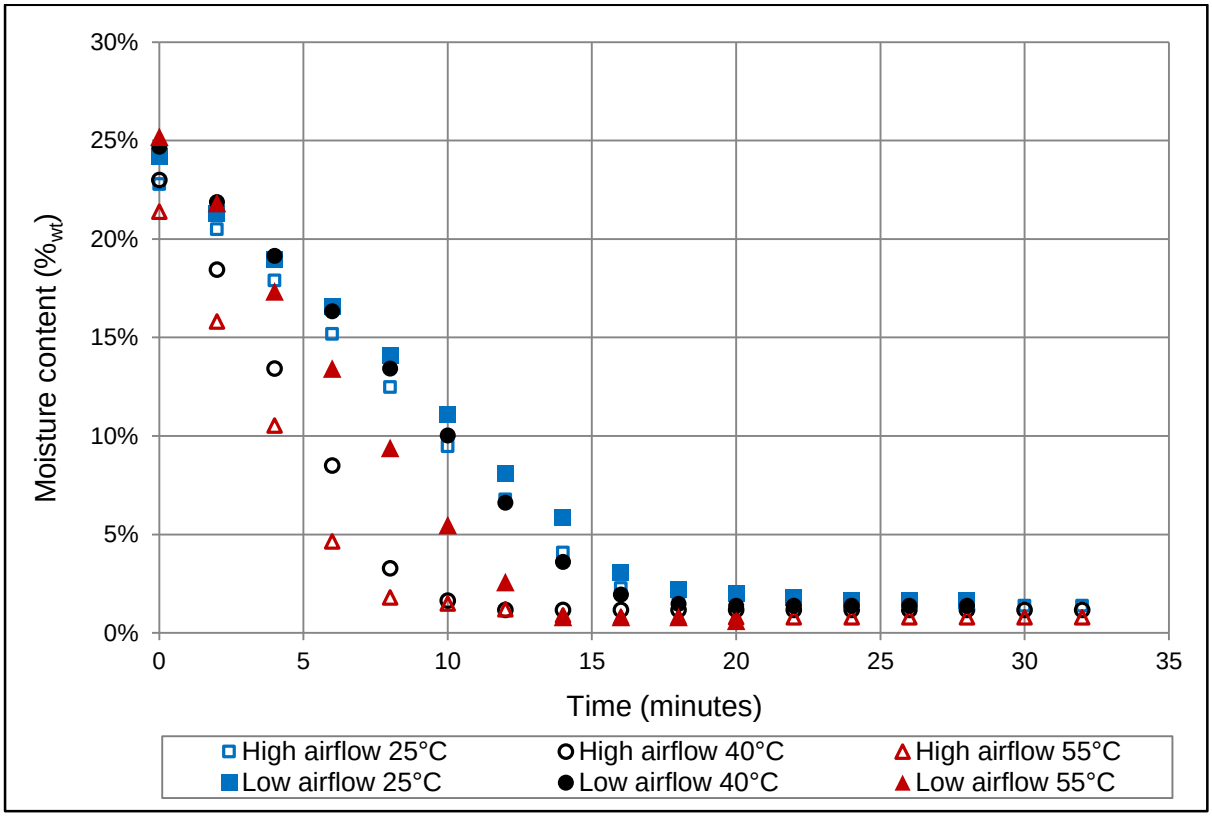

Figure 4.6. Drying of filter cakes at low and high airflow in a fluidised bed at 25°C, 40°C and 55°C and 30% RH

The results from Figure 4.6. indicated that the drying rate of the filter cakes placed in the fluidised bed was improved significantly when using high airflow rates. However this only seemed to be true for the higher temperatures of 40°C and 55°C. The difference in the drying rate between the low and high airflow conditions at 25°C, proved to be so small that it falls within experimental error. The high airflow rate at 25°C proved to have a similar drying rate than the samples dried at low airflow conditions.

As described in Chapter 2.6., an increase in the air velocity will bring forth a larger drag force on the particles and more of the particles will break loose from the wet sample to be fluidised (Syahrul *et al*., 2002). An increase in the airflow rate caused vigorous mixing that most likely caused more interaction between the drying air and the wet solid particles. As a result, more moisture was captured and transferred away by the up flowing drying air, leading to a faster drying rate. Furthermore the higher airflow was also able to replace the newly formed vapour with drier air at a much faster rate. Therefor the higher airflow caused the system to reach a concentration gradient more rapidly resulting in a faster drying rate.

4.3.4. Temperature of drying air

The drying curves at 25°C, 40°C and 55°C were compared at each relative humidity condition, to investigate the effect of the drying air temperature. Figure 4.7. shows the influence of temperature on the drying rate at 30% relative humidity and a high airflow rate. The results were similar at relative humidity conditions of 50% and 70% and the results thereof can be found in Appendix B.

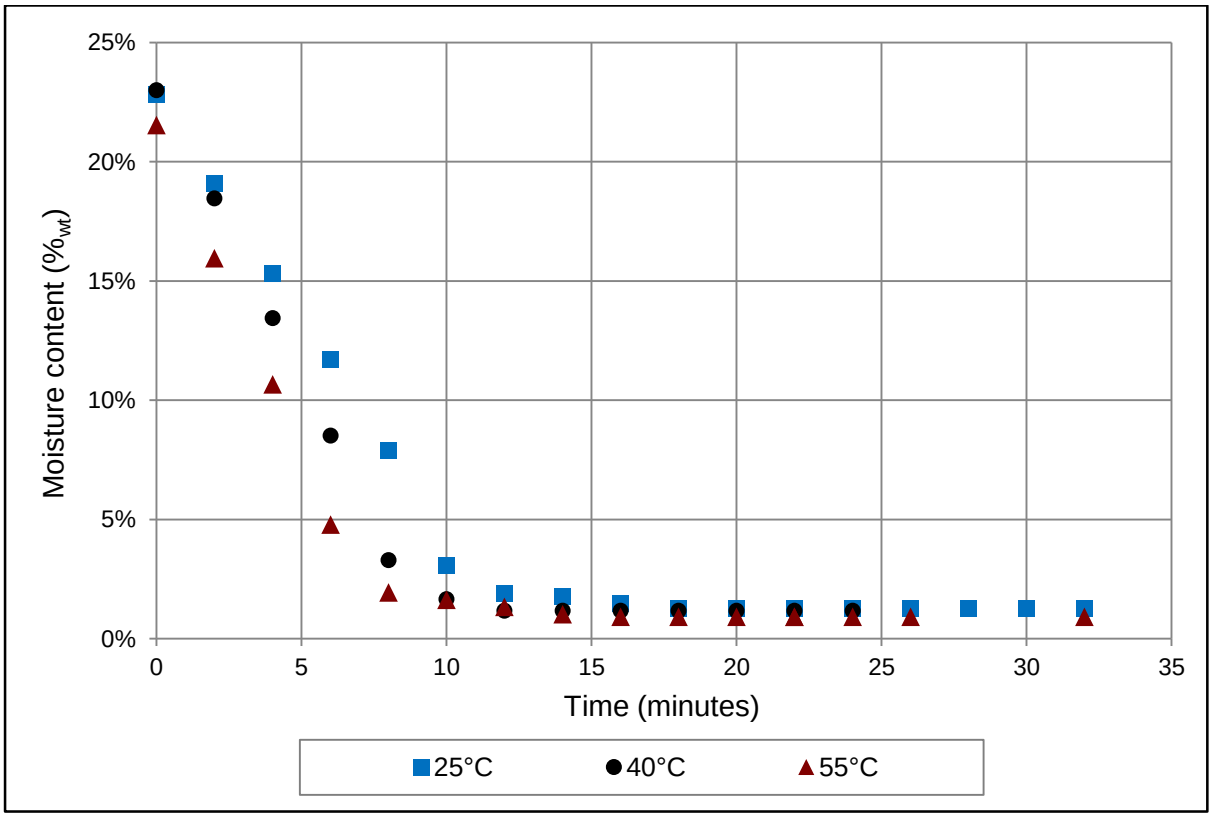

Figure 4.7. Drying of filter cakes in a fluidised bed at 25, 40 and 55°C and 30% RH

The results from Figure 4.7. showed that the drying rate for all three temperatures were similar. The small changes in the drying rates indicated that an increase in temperature led to an increase in the drying rate. However, there were only small changes in the drying rate mainly due to the fact that only temperatures below 60°C were used, thus not using high temperatures as a driving force for more dewatering. In addition the minor temperature difference between these temperatures below 60°C, led to similar drying rates. It could therefore be concluded that the rate of mass transfer in the pores was limiting and the temperature was not changed significantly.

4.3.5. Influence of temperature and relative humidity

This section of work focuses on determining the influence of the temperature as well as relative humidity on the drying rate. The filter cakes of 100g each and a moisture content of about 25%$_{wt}$ were fed to the fluidised bed operating with warm air at 25°C, 40°C and 55°C. The air entering the fluidised bed was conditioned to maintain a relative humidity of 30% and 50% with an airflow rate of 1.5-1.7m/s. Figure 4.8. shows the influence of temperature and humidity on the drying rate. Note that the hollow data points were added for readability and represent the data of 30% relative humidity.

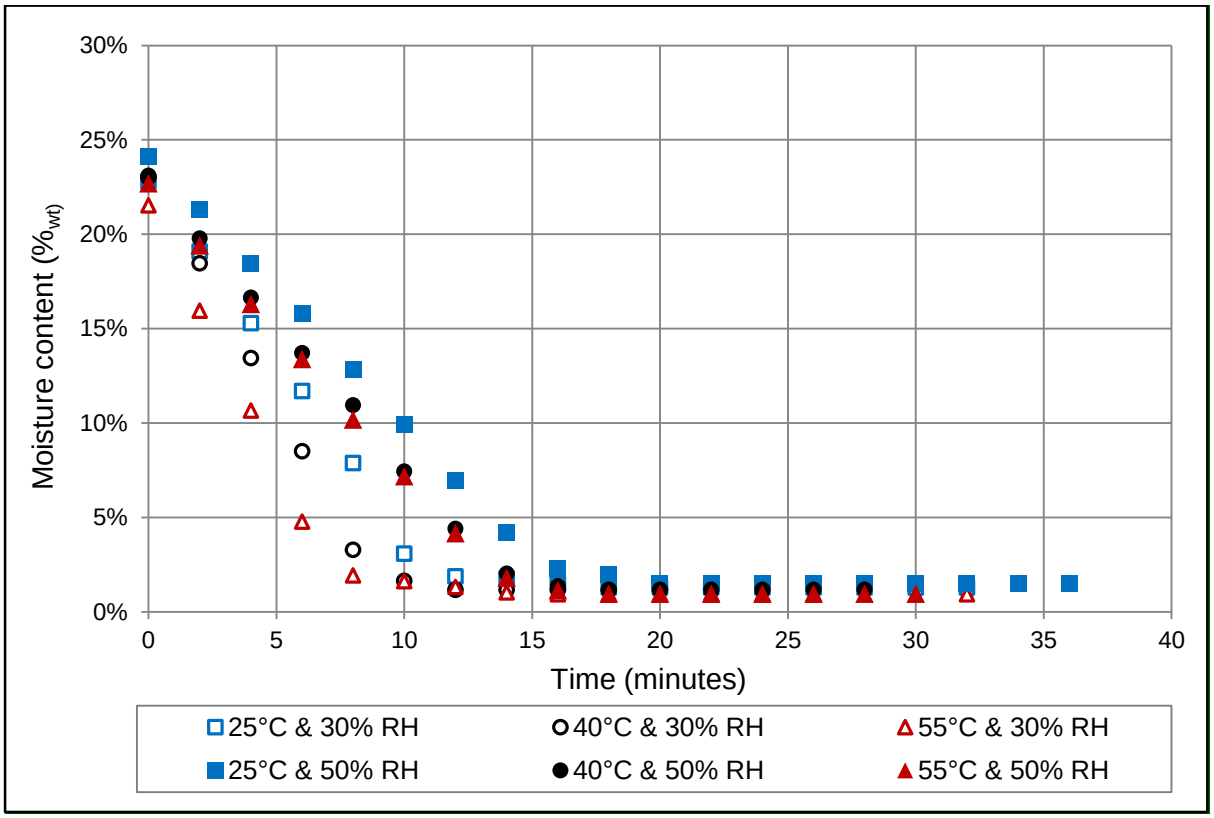

Figure 4.8. Drying of filter cakes in a fluidised bed at 25°C, 40°C and 55°C and 30 and 50% RH

The results yielded a better idea whether the temperature or relative humidity contributed the most to the drying rate. The lower relative humidity of 30% showed to increase the drying rate compared to the 50% relative humidity condition. This is expected as lower humidity conditions and thus lower partial pressures of the drying air increases its ability to absorb moisture from the wet coal sample at a faster rate.

It was clear that the drying rate for all three temperatures was alike at both relative humidity conditions however more so for the 50% relative humidity. The small changes in the drying rates indicated that an increase in temperature led to an increase in the drying rate across both humidity conditions, which is similar to the results in Section 4.3.4. In addition it was also clear that the drying rates in the fluidised bed were much less sensitive to the temperature just as it was to relative humidity.

4.3.6. Conclusions about the operating parameters

According to Asmatulu & Yoon (2012) dewatering of fines primarily relies on the efficiency of the air phase replacing the moisture. High airflow with lower partial pressures proved to be able to absorb more moisture from the fines, without using high temperatures to evaporate the water from the fine coal. It was clear that between temperature and airflow rate that variations in airflow rate was a bigger contributor to the faster drying rates. However, the elevated temperatures increased the drying rate at the higher airflow conditions.

In conclusion it was proven that the airflow and relative humidity of the drying air contributed to faster drying rates. The temperature didn't prove to have such a big contribution, however higher temperatures did increase the drying rate for higher airflow and lower humidity conditions.

4.4. Repeatability tests

A series of experiments in the fluidised bed were repeated in order to test the reproducibility of the experiments runs. The fluidised bed and the experimental procedures proved to deliver results that fall in a very narrow range from one another.

The average was determined using Equation 4.3 and the standard deviation for every data point was determined by Equation 4.4. Where x is a data point, $\bar{x}$ is the average, n is the amount of runs and S is the standard deviation.

$$\bar{x} = \frac{\sum_1^n x_i}{n} \quad \textbf{(4.3)}$$

$$S = \sqrt{\frac{1}{n-1}\sum_{1}^{n}(x_i - \bar{x})^2} \quad \textbf{(4.4)}$$

The average and standard deviation was calculated for every time interval. Only tw repeatability tests are shown in this chapter and the rest of the results can be found in Appendix B.

The maximum standard deviation was 2.39%$_{wt}$ and the minimum standard deviation was 0.05%$_{wt}$. The repeatability results can be found in Figure 4.9. and the lower and upper limits shown in Figure 4.9. are the standard deviation from the average between the two experiments.

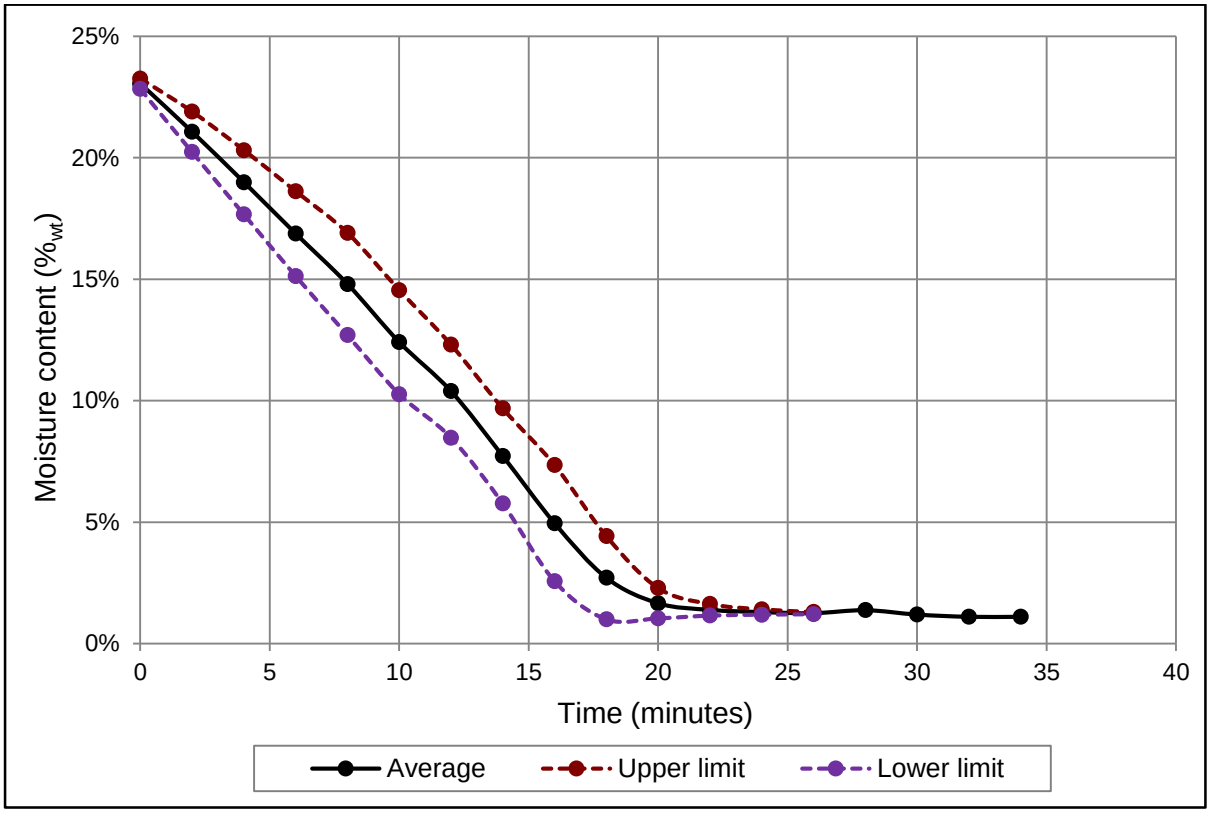

Figure 4.9. Average and standard deviation of repeats done at 40°C and 70% RH

The calculated results of the experimental run with the smallest range of deviation can be seen in Figure 4.10. The maximum standard deviation was 1.13%$_{wt}$ and the minimum standard deviation was 0.06%$_{wt}$.

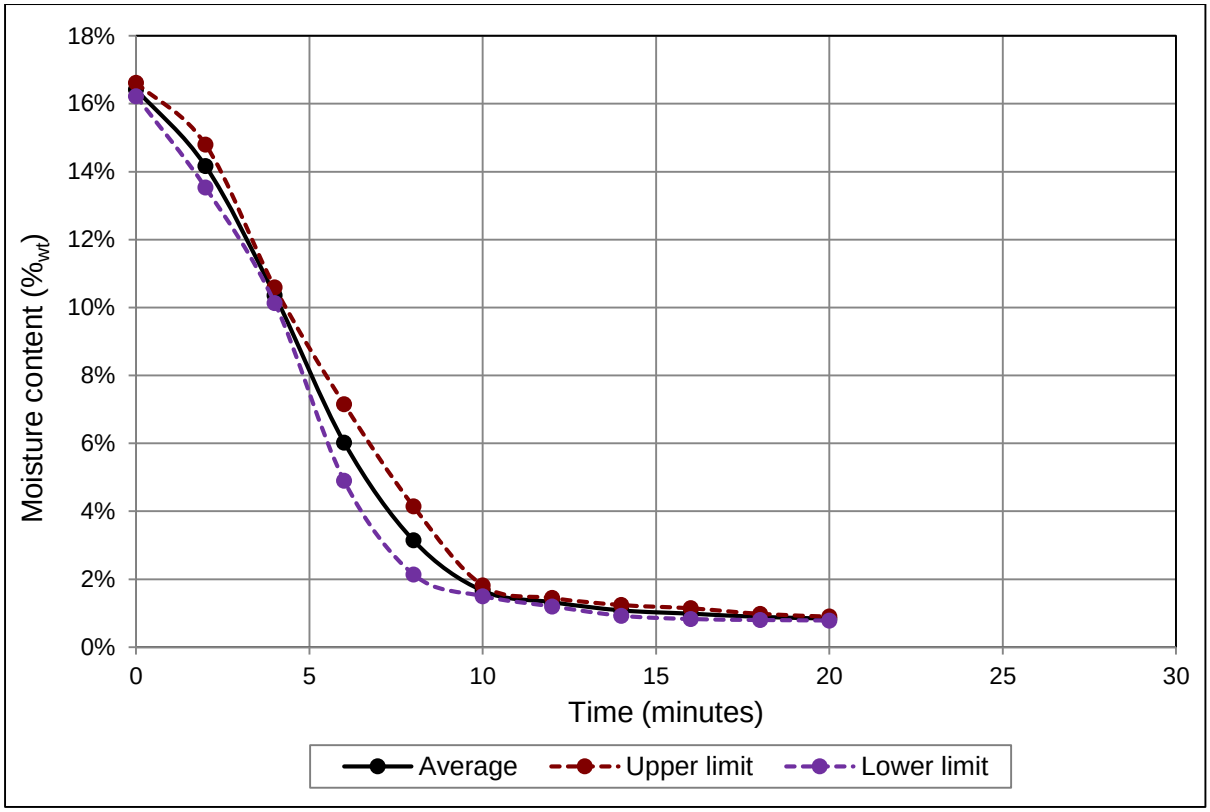

Figure 4.10. Average and standard deviation of repeats done at 55°C and 50% RH

A confidence interval, σ, of 95% was chosen and Equation 4.5 is an excel® function that was used to determine the Z-interval. The percentage error was calculated using Equation 4.6.

$$Z_{interval} = CONFIDENCE(1-\sigma, S, n) \quad \textbf{(4.5)}$$

$$\%\ Error = \left(\frac{2\,(Z_{interval})}{\bar{x}}\right)100 \quad \textbf{(4.6)}$$

With the repeated experiments the minimum error was 0.03% and the maximum error was 1.75%, both within a confidence interval of 95%.

4.5. Model fit and drying performance

This section focuses on determining the drying rate for the experiments completed in order to compare the efficiency of all the operating conditions. These include the temperatures, relative humidity and airflow conditions. The results from Section 4.3. showed that the drying rates for the coal samples dried in the fluidised bed were all linear as illustrated by the solid line in Figure 4.9. In addition, the drying rate was linear up until it reached a point within the range between 1-2%$_{wt}$ from the final equilibrium moisture content. This is shown by the dotted line in Figure 4.11. At this point the drying rate slows down to such an extent that it seems to be a near-constant drying rate.

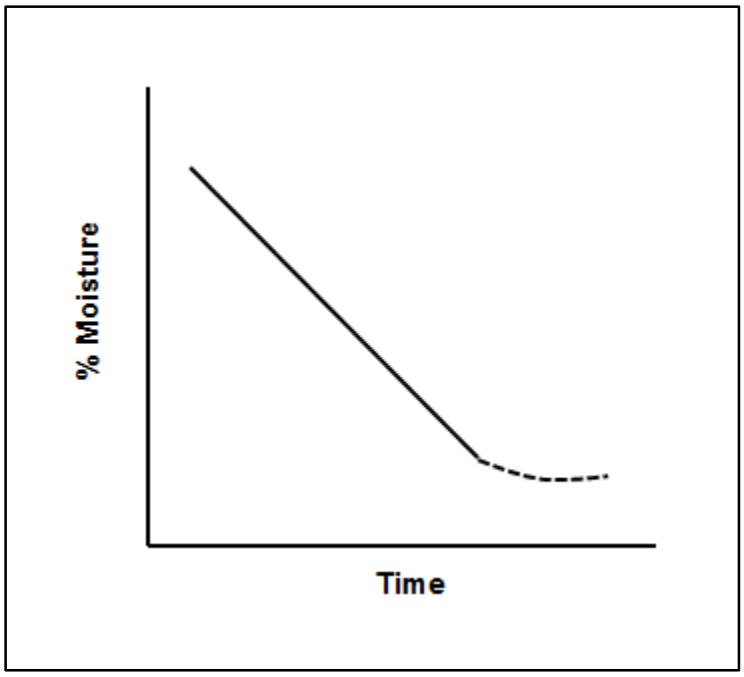

Figure 4.11. Diagram for reaction rate

As described by Fogler (2006), the linear part of the drying rate is a typical zero-order drying model. This means that the rate of drying is independent of the moisture content in the coal sample. The drying rate is just the removal of moisture per unit time and can be illustrated by Equation 4.7 and the integrated form can be seen in Equation 4.8. Where r is the drying rate, t is the time, k is the drying rate coefficient, $[\%\, moisture]_t$ is the moisture at a specific time and $[\%\, moisture]_0$ is the initial moisture content.

$$r = -\frac{d[\%moisture]}{dt} = k \quad \textbf{(4.7)}$$

$$[\%\, moisture]_t = kt + [\%moisture]_0 \quad \textbf{(4.8)}$$

Table 4.1. gives the drying times needed to reach an equilibrium moisture content for all the samples placed in the fluidised bed at all the temperatures, humidity and airflow conditions. The minimum fluidisation airflow rate was about 0.8-1.1m/s and the high airflow fluidisation velocity causing vigorous mixing was 1.5-1.7m/s.

Table 4.1. Drying times (min) in the fluidised bed needed to reach equilibrium moisture content

Temperature	Low airflow	High airflow		
	30% RH	30% RH	50% RH	70% RH
25°C	16	12	16	20
40°C	16	10	14	18
55°C	14	8	14	20

The lowest drying times were at high airflow conditions with a relative humidity of 30%. Lower humidity conditions and thus lower partial pressures of the drying air increased its ability to absorb moisture from the wet coal samples at a faster rate. The drying times at 70% relative humidity are even slower than for the samples dried with a lower airflow rate.

The results of the drying rates, as calculated by Equation 4.7, can be found in Table 4.2. Note that as indicated by Equation 4.7 that the drying rate is equal to the drying rate coefficient as well.

Table 4.2. Drying rates or drying rate coefficient (%moisture/min) in the fluidised bed

Temperature	Low airflow	High airflow		
	30% RH	30% RH	50% RH	70% RH
25°C	0.013	0.018	0.014	0.011
40°C	0.015	0.023	0.015	0.012
55°C	0.018	0.025	0.015	0.011

Figure 4.12. shows how well the zero-order drying model predicted the experimental data for a filter cake dried in a fluidised bed at 40°C and 30% relative humidity. Results of the remaining drying model fits can be found in Appendix B.

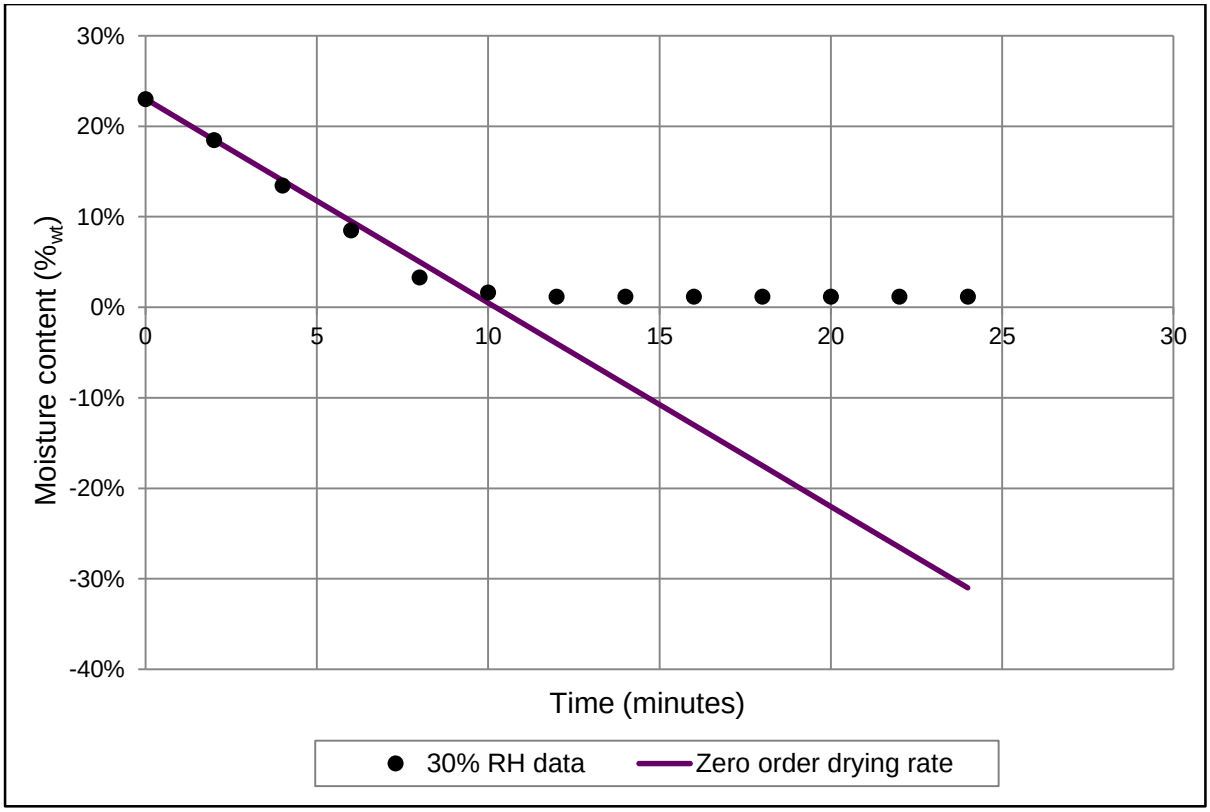

Figure 4.12. Comparison between drying models and experimental data

It is clear from the data plots in Figure 4.12. that the zero-order drying model was only able to predict the linear part of the experimental data. When the drying rate decreases at a point near the final moisture content, the drying model was no longer applicable. However the zero-order drying model is useful to predict the first part of the drying rate and moisture content of samples dried at various conditions. It can also give an indication of what the final moisture content of the bulk coal sample would be as it is able to predict the moisture up to about the equilibrium moisture content.

Figure 4.13. is a bar diagram to compare the drying rates for all the conditions tested in the fluidised bed. Higher temperatures of 40°C and 55°C resulted in faster drying rates at the lower relative humidity conditions of 30%. An increase in temperature did lead to an increase in the drying rate for higher airflow and lower humidity condition of 30%. Then again as the relative humidity increased to 50% and 70%, the increase in temperature did not have a large influence. During the experimental work it was noticed that at the high relative humidity and temperature conditions, the climate chamber and fluidised bed was filled with condensate that got trapped, especially on the sides of the vessel. The system had to remove the condensate as well as remove the moisture from the coal and this could be a reason for the slower drying rate at these conditions.

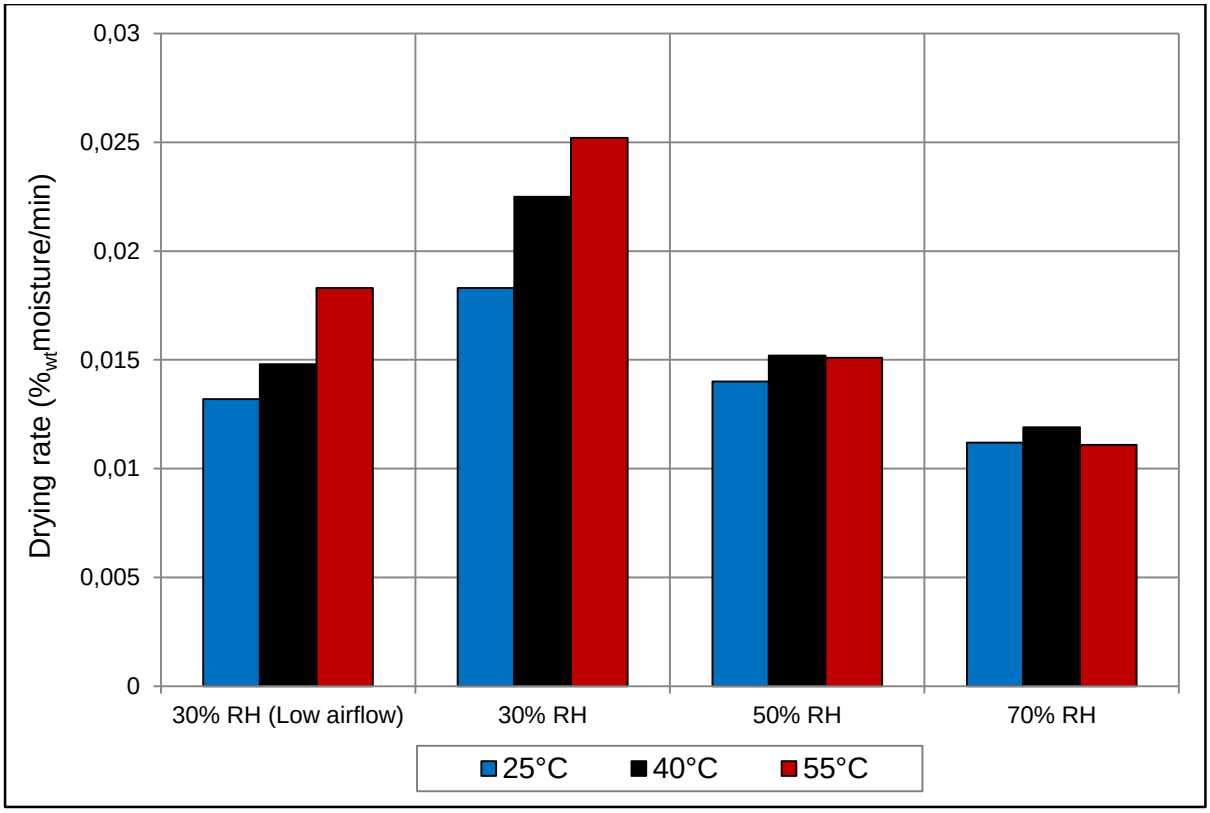

Figure 4.13. Comparison between drying rates in the fluidised bed

In terms of the fastest drying time and drying rate in the fluidised bed, it was concluded that the most efficient condition is airflow above minimum fluidisation point causing vigorous mixing and maximum contact with the drying air. In addition to the high airflow it was concluded that 30% relative humidity and 55°C resulted in the fastest drying time. However this is not necessarily the most energy efficient conditions. A study on the energy needed for drying at all the above mentioned conditions will be conducted and discussed in Chapter 5.

Results from Du Preez (2012) showed that the release of moisture from coal at controlled temperature and relative humidity conditions without airflow was linear. Levy *et al.* (2006) also did a study on drying of wet fine coal in a bubbling fluidised bed at temperatures ranging from 43°C to 60°C and a range of relative humidity conditions. Coal with a size distribution of between -4mm+0.3mm was used at high airflow conditions causing bubbling. The results showed that the drying rate in the bubbling fluidised bed was also linear until it reached a point near the final moisture content. It was also shown that there is a linear correlation between the drying rate and an increase in the airflow. In addition it was proved that increasing the airflow rate resulted in a higher drying rate.

4.6. Effect of coal characteristics and properties on the drying rate

Two bulk coal samples, one vitrinite rich and the other inertinite rich, were conditioned at 25°C and 80% RH for about two hours to reach equilibrium moisture content. Each sample was placed onto the balance in the climate chamber consecutively. The relative humidity was reduced in a stepwise manner, in steps of 10% from 80% down to 30%. This was done at 40°C and static conditions without airflow. The moisture content was determined after equilibrium moisture content was reached at each step as shown in Figure 4.14.

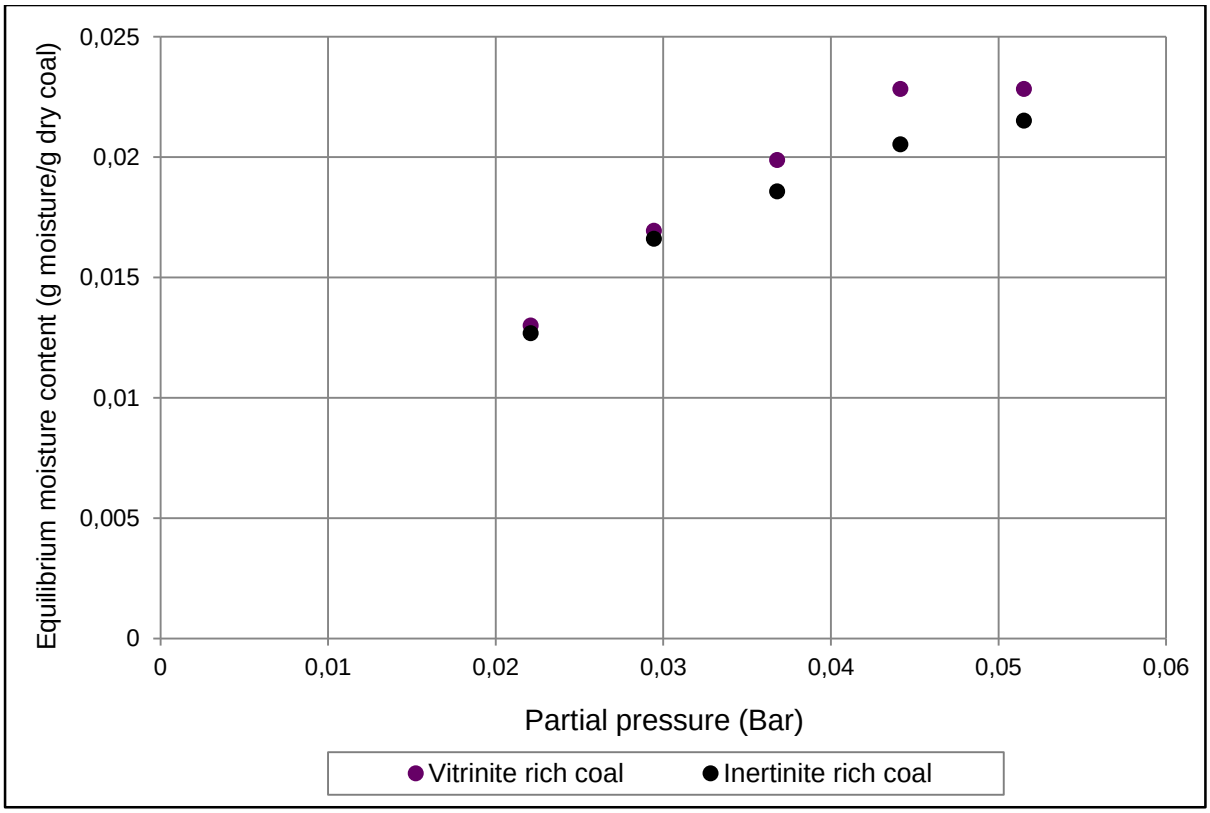

Figure 4.14. Desorption isotherm of vitrinite and inertinite rich coal samples at 40°C and a humidity range of 70% to 30%

The results yielded a better understanding of how these two coal types responded in the same conditions, before introducing airflow. The phase change is driven by an increase or decrease in the vapour pressure of the water surrounding the coal particles. The results from Figure 4.14. show that a decrease in the relative humidity led to a lower moisture content for both the vitrinite and inertinite rich coal. It can be seen from Figure 4.14. that at low relative humidity conditions both coal samples contained nearly the same moisture and as the moisture in the surrounding air increased, a bigger difference in the moisture uptake between the two coal samples could be noted. Furthermore the vitrinite rich coal was able to absorb more moisture than the inertinite rich coal at all relative humidity conditions.

Asmatulu & Yoon (2012) stated that finer particles are more difficult to dewater mainly because they have a larger surface area compared to coarser particles. The larger surface area creates surface and capillary forces that prevent the moisture from leaving the finer coal particles. The vitrinite rich coal had more fine particles in the sample compared to the inertinite rich coal, which could be the reason for the higher moisture content. According to Van der Merwe & Campbell (2002) finer particles will not only absorb more moisture, but will also lead to a faster moisture uptake rate.

In addition the vitrinite rich coal also had a higher mineral matter content. Van der Merwe & Campbell (2002) also observed that a higher mineral matter content in fine coal resulted in a higher moisture uptake as the mineral matter acts as a hydrophilic site. Work done by Rong & Hitchins (1995) as well as Du Preez (2012) proved that mineral matter and especially clay type minerals in coal is the main reason for moisture absorption. It is likely that the vitrinite-rich coal retained moisture, because of its high clay content.

As the relative humidity was lowered from 70% to 30% the vitrinite rich coal held on to the moisture mainly due to its high mineral matter content and finer particles. The inertinite rich coal was more porous and showed to release the moisture when relative humidity was lowered from 70% to 30%. The pores made it possible for drying air to percolate through the samples. Rong & Hitchins (1995) did a study on the dewatering of fine coal and also found that a higher porosity made it possible for more water to be released from the coal, depending on the type porosity.

The next set of experiments were completed to determine the influence of coal characteristics and properties of vitrinite as well inertinite rich coals on the drying rate, but at this stage airflow was introduced. The same tests were repeated in the fluidised bed cell, but this time introducing high airflow above minimum fluidising velocity at about 1.5-1.7 m/s causing vigorous mixing. Filter cakes of 100g and a moisture content of about 25%$_{wt}$ were fed and dried in a fluidised bed with warm air at 40°C. The air entering the fluidised bed was controlled at relative humidities of 30%, 50% or 70%. Table 4.3. gives the comparison between the drying rates.

Table 4.3. Drying rates (%moisture/min) in the fluidised bed at 40°C

Coal sample	30% RH	50% RH	70% RH
Inertinite rich coal	0.0225	0.0152	0.0119
Vitrinite rich coal	0.0218	0.0125	0.0101

The inertinite rich coal released more moisture at a faster rate compared to the vitrinite rich coal. This confirms the results that were also found at static conditions, where the inertinite rich coal also released more moisture. It is presumed that due to the fact that the inertinite rich coal is more porous and contains less mineral matter and finer particles, it was able to release moisture at a faster rate. This is also proved by the results showed in Table 4.4.

Table 4.4. Final moisture content ($\%_{wt}$) of samples dried in the fluidised bed at 40°C

Coal type	30% RH	50% RH	70% RH
Inertinite rich coal	1.16	1.18	1.23
Vitrinite rich coal	1.66	1.55	1.89

The inertinite rich coal was able to release more moisture and ended up with a lower final moisture content after drying in the fluidised bed. However the vitrinite rich coal contained more moisture after drying at the same conditions.

4.7. Effect of initial moisture content on the drying rate

Filter cakes of 100g each and a moisture content of about $15\%_{wt}$ as well as $25\%_{wt}$ were dried in a fluidised bed with warm air at 55°C and a relative humidity of 50%. Figure 4.15. shows the drying curves at these conditions and gives an indication of how the initial moisture content influences the drying rate and final moisture content.

The samples with the lower moisture and higher moisture content took about 10 minutes and 20 minutes, respectively, to dry to their final equilibrium moisture values. Both samples had similar final moisture contents, which would make sense as both were inertinite rich coal with similar characteristics and properties. It also proved that the initial moisture content didn't affect the final moisture content as the moisture just shifted from the wet coal to the drier flowing air, until the samples reached their final moisture contents.

Calculations show that the drying rate of the sample with the lower moisture content was $0.0144 \frac{\%\, moisture}{min}$ and the drying rate of the sample with the higher moisture content was $0.0143 \frac{\%\, moisture}{min}$. Both curves in Figure 4.15. showed to have similar drying rates. As stated in Section 4.4 the linear part of the drying rate is a typical zero-order reaction. This means that the rate of drying is independent of the initial moisture content in the coal sample as can be seen in Figure 4.15.

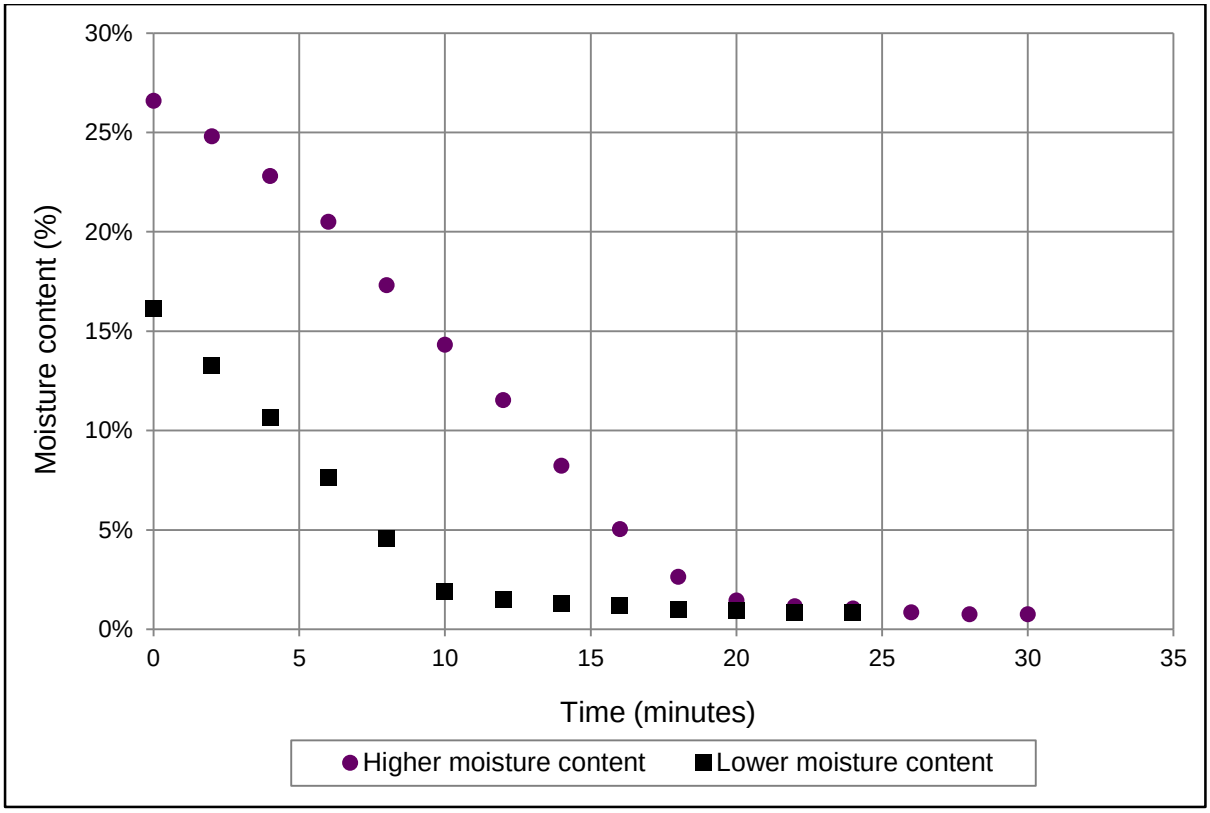

Figure 4.15. Drying of 15%$_{wt}$ and 25%$_{wt}$ filter cakes in a fluidised bed at 55°C and 50% RH

4.8. Observations during the drying process

Some non-ideal fluidising conditions occurred in tests using the fluidised bed. One example is where the wet coal particles get stuck to the side of the fluidising vessel. It was noted during the experimental work that the airflow wasn't able to sufficiently dry the particles that became attached to the side of the cylinder. This occurrence is explained in Appendix B.

The filter cakes that were dried in the fluidised bed were a wet heap at the beginning of the experiment and the particles did not move with the up flowing air. It was observed during the experimental run that some of particles, as well as clusters of particles, broke away from the wet heap and flowed upwards with the drying air. This started happening when the bulk coal sample reached a moisture content of about 15%$_{wt}$. When the bulk moisture content got to a point of between 5-7%$_{wt}$, the entire sample was able to be suspended in the up flowing air. Terblanche (2011) as well as Willemse (2011) studied density separation of fine coal with other fluidised bed apparatus, at the North-West University. They also found that complete and effective density separation is only possible with fine coal with a moisture content of about 5%$_{wt}$. It was therefore proven that drying in the fluidised bed could be possible to such an extent that effective density separation can follow the drying process.

4.9. Conclusion

Introducing airflow to the system led to a lower moisture content in the coal samples, but also proved to have the ability to increase the drying rate. It was determined that the airflow had the ability to remove more free moisture from the filter cake. In addition more inherent moisture could also be removed by using upward flowing air, resulting in a lower equilibrium moisture content. In conclusion it was proven that the airflow and relative humidity of the drying air contributed to faster drying rates. The temperature did not prove to have a big contribution, however higher temperatures did increase the drying rate for higher airflow and lower humidity conditions.

The larger surface areas of particles create surface and capillary forces that prevent the moisture from leaving the finer coal particles. A higher mineral matter content in fine coal resulted in a higher moisture uptake. A higher porosity made it possible for more water to be released from the coal samples.

The linear part of the drying rate is typical zero-order drying model. This means that the rate of drying is independent of the moisture content in the coal sample. In terms of the fastest drying time and drying rate in the fluidised bed, it was concluded that the most efficient condition is airflow above minimum fluidisation point causing vigorous mixing and maximum contact with the drying air. In addition to the high airflow it was concluded that 30% relative humidity and 55°C resulted in the fastest drying time.

CHAPTER 5 – ENERGY CONSIDERATIONS

5.1. Introduction

From Chapter 4.5. it was concluded that the fastest drying rate was at 30% relative humidity and 55°C, at high airflow conditions. However these are not necessarily the most energy efficient conditions and therefore this chapter focuses on the energy considerations made. This means that the energy required for the drying process should be less than the energy gained by improving the calorific value of coal. The total energy required for the drying process included the following variables:

- Phase change of water for evaporation including change in the enthalpy of the water
- Conditioning of the air by the climate chamber
- Work done by the blower

The total energy consumption was determined for coal dried to a moisture content of 10%$_{wt}$, 5%$_{wt}$ and lastly to its inherent moisture content. This information gives an indication whether energy consumption for drying is effective when drying up to certain moisture content, specifically by taking the improvement of calorific value into consideration. In conclusion the energy consumption was compared to other drying technologies.

5.2. Energy required for the drying process

To begin this energy study, an analysis was done to determine how much energy is required to condition air at various temperature and humidity conditions. This is only for the changes in the air and water system during drying in order to give an indication of which conditions might lead to a higher or lower power requirement by air conditioning systems. Thereafter the energy required by the climate chamber and blower was determined for each test run to dry the inertinite coal samples to its inherent moisture. Finally a comparison was done on the total energy required for drying wet coal samples to a variety of final moisture contents.

5.2.1. Conditioning of air

First and foremost a psychrometric chart was used to determine the enthalpy needed to condition the air at specific temperature and humidity conditions. The results thereof are given in Table 5.1.

Table 5.1. Enthalpy at specific temperature and humidity conditions (kJ/kg dry air)

Temperature	30% RH	50% RH	70% RH
25°C	40.14	50.30	60.59
40°C	75.98	100.73	126.24
55°C	134.46	191.71	252.96

The enthalpy for air at an average room temperature of 25°C and average relative humidity of 50%, was 50.3 $\frac{kJ}{kg\ dry\ air}$. These are the average conditions for South Africa during summer time and this enthalpy value was used for further calculations. Equation 5.1 was used to determine the delta enthalpy, $\widehat{H}$, at saturation needed to condition the air from the average room temperature and relative humidity. The results can be found in Table 5.2.

$$\Delta \widehat{H} = \widehat{H}_2 - \widehat{H}_1 \quad \textbf{(5.1)}$$

Table 5.2. Delta enthalpy at saturation (kJ/kg dry air)

Temperature	30% RH	50% RH	70% RH
25°C	-10.16	0.00	10.29
40°C	25.68	50.43	75.95
55°C	84.16	141.41	202.66

The humid volume, $\hat{V}_H$, was determined by using the psychrometric chart as well. The data represents the volume occupied by 1kg of dry air including the water vapour that accompanies the dry air. The results can be found in Table 5.3.

Table 5.3. Humid volume (m^3/ kg dry air)

Temperature	30% RH	50% RH	70% RH
25°C	0.85	0.86	0.86
40°C	0.91	0.92	0.93
55°C	0.97	1.01	1.04

The total volume or air that needed to be conditioned includes the volume in the climate chamber, fluidised bed as well as in the pipes. The calculations of the volumes are given by Equation 5.2 to 5.4 and the total volume can be calculated by Equation 5.5.

$$Volume_{climate\ chamber} = 100L = 0.1m^3 \quad \textbf{(5.2)}$$

$$Volume_{fluidised\ bed} = \frac{\pi}{4} D^2 h = \frac{\pi}{4} (0.1m)^2 \cdot 0.6m = 0.005\ m^3 \quad \textbf{(5.3)}$$

$$Volume_{pipes} = = \frac{\pi}{4} D^2 h = \frac{\pi}{4} (0.05m)^2 \cdot 1m = 0.002\ m^3 \quad \textbf{(5.4)}$$

$$Volume_{total} = Volume_{climate\ chamber} + Volume_{fluidised\ bed} + Volume_{pipes} = 0.152m^3 \quad \textbf{(5.5)}$$

Equation 5.6 was used to determine the mass of dry air in the system, while Equation 5.7 was used to determine the energy needed to condition the air. The results can be found in Table 5.4.

$$m_{DA} = \frac{1}{\hat{V}_H} \cdot V_{DA} \quad \textbf{(5.6)}$$

$$Q_i = m_{DA} \cdot \Delta\hat{H} \quad \textbf{(5.7)}$$

Table 5.4. Energy (kJ) needed to condition the drying air

Temperature	30% RH	50% RH	70% RH
25°C	-1.81	0.00	1.81
40°C	4.31	8.34	12.36
55°C	13.14	21.36	29.56

The climate chamber was able to reach low temperatures of 25°C, 40°C and 55°C within minutes. It was, however more demanding for the climate chamber to reach the prescribed humidity conditions. Humidity is a function of temperature and by controlling the temperature to set point, the relative humidity changed accordingly. The climate chamber conditioned the air temperature to a set point first and thereafter the relative humidity. Consequently it took about 10 minutes to reach the set point temperature and relative humidity of 50% and 70%. The climate chamber was only able to reach a 30% relative humidity after about 20 minutes.

In addition it was also assumed that the amount of energy needed during the course of the experiment was equivalent to the energy needed for pre-conditioning to reach the set point temperature and relative humidity. The temperature changed as the blower added extra heat to the system in addition the relative humidity also changed as the moisture from coal samples was captured into the drying air. Therefore the total time required to condition the air was determined by the sum of time needed to condition the air prior to the experiment and during the experiment, as illustrated by Equation 5.8. The total time required to condition the air for each test run can be found in Table 5.5.

$$t_{total} = t_{pre-conditioning} + t_{experiment} \quad \textbf{(5.8)}$$

Table 5.5. Time (min) required for conditioning of air

Temperature	Low airflow	High airflow		
	30% RH	30% RH	50% RH	70% RH
25°C	36	32	26	30
40°C	36	30	24	28
55°C	34	28	24	30

After the pre-conditioning of the air, the experimental run took place and some experiments took place with low airflow rates and others with higher airflow rates. The experimental runs using lower airflow rates took longer than those with higher airflow.

The power needed for conditioning the air was calculated with Equation 5.9., where W_i is the power in $Watt$ or in $\frac{J}{S}$ and t is the time in $seconds$. The results can be found in Table 5.6.

$$W_i = \frac{Q_i}{t} \quad \textbf{(5.9)}$$

Table 5.6. Power (Watt or J/s) needed to condition the air

Temperature	Low airflow	High airflow		
	30% RH	30% RH	50% RH	70% RH
25°C	-0.84	-0.94	0.00	1.01
40°C	1.99	2.39	5.79	7.36
55°C	6.44	7.82	14.83	16.42

Figure 5.1. gives a comparison between the amount of energy required at various temperatures and relative humidity conditions. The results give a better understanding of the energy needed for air water system during drying.

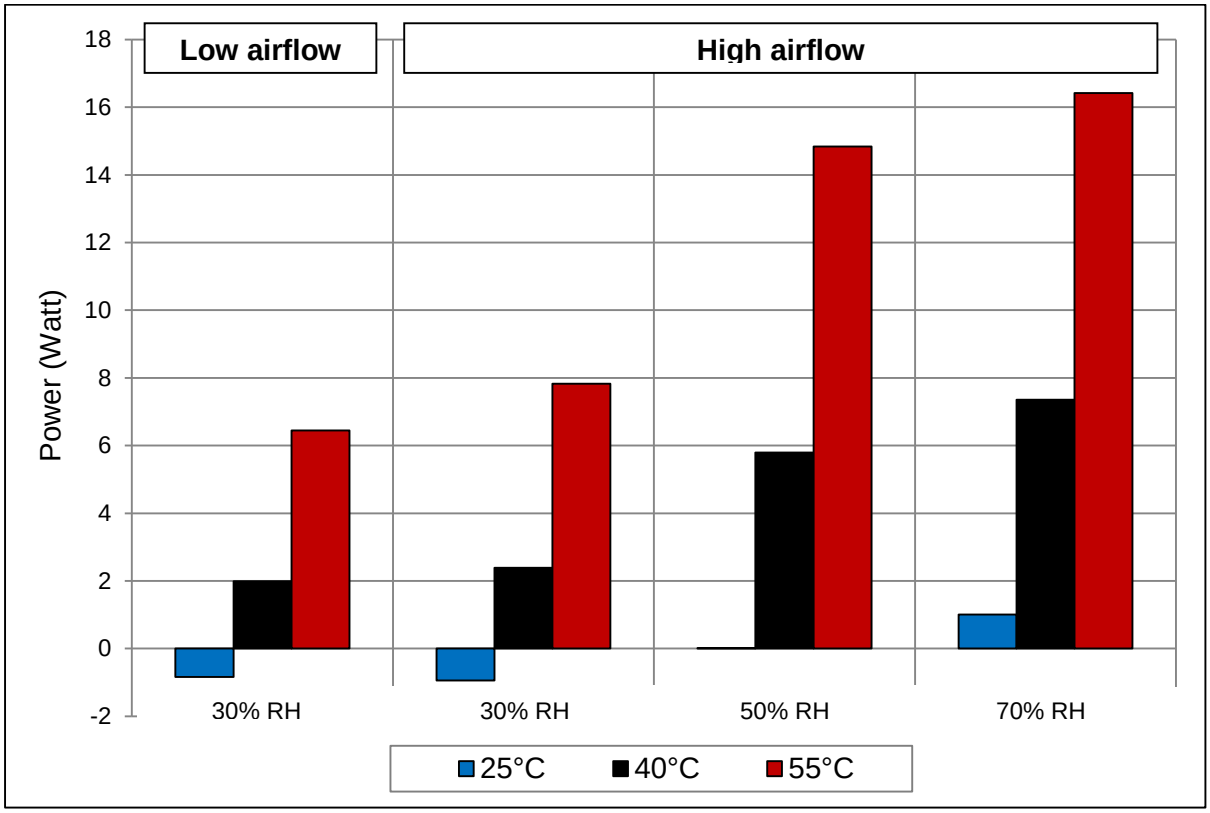

Figure 5.1. Power (Watt or J/s) needed for air-water system

Experiments with a relative humidity of 70% and a high temperature of 55°C required the most power. No conditioning of air took place at a temperature of 25°C and a relative humidity of 50%, as the surrounding air had similar temperature and relative humidity conditions. This is the reason why the power value is zero, as shown in Figure 5.1. It is clear from Figure 5.1. that an increase in temperature requires more power. It is interesting to notice that more than double the power is needed with each temperature increase across all the relative humidity conditions. On the other hand, increases in the relative humidity led to a more gradual increase in the amount of power needed in the air-water system.

The climate chamber used a total power of 2000 Watt and the values in Table 5.6. are small in comparison to the total power needed to run the climate chamber. It was assumed that these power changes in the air-water system during drying, gave an indication of which conditions might lead to a higher or lower power requirement by the climate chamber.

5.2.2. Climate chamber

The power needed by the climate chamber to run at all the conditions was approximately 2000 Watt. However, conditioning the air to higher or lower temperature and relative humidity conditions caused the climate chamber to have a higher or lower power usage. It wasn't clear what the precise deviation from 2000 Watt was, as the power usage continually corresponded to each change in the temperature and relative humidity conditions. It was therefore decided to add the power changes in the air water system as calculated in Section 5.2.1., to the total power needed by the climate chamber. No conditioning for the air water system took place at a temperature of 25°C and a relative humidity of 50%, as the surrounding air had similar temperature and relative humidity conditions. However the temperature and humidity changed constantly during the experimental run and the climate chamber had to run to maintain the prescribed conditions.

As the climate chamber had to condition the air prior to the experiment and during the experiment, the time values calculated and shown in Table 5.5. were used. Equation 5.10 was used to determine the amount of energy, Q_c, needed for the total time the climate chamber was used for each experiment. The symbol W_c indicates the total power of the climate chamber, while W_i refers to the power needed for the air-water system during drying. The results of Equation 5.10 are given in Table 5.7.

$$Q_c = (W_c + W_i)\, t \qquad \textbf{(5.10)}$$

Table 5.7. Total energy (kJ) required by the climate chamber

Temperature	Low airflow	High airflow		
	30% RH	30% RH	50% RH	70% RH
25°C	4318	3838	3120	3602
40°C	4324	3604	2888	3372
55°C	4093	3373	2901	3630

The low airflow rates required the most energy, while the 30% and 70% relative humidity conditions also required more energy than the 50% relative humidity conditions. The highest contributor is the slower drying rates for the lower airflow rates and 70% relative humidity, that resulted in longer drying times. In addition the 30% relative humidity also took more time to condition that led to a higher energy demand.

5.2.3. Blower

The blower used a total of 700 Watt at the high airflow rate of between 1.5-1.7m/s and 350 Watt at the low airflow rate of between 0.8-1.1m/s. The blower was only switched on after the air was conditioned to its set point temperature and relative humidity. Therefore, only the drying time for each sample was used to determine the energy usage required by the blower. Table 5.8. gives the drying times for the samples placed in the fluidised bed at all the temperature, humidity and airflow conditions.

Table 5.8. Drying times (min) in the fluidised bed

Temperature	Low airflow	High airflow		
	30% RH	30% RH	50% RH	70% RH
25°C	16	12	16	20
40°C	16	10	14	18
55°C	14	8	14	20

Equation 5.11 was used to determine the amount of energy, Q_b, needed for the total time the blower was used for each experiment. The symbol W_b indicates the power usage of the blower. The results of Equation 5.11 can be found in Table 5.9.

$$Q_b = W_b \cdot t \quad \textbf{(5.11)}$$

Table 5.9. Total energy (kJ) required by the blower

Temperature	Low airflow	High airflow		
	30% RH	30% RH	50% RH	70% RH
25°C	336	504	672	840
40°C	336	420	588	756
55°C	294	336	588	840

The results indicated that the blower required significantly less energy than the climate chamber. The results show that a lot less energy was needed for the lower airflow rates and less energy was used for experiments with shorter drying times.

5.2.4. Total energy required

The total energy required was calculated as the sum of the energy needed from the climate chamber as well as the blower, as shown in Equation 5.12. The final energy values from Section 5.2.2. and 5.2.3. were used in the calculations. The results for the energy required can be seen in Table 5.10. and in Figure 5.2. as well.

$$Q = Q_c + Q_b \quad \textbf{(5.12)}$$

Table 5.10. Total energy (kJ/kg load) required by the climate chamber and blower

Temperature	Low airflow	High airflow		
	30% RH	30% RH	50% RH	70% RH
25°C	4654.19	4342.19	3792.00	4441.81
40°C	4660.31	4024.31	3476.34	4128.36
55°C	4387.14	3709.14	3489.36	4469.56

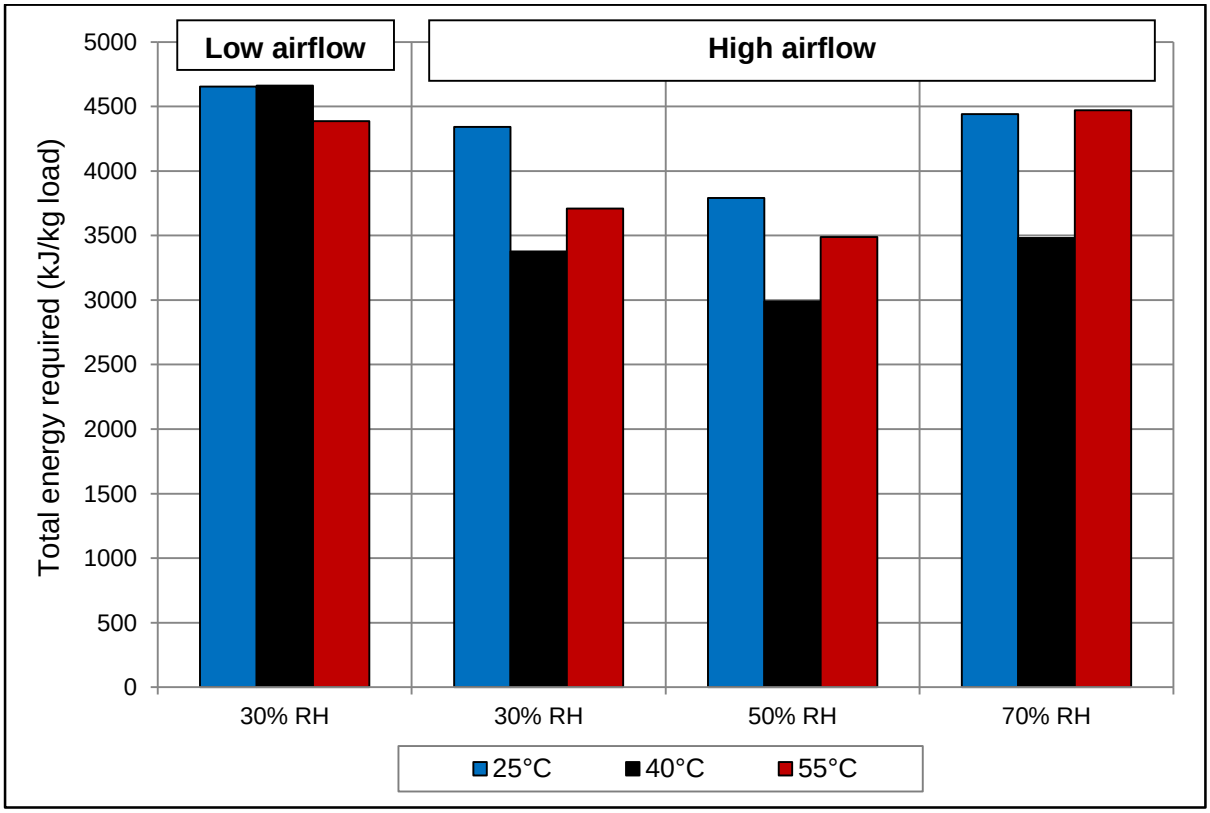

Figure 5.2. Total energy (kJ/kg load) required by the climate chamber and blower

The low airflow conditions required more energy, while the 70% relative humidity conditions also required more energy. The slower drying rate for both the low airflow rate and 70% relative humidity resulted in longer drying times that the blower and climate chamber had to run, leading to more energy consumption. The 30% relative humidity had the fastest drying rate, however it wasn't as energy efficient as the climate chamber needed more time to condition the air at these low relative humidity conditions.

The higher temperatures of 40°C and 55°C proved to have a higher drying rate, yet the amount of energy required to condition and maintain that temperature was less or equal to the lower temperature of 25°C.

In terms of the fastest drying time and drying rate in the fluidised bed, it was concluded that the most efficient condition is airflow above minimum fluidisation point causing vigorous mixing and maximum contact with the drying air. In addition to the high airflow it was concluded that 30% relative humidity and a temperature of 55°C resulted in the fastest drying time. However the most energy efficient condition proved to be at 50% relative humidity at a temperature of 40°C or 55°C. Much less air conditioning was required to maintain 50% relative humidity as the average surrounding relative humidity is about 50% and the power was mainly required to raise and maintain the temperature.

It was therefore more effective to use air at slightly elevated temperatures and relative humidity conditions close to the relative humidity of the surrounding air that is drawn in by the blower. Considering that the air has to have a relative humidity of 50% and lower to maintain a high moisture concentration gradient for effective and fast drying.

5.2.5. Energy requirement to dry coal to various final moisture contents

A comparison was done on the total energy required for drying wet coal samples to moisture content of $10\%_{wt}$, $5\%_{wt}$ and to its inherent moisture content. The total energy requirements for drying up to $10\%_{wt}$ and $5\%_{wt}$, were also calculated with the same method as drying to its inherent moisture content, that was discussed in Section 5.2.1. to 5.2.4. The main difference was a change in the drying times, which resulted in a change in the energy requirement. It took more time to remove moisture to its inherent moisture content, than to dry to a moisture content of $5\%_{wt}$. The shortest drying time was when the moisture was only reduced to$10\%_{wt}$. The results for the energy required can be seen in Table 5.11.

Table 5.11. Total energy (kJ/kg load) required for drying to different final moisture contents

Moisture content	Temperature	Low airflow	High airflow		
		30% RH	30% RH	50% RH	70% RH
10%$_{wt}$	25°C	3808.19	3370.19	2820.00	3145.81
	40°C	**3814.31**	3214.31	**2504.34**	2832.36
	55°C	3541.14	3061.14	2517.35	3011.57
5%$_{wt}$	25°C	**4372.19**	3856.19	3306.00	3955.81
	40°C	4237.31	3538.31	**3152.34**	3642.36
	55°C	3823.14	3385.14	3165.35	3821.57
Inherent	25°C	4654.19	4342.19	3792.00	4441.81
	40°C	**4660.31**	4024.31	**3476.34**	4128.36
	55°C	4387.14	3709.14	3489.36	4469.56

The minimum and maximum values are highlighted in Table 5.11 and shown in Figure 5.3.

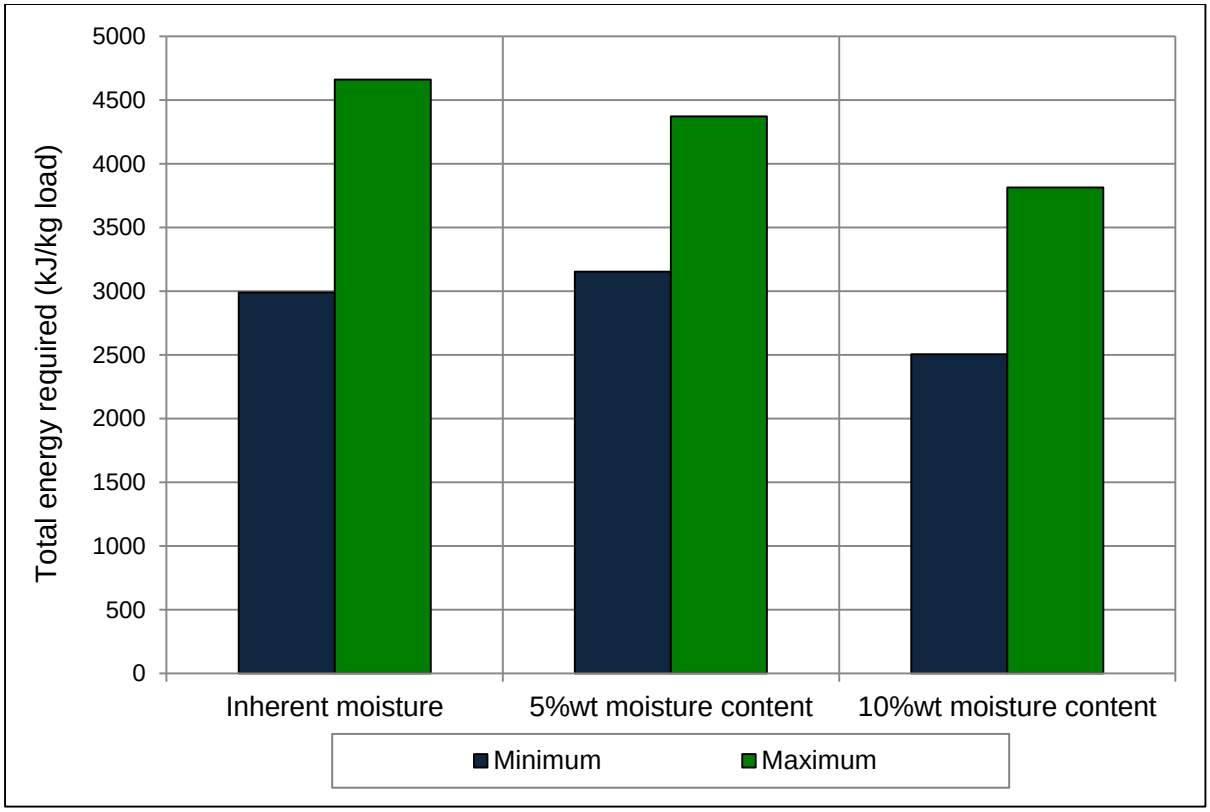

Figure 5.3. Minimum and maximum energy (kJ/kg load) required to dry to different final moisture contents

The results from Table 5.11. and Figure 5.3. showed that it required more energy to remove more moisture from the fine coal sample, mainly due to the longer drying times. Drying the sample up to its inherent moisture required a minimum and maximum energy of 3476.34 $kJ/kg\ load$ and 4660.31 $kJ/kg\ load$, respectively. The total minimum and maximum energy needed to dry the coal samples up to 5%$_{wt}$, was 3152.34 $kJ/kg\ load$ and 4372.19 $kJ/kg\ load$. Moreover the minimum and maximum energy needed to dry the coal samples up to 10%$_{wt}$, was 2504.34 $kJ/kg\ load$ and 3814.31 $kJ/kg\ load$. The difference across the minimum and maximum energy values is gradual as illustrated in Figure .5.3.

5.3. Upgrading of coal: Improvement of calorific value

The calorific values of the vitrinite and inertinite coal samples were determined before and after drying in the fluidised bed. The moisture content of both the filter cake samples was about 25%$_{wt}$. Furthermore the calorific value of the filter cakes was determined as received and not on an air-dried basis. After drying each of the samples at 40°C and 30% relative humidity, the calorific value was determined again. The results are given in Table 5.12.

Table 5.12. Calorific values before and after drying filter cakes (As received)

Moisture content	Sample Identification	Vitrinite rich coal	Inertinite rich coal
10%$_{wt}$	Calorific value of filter cake (MJ/kg)	5.28	16.54
	Calorific value of dried sample (MJ/kg)	10.7	21.96
5%$_{wt}$	Calorific value of filter cake (MJ/kg)	5.28	16.54
	Calorific value of dried sample (MJ/kg)	12.5	23.77
Inherent	Calorific value of filter cake (MJ/kg)	5.28	16.54
	Calorific value of dried sample (MJ/kg)	13.87	25.07

The calorific value of both the vitrinite and inertinite rich coal almost doubled after drying, mainly due to the major moisture reduction. The results show that drying of wet filter cakes with a fluidised bed proved to be viable, as the calorific value increased significantly as well. The improvement of the calorific value was calculated using Equation 5.13 and the results are shown in Table 5.13.

$$Improved\ CV = CV\ of\ dried\ sample - CV\ of\ filter\ cake \quad \textbf{(5.13)}$$

The minimum and maximum values for the energy consumed during drying was converted from $kJ/kg\ load$ to $MJ/kg\ load$ and listed in Table 5.13. The difference between energy consumed and improved energy value of the coal was calculated with Equation 5.14 and the results are shown in Table 5.13.

$$Calculated\ difference\ in\ energy = Improved\ CV - Energy\ consumed \quad \textbf{(5.14)}$$

Table 5.13. Energy calculations: Upgrading of coal

Moisture content	Sample Identification	Vitrinite rich coal	Inertinite rich coal
10%$_{wt}$	Energy consumed for drying (MJ/kg)	2.99 - 3.48	2.50 - 3.81
	Improvement of calorific value (MJ/kg)	5.42	5.42
	Energy gain (MJ/kg)	2.43 - 1.94	2.92 - 1.61
5%$_{wt}$	Energy consumed for drying (MJ/kg)	3.64 - 4.45	3.15 - 4.37
	Improvement of calorific value (MJ/kg)	7.22	7.23
	Energy gain (MJ/kg)	3.58 - 2.77	4.08 - 2.86
Inherent	Energy consumed for drying (MJ/kg)	4.02 - 4.78	2.99 - 4.66
	Improvement of calorific value (MJ/kg)	8.59	8.53
	Energy gain (MJ/kg)	4.57 - 3.81	5.54 - 3.87

The results in Table 5.13. indicate that less energy was used for drying than the energy improvement of the coal samples after drying. These results show that all the drying processes at all the airflow rates, temperature and relative humidity conditions were energy efficient. In addition, the process was also energy efficient to dry to all the various final moisture contents. From Table 5.13 it can also be seen that the result for vitrinite and inertinite coal samples were similar, however drying of inertinite rich coal was slightly more energy efficient. This can be confirmed by the occurrence of the drying rate for inertinite rich coal that was also a little faster than the drying rate for the vitrinite rich coal, as discussed in Chapter 4.6. The results also indicated that it was more energy efficient to dry the vitrinite and inertinite coal samples to its inherent moisture content, than drying to a moisture content of 5%$_{wt}$ or 10%$_{wt}$. Drying within the fluidised bed proved to be more cost effective, as the lowest possible moisture content was achieved using the least energy possible to obtain the higher calorific values.

5.4. Comparison to other drying technologies

This section of work focuses on determining whether the fluidised bed is energy efficient in comparison to other existing technologies. The energy needed to remove a certain mass of moisture from a coal sample can be calculated with Equation 5.15. Where Q_c refers to the energy required by the climate chamber, Q_b refers to the energy required by the blower and m_w refers to the mass of moisture that is removed during the drying process.

$$Q_w = {}^{(Q_c + Q_b)}/_{m_w} \quad \textbf{(5.15)}$$

The results for the energy required per mass of moisture removed were calculated using Equation 5.15 and listed in Table 5.14. The results were calculated for drying to a moisture content of 10%$_{wt}$, 5%$_{wt}$ and to its inherent moisture content.

Table 5.14. Total energy (kJ/kg moisture removed) required for drying to different final moisture contents

Moisture content	Temperature	Low airflow	High airflow		
		30% RH	30% RH	50% RH	70% RH
10%$_{wt}$	**25°C**	2800.14	2785.28	1905.41	2231.07
	40°C	2686.13	2571.45	1956.52	2195.63
	55°C	2095.35	**2860.88**	**1892.75**	2428.68
5%$_{wt}$	**25°C**	**2301.15**	2229.01	1704.12	1977.91
	40°C	2097.68	1999.04	**1600.17**	1867.88
	55°C	1811.91	2051.60	1606.78	2000.82
Inherent	**25°C**	1988.97	**2019.62**	1606.78	1898.21
	40°C	1941.79	1493.94	**1294.52**	1493.72
	55°C	1668.12	1827.16	1510.55	1968.97

Drying the sample up to its inherent moisture required a minimum and maximum energy of 1294.52 kJ/kg_{H_2O} and 2019.62 kJ/kg_{H_2O}, respectively. The total minimum and maximum energy needed to dry the coal samples up to 5%$_{wt}$, was 1600.17 kJ/kg_{H_2O} and 2301.15 kJ/kg_{H_2O}. In addition the minimum and maximum energy needed to dry the coal samples up to 10%$_{wt}$, was 1892.75 kJ/kg_{H_2O} and 2860.88 kJ/kg_{H_2O}. Less energy (kJ/kg moisture removed) when drying the coal samples with an inherent moisture content.

As stated in Chapter 2.5., thermal drying usually refers to a process where moisture is removed from wet solid particles by using a drying medium that is in the gaseous state. The moisture is then evaporated and carried away by the drying medium (Syahrul *et al.*, 2002). According to Felder & Rousseau (2005) energy of 2256.9 kJ/kg is needed to evaporate 1kg of water at a temperature of 100°C and at atmospheric pressure. The results from Table 5.14. shows that the energy required for drying was lower than 2256.9 kJ/kg for the majority of the airflow, temperature and relative humidity conditions in the fluidised bed. This proves that using fluidised air at temperatures below 60°C used less energy than needed for thermal drying techniques operating with temperatures higher than the boiling point of water.

Wilson *et al.* (1992) did a study on low rank coal and listed a number of dryer types and the energy they consumed per unit moisture removed. These values are listed in Table 5.15.

Table 5.15. Energy consumption for different dryers; taken from Wilson *et al*. (1992)

Type of dryer	Energy consumption (kJ/kg H_2O)
Rotary dryer	3700
Rotary tube dryer	2950-3100
Chamber dryer	3150
Pneumatic dryer	3100
High temperature fluid bed dryer	3100-3500
Fleissner process (superheated steam)	1750

The energy consumption for the fluidised bed is lower than for all the dryer systems listed in Table 5.15., this includes the mechanical dewatering and thermal drying systems. Almost all the dryers listed in Table 5.15. consumed more energy than 2256.9 kJ/kg, the basic indication of energy needed for a thermal drying operation.

Figure 5.4. illustrates the comparison between the fluidised bed and the other drying systems. The results show that energy consumption was efficient using a fluidised bed to dry to a moisture content of 10%$_{wt}$, 5%$_{wt}$ and to its inherent moisture content. This is just a preliminary correlation; however the fluidised bed used in this study proved to be much more energy efficient.

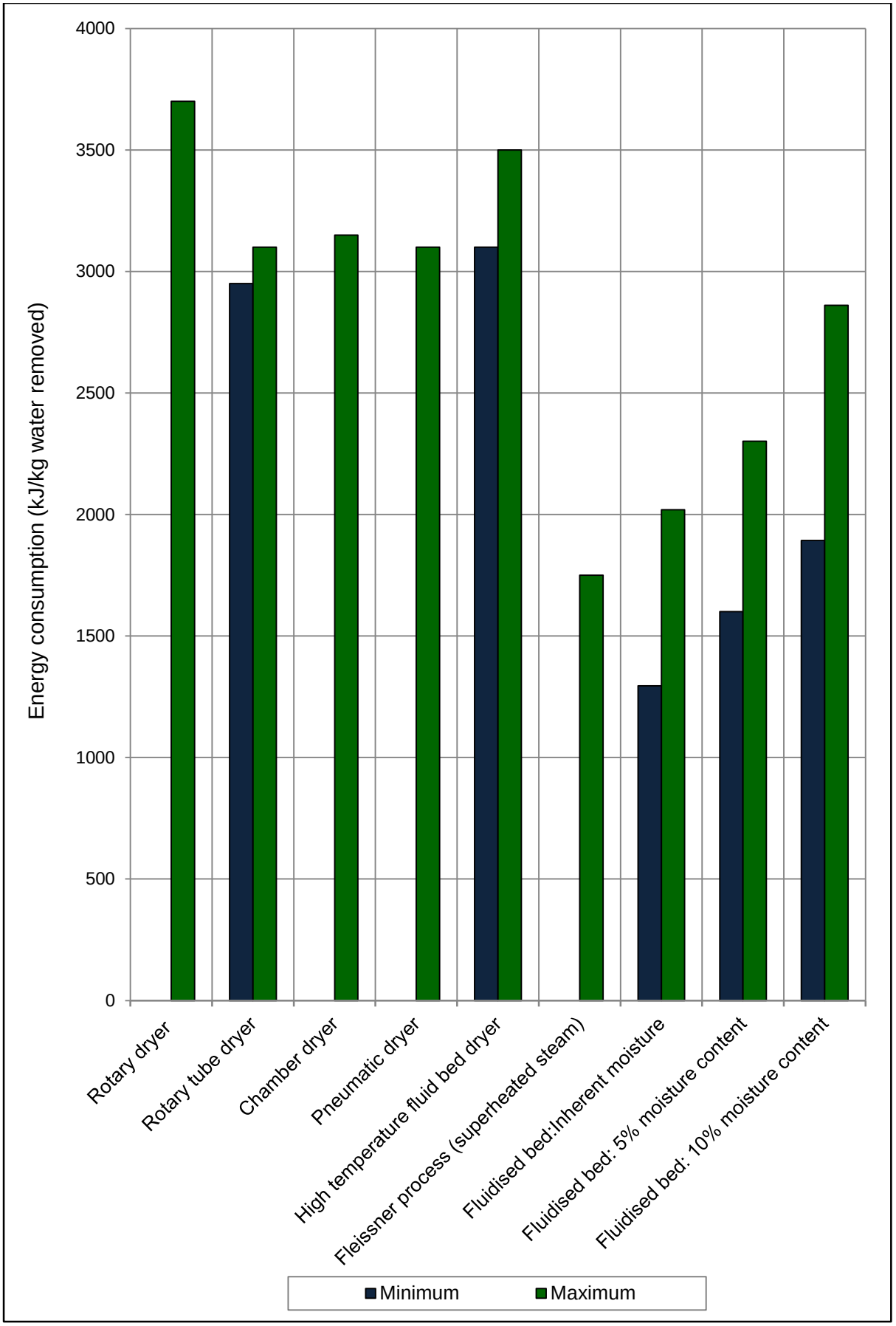

Figure 5.4. Comparison between the fluidised bed and the other drying systems

5.5. Conclusion

The most energy efficient conditions proved to be at 50% relative humidity at a temperature of 40°C or 55°C. Much less air conditioning was required to maintain 50% relative humidity as it was the average surrounding relative humidity. It was therefore more effective to use air at slightly elevated temperatures and relative humidity conditions close to the relative humidity of the surrounding air that is drawn in by the blower. Considering that the air has to have a relative humidity of 50% and lower to maintain a high moisture concentration gradient for effective and fast drying.

All the drying processes at all the airflow rates, temperature and relative humidity conditions were energy efficient. In addition the process was also energy efficient to dry to a moisture content of $10\%_{wt}$, $5\%_{wt}$ and to its inherent moisture content. The calorific value of both the vitrinite and inertinite rich coal almost doubled after drying, mainly due to the major moisture reduction. Drying of wet filter cakes with a fluidised bed proved to be viable, as the calorific value increased significantly. The fluidised bed used in this study proved to be much more energy efficient than all the dryer systems compared to.

CHAPTER 6 – CONCLUSIONS AND RECOMMENDATIONS

6.1. Introduction

Final conclusions were made from the results and discussions in Chapter 4 as well as the energy balances from Chapter 5. Recommendations were made for further research to get a more thorough understanding of the research topic. Note that the conclusions and recommendations are numbered and correspond to the objectives of study stated in Chapter 1.3. To end this chapter, Section 6.4. lists the contributions that were made to the research field and industry.

6.2. Final conclusions

The following conclusions were drawn to meet the objectives specified in Chapter 1.3:

1) The amount of equilibrium moisture, changes to correspond to the changes in the surrounding temperature and relative humidity. This would mean that the temperature and relative humidity of the drying air will affect the final moisture content of the wet coal particles dried within the fluidised bed.

2) The samples reached an equilibrium moisture content at each of the relative humidity conditions and it was clear that a decrease in the relative humidity lead to a lower moisture content. Higher temperatures of the drying air were able to reduce the equilibrium moisture content, especially when drying the coal samples containing less moisture at the lower relative humidity conditions. The vitrinite rich coal was able to absorb more moisture than the inertinite rich coal at all relative humidity conditions, as the vitrinite rich coal sample contained more mineral matter as well as fines. The inertinite rich was more porous and showed to release the moisture when relative humidity was lowered.

3) A laboratory scale fluidised bed was designed and built as shown in Chapter 3. The fluidised bed and the experimental procedures proved to deliver results that fall in a very narrow range from one another, with a maximum standard deviation of 2.39%$_{wt}$. High airflow with lower partial pressures proved to be able to absorb more moisture from the fines, without using high temperatures to evaporate the water from the fine coal. In conclusion it was proven that the airflow and relative humidity of the drying air at low temperatures contributed to faster drying rates. The temperature didn't prove to have

such a big contribution, however higher temperatures did increase the drying rate at higher airflow and lower humidity conditions.

4) It was determined that the drying rate for coal with an equilibrium moisture content and filter cakes containing free moisture, was both linear until it reached an equilibrium with the drying air conditions. The linear part of the drying rate is typical zero-order drying model and the rate of drying is independent of the moisture content in the coal sample. The results from the experimental data showed that the drying rates for the coal samples dried in the fluidised bed were all linear. In addition the drying rate was linear up until it reached a point within the range between 1-2%$_{wt}$ from the final equilibrium moisture content. It was concluded that the most efficient condition is airflow above minimum fluidisation point causing vigorous mixing and maximum contact with the drying air. In addition to the high airflow it was determined that 30% relative humidity and 55°C resulted in the fastest drying time.

5) The zero-order drying model used to compare the experimental data is useful to predict the first part of the drying rate and moisture content of samples dried at various conditions. It can also give an indication of what the final moisture content of the bulk coal sample would be, as it is able to predict the moisture up to about the equilibrium moisture content.

6) The inertinite rich coal released more moisture at a faster rate compared to the vitrinite rich coal. This confirms the results that were also found at static conditions, where the inertinite rich coal also released more moisture. It is presumed that due to the fact that the inertinite rich coal is more porous and contains less mineral matter and finer particles, it was able to release moisture at a faster rate.

7) It was determined that the drying rate for coal with an equilibrium moisture content and filter cakes containing free moisture, was both linear until it reached an equilibrium with the drying air conditions. The initial moisture content didn't affect the drying rate as it is independent of the moisture content in the coal sample.

8) The most energy efficient conditions proved to be at high airflow at 50% relative humidity and a temperature of 40°C or 55°C. Much less air conditioning was required to maintain 50% relative humidity as it was the average surrounding relative humidity. It was therefore more effective to use air at slightly elevated temperatures and relative humidity conditions close to the relative humidity of the surrounding air that is drawn in by the blower. Considering that the air has to have a relative humidity of 50% and lower to maintain a high moisture concentration gradient for effective and fast drying.

9) Less energy was used for drying than the improvement of calorific values of the coal samples after drying. These results show that all the drying processes at all the airflow rates, temperature and relative humidity conditions were energy efficient. In addition the process was also energy efficient to dry to all the various final moisture contents. The calorific value of both the vitrinite and inertinite rich coal almost doubled after drying, mainly due to the major moisture reduction.

10) The overall energy consumption for the fluidised bed is lower than for all the dryer systems compared to, including thermal and mechanical dryer systems.

6.3. Recommendations for further studies

The following recommendations were made for each section of work and numbered according to the objectives specified in Chapter 1.3:

1) It is advised to investigate more temperature and relative humidity conditions within the climate chamber. In addition it would also be helpful to determine the time needed to reach equilibrium at each temperature and relative humidity set point. This would yield a better understanding of the conditions of air drying that would use more time and, ultimately, energy to pre-condition and maintain.

2) It is recommended that a detailed mineral analysis should be done in order to determine the effect of the various minerals on the desorption kinetics. It would yield the best results if pure minerals are placed in the climate chamber to compare their contribution to the moisture adsorption or desorption. It is also suggested to investigate the pore network of the coal samples and not only the open area per mass of sample. This would result in a better understanding of the drying process and the way coal absorbs or releases moisture. It is also advised that the moisture related to each sample should be determined not only by the quantity but also percentage and type of moisture present. From this it can be determined what the drying rate would look like when each of these moisture levels is reached during drying.

3) It is recommended to build a pilot scale fluidised bed for further studies in fluidised bed drying. In addition alternative methods to condition the air, should be tested to replace the function of the climate chamber. In addition it is also recommended to do test work on a larger variety of coal from different seams. This would give a larger range of data investigating more coal properties and characteristics and also determine how they influence the drying rate in the fluidised bed. Drying pure minerals would also provide more complete data for further research. It is suggested to complete test runs with a

larger temperature, relative humidity and airflow rate range. This would yield a fuller range of data to get a better understanding of how these parameters interact with each other.

4) Complete test runs with a larger temperature and airflow range. It is advised to investigate different airflow rates and patterns to get a better understanding of the how the airflow rate influences the drying.

5) Find or construct a drying model that would describe the drying rate by including variables like particle size, airflow rate, temperature and relative humidity as well. Complete test runs with a larger temperature, relative humidity and airflow range. This would provide sufficient data to construct a drying model that would describe the drying rate more accurately.

6) Complete more test runs with coal from different seams that also contain either more vitrinite or inertinite, to determine the accuracy of the result from this study.

7) It is advised that the moisture related to each sample should be determined not only by the quantity but also percentage and type of moisture present. From this it can be determined what the drying rate would look like when each of these moisture levels is reached during drying.

8) It is advised to design the pilot scale in such a way that the energy required could be determined more accurately.

9) It is suggested to complete energy balances with data from the pilot scale fluidised bed as well. It is recommended to do petrographic analysis as well as determine the particle size distribution after fluidisation, to determine the changes in structure and size of the coal particles. These would also affect the upgrading of coal and quality of the final product.

10) Compare the data with drying systems in industry, using similar coal.

6.4. Contributions made to research field and industry

It was determined by this study that drying of fine coal is possible using air at temperatures below 60°C. In addition it was proven that the airflow and relative humidity of the drying air at these temperatures contributed to faster drying rates. The drying rates for the coal samples dried in the fluidised bed were all linear, up until it reached a point within the range between 1-2%$_{wt}$ from the final equilibrium moisture content of the bulk coal sample. It was also concluded that drying was more efficient using airflow causing a low pressure than high pressure low airflow systems. It was determined that filter cakes can be dried in the fluidised bed to a point where effective fluidisation can follow. All the drying processes at all the airflow rates, temperature and relative humidity conditions were energy efficient. This process was shown to be energy positive, resulting in an overall energy gain. The overall energy consumption for the fluidised bed is lower than for all the dryer systems compared to and it compared favourably with other thermal drying technologies. It was therefore shown that this is a viable technology for the dewatering of fine coal.

BIBLIOGRAPHY

Asmatulu, R. & Yoon, R.H. 2012. Effects of Surface Forces on Dewatering of Fine Particles. (*In* Separation Technologies for Minerals, Coal and Earth Resources. Society of Mining, Metallurgy, and Exploration, Inc. (SME). p. 95-101).

Bourgeois, F., Barton, W., Buckley, A., McCutcheon, A., Clarckson, C. & Lymon, G. 2000. Project 3087: Fundamentals of fine coal dewatering. http://acarp.com.au/Completed/Coal_ preparation/briefs/ Date of access: 10 Sep. 2012.

Buckley, A.N. & Nicol, S.K. 1995. Surface-related moisture retention characteristics of coal. Investigation Report CETIIR273, CSIRO, North Ryde, Australia. p. 65.

Campbell, Q.P. 2006. Dewatering of fine coal with flowing air using low pressure drop. Potchefstroom: NWU. (Thesis - PhD).

Chua, K.J. % Chou, S.K. 2003. Low-cost drying for developing countries. *Trends in Food Science and Technology*, 14:519-628.

De Korte, G.J. & Mangena, S.J. 2004. Thermal Drying of Fine and Ultra-fine Coal. Report No. 2004 - 0255, Division of Mining Technology, CSIR. p. 5-9.

Du Preez, S.M. The influence of minerals on the moisture adsorption and desorption properties of South African fine coal. 2012. Potchefstroom: NWU. (Dissertation - Masters).

Dwari, R.K. & Rao, K.H. 2007. Dry beneficiation of coal - a review. *Mineral Processing and Extractive Metallurgy Review*, 8(3):177-234.

Eberhard, A. 2011. The future of South African coal: Market, investment and policy challenges. http://iis-db.stanford.edu/pubs/23082/WP_100_Eberhard_Future_of_South_African_Coal.pdf Date of access: 21 Aug. 2012.

Falcon, R. & Ham, A.J. 1988. The characteristics of South African coals. *Journal of the South African Institute of Mining and Metallurgy*, 88(5):145-161.

Felder, R.M. & Rousseau, R.W. 2005. Elementary Principles of Chemical Processes. 3rd ed. United States of America: John Wiley & Sons Inc.

Firth, B. & Swanson, A. 2002. Opportunities for improved fine coal treatment. (*In* 14th International Coal Preparation Congress and Exhibition. Johannesburg: South African Institute of Mining and Metallurgy. p. 451-456).

Fogler, H.S. 2006. Elements of chemical reaction engineering. 4th ed. Pearson Education Inc.

Fourie, P.J.F., Van Der Walt, P.J. & Falcon, L.M. 1980. The beneficiation of fine coal by dense-medium. *Journal of the South African Institute of Mining and Metallurgy*:357-361.

Hatt, R. 2003. Moisture Impacts on Coal Handling and Heat Rate. http://www.coalcombustion.com/PDF%20Files/MOISTURE%2003.pdf Date of access: 20 Aug. 2013.

Jangam, S.V., Kuma, J.V.M. & Mujumdar, A.S. 2011. Critical Assessment of Drying of Low Rank Coal. Technical Report M3TC-2011-01, Minerals, Metals and Materials technology Centre, National university of Singapore. p. 1-28.

Jeffrey, L.S. 2004. A preliminary investigation into the geotechnical interpretation of geophysical logs. Coaltech 2020.

Karthikeyan, M., Zhonghua, W. & Mujumdar, A.S. 2009. Low-Rank Coal Drying Technologies - Current Status and New Developments. *Drying Technology: An International Journal*, 27(3):403-415.

Keles, S., Luttrell, G., Yoon, R., Estes, T., Schultz, W. & Bethell, P. 2010. Development of the Centribaric™ Dewatering Technology. *International Journal of Coal Preparation and Utilization*, 30(2-5):204-216.

Koretsky, M.D. 2004. Engineering and Chemical Thermodynamics. 2nd ed. Hoboken, New Jersey, USA: John Wiley & Sons Inc.

Kunii, D. & Levenspiel, O. 1991. Fluidization Engineering. 2nd ed. New York: Wiley.

Lawluvl, H. & Ayensu. 1998. Thermal Stimulated Moisture Desorption and Drying Characteristics of Tropical Hardwood. (*In* VAHPU Conference proceedings. Ghana. p. 121-130).

Lemley, A., Wagenet, L. & Kneen, B. 1995. Activated Carbon Treatment of Drinking Water. http://www.sswn.info/sites/default/files/toolbox/LEMLEY%20et%20al%201995%20a%20Typical%20Carbon%20Particle.jpg Date of access: 22 May 2012.

Le Roux, M. An investigation into an improved method of dewatering fine coal. 2003. Potchefstroom: NWU. (Dissertation - Masters).

Le Roux, M., Campbell, Q.P. 2003. An Investigation into an Improved Method of Fine Coal Dewatering. *Minerals Engineering*, 16(10):999-1003.

Levy, E.K., Caram, H.S., Yao, Z., Wei, Z. & Sarunac, N. 2006 Kinetics of Coal Drying in Bubbling Fluidized Beds. (*In* Proceedings Fitfth World Congress on Particle Technology. Orlando, Florida. p. 1-6).

Luo, Z., Zhu, J., Fan, M., Zhao, Y. & Tao, X. 2007. Low Density Dry Coal Beneficiation Using an Air Dense Medium Fluidised Bed. *Journal of China University of Mining & Technology*, 17(3):306-309.

Luo, Z.F., Zhu, J.F., Tang, L.G., Zhao, Y.M., Guo, J., Zuo, W. & Chen, S.L. 2010. Fluidization characteristics of magnetite powder after hydrophobic surface modification. *International Journal of Mineral Processing*, 94(2010):166-171.

Mahajan, O.P. & Walker, Jr, P.L. 1978. Analytical Methods for Coal and Coal Products: Volume 1. Academic Press, Inc. p. 125-162.

Mangena, S.J., De Korte, G.J., McCrindle, R.I. & Morgan, D.L. 2003. The amenability of some Witbank bituminous ultra fine coals to binderless briquetting. *Fuel Processing Technology*, 85(2004):1647-1662.

Mohanty, M.K., Akbari, H. & Luttrell, G.H. 2012. Fine Coal Drying and Plant Profitability. (*In* Challenges in Fine Coal Processing, Dewatering, and Disposal. Society of Mining, Metallurgy, and Exploration, Inc. (SME). p. 329-344).

Nellis, G. & Klein, S. 2012. Heat Transfer. http://www.cambridge.org/us/engineering/author/nellisandklein/ Date of access: 15 Apr. 2013.

Osborne, D.G. 1988. Coal Preparation Technology: Volume 1. London: Graham & Trotman Limited.

Reddick, J.F., Von Blottnitz, H. & Kothuis, B. 2007. A cleaner production assessment of the ultra-fine coal waste generated in South Africa. *The Journal of The South African Institute of Mining and Metallurgy*, 107:811-816.

Rhodes, M. 2008. Introduction to Particle Technology. 2nd ed. England: John Wiley & Sons, Ltd. p. 169-199.

Rong, R.X. & Hitchins, J. 1995. Preliminary study of correlations between fine coal characteristics and properties and their dewatering behaviour. *Minerals Engineering*, 8(3):293-309.

Syahrul, S., Dincer, I. & Hamdullahpur, F. 2002. Thermodynamic modeling of fluidised bed drying of moist particles. *International Journal of Thermal Sciences*, 42(2003):691-701.

Terblanche, A.N. 2011. Dry beneficiation of fine coal using a fluidised bed. Final year project report. Potchefstroom: NWU. (Unpublished).

University of Colorado at Boulder. 2009. Technology: Fluidization. http://www.colorado.edu/che/TeamWeimer/ResearchInterests/Fluidization.htm Date of access: 21 May 2012.

University Corporation for Atmospheric research. 2010. http://stream2.cma.gov.cn/pub/comet/HydrologyFlooding/UnderstandingtheHydrologicCycleInternationalEdition/comet/hydro/basic_int/hydrologic_cycle/media/graphics/vapor_pressure_deficit.jpg Date of access: 16 Mar. 2013.

University of Texas. 2013. http://ch302.cm.utexas.edu/svg302/phase-diagram-water.svg Date of access: 16 Mar. 2013.

Unsworth, J.F., Fowler, C.S. & Jones, L.F. 1989. Moisture in coal: Maceral effects on pore structure. *Fuel*, 68:18-26.

Van der Merwe, D.C.S., & Campbell, Q.P. 2002. An Investigation into the Moisture Absorption Properties of Thermally Dried South African Fine Coal. *Journal of the South African Institute of Mining and Metallurgy*. 102(7):417-419.

Wakeman, R.J. 1984. Residual Saturation and Dewatering of Fine Coals and Filter Cakes. *Powder Technology*, 40:53-63.

Willemse, V.J. 2011. Dry beneficiation of coal using a fluidised bed. Final year project report. Potchefstroom: NWU. (Unpublished).

Wilson, W.G., Young, B.C. & Irwin, W. 1992. Low-rank coal drying advances. *Coal*, 24-27.

World Coal Assosiation. 2012. http://www.worldcoal.org/coal/where-is-coal-found/ Date of access: 27 Aug. 2012.

World Petroleum Council. 2011. Fuel for Life. http://www.world-petroleum.org/index.php?/Latest-Publications/howtheenergyindustryworks2009.html Date of access: 21 Aug. 2012.

Zhonghua, W. & Mujumdar, A.S. 2011. Drying in Mineral Processing Industry: Potential for Innovation. Technical Report M3TC-2011-01, Minerals, Metals and Materials technology Centre, National university of Singapore. p. 65-77.

APPENDIX A

A.1. Maceral analysis of the inertinite rich sample

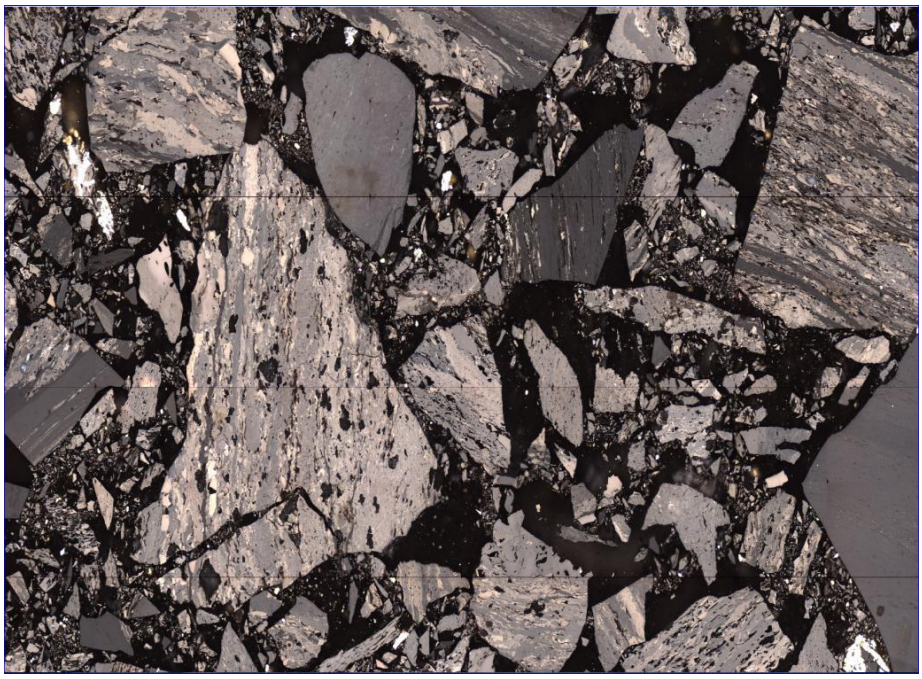

Figure A.1. Scanned overview of inertinite rich sample

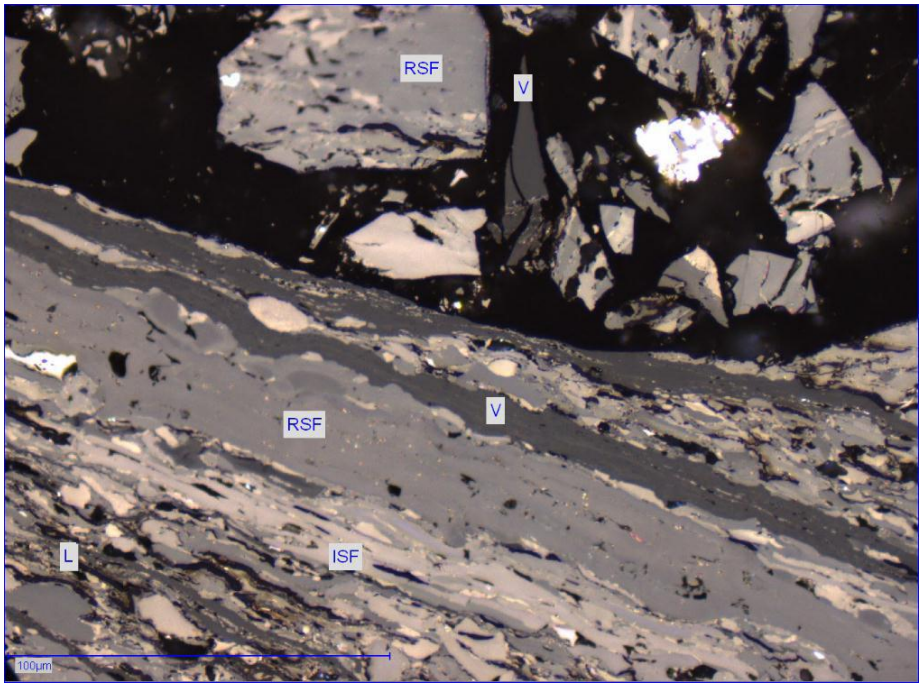

Figure A.2. Particles of vitrinite (V), reactive semi Fusinite (RSF), semi Fusinite (ISF) and liptinite (L)

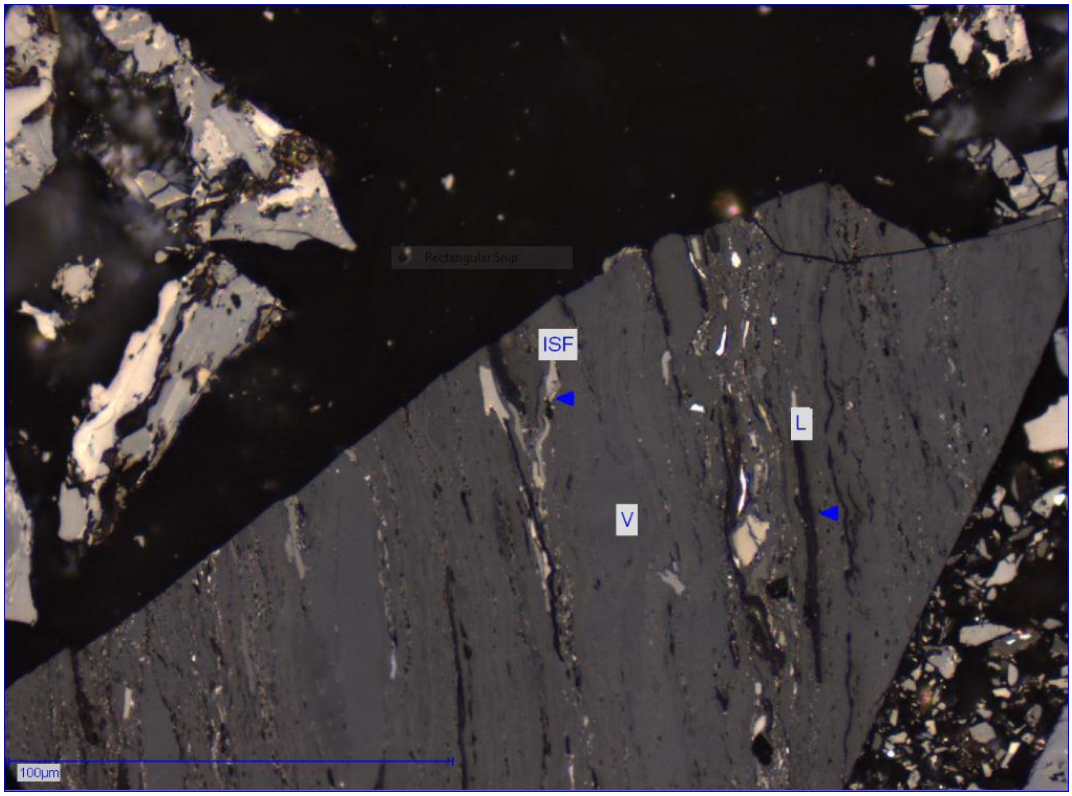

Figure A.3. Particles of semi fusinite (ISF), vitrinite (V) and liptinite (L)

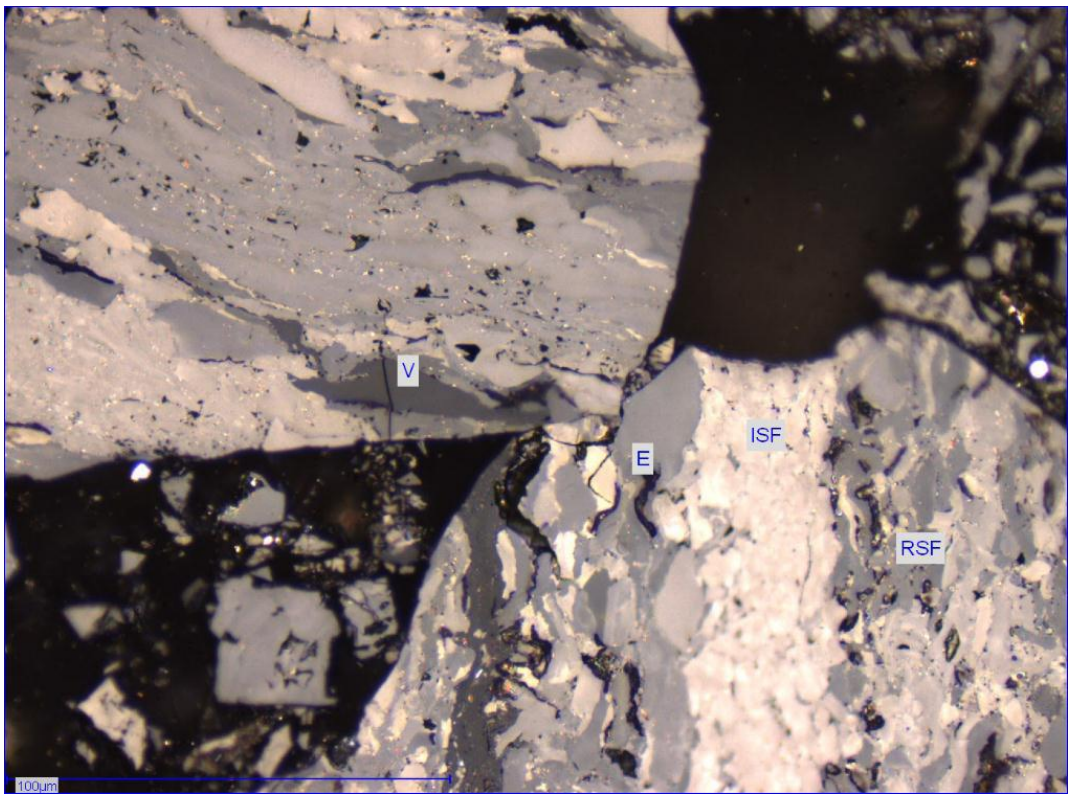

Figure A.4. Particles of vitrinite (V), semi fusinite (ISF), reactive semi fusinite (RSF) and liptinite (L)

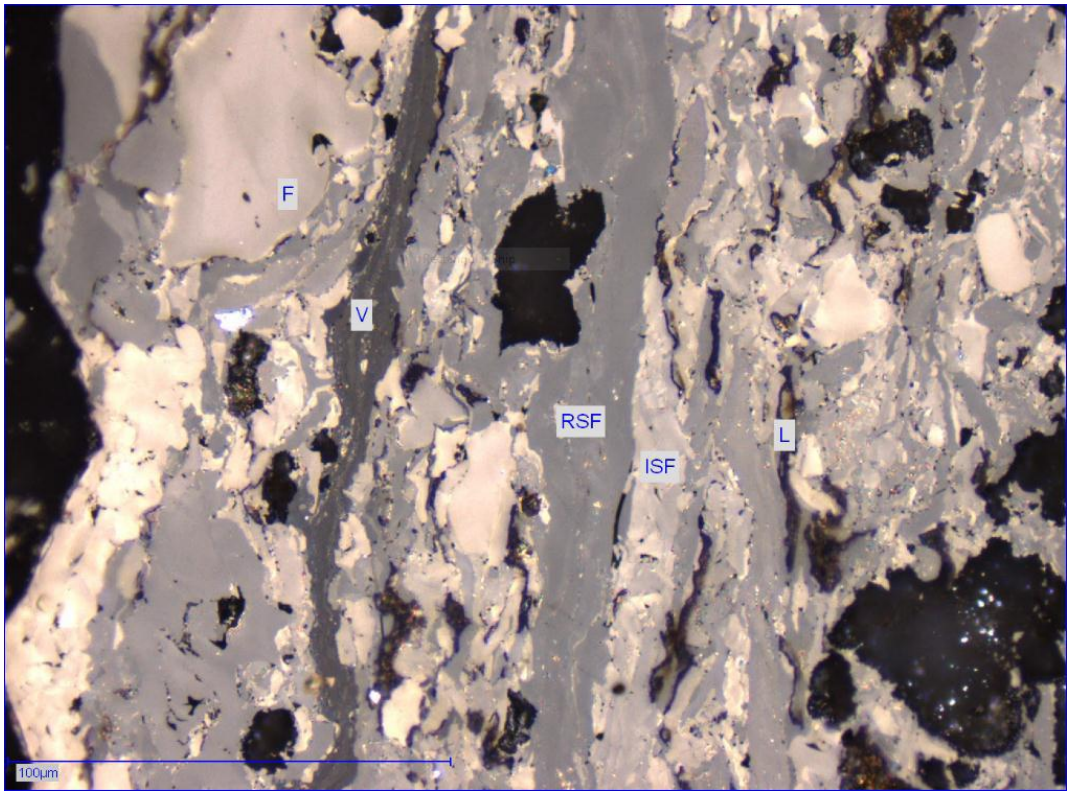

Figure A.5. Particles of vitrinite (V), reactive semi fusinite (RSF), semi fusinite (ISF) and liptinite (L)

A.2. Maceral analysis of the vitrinite rich sample

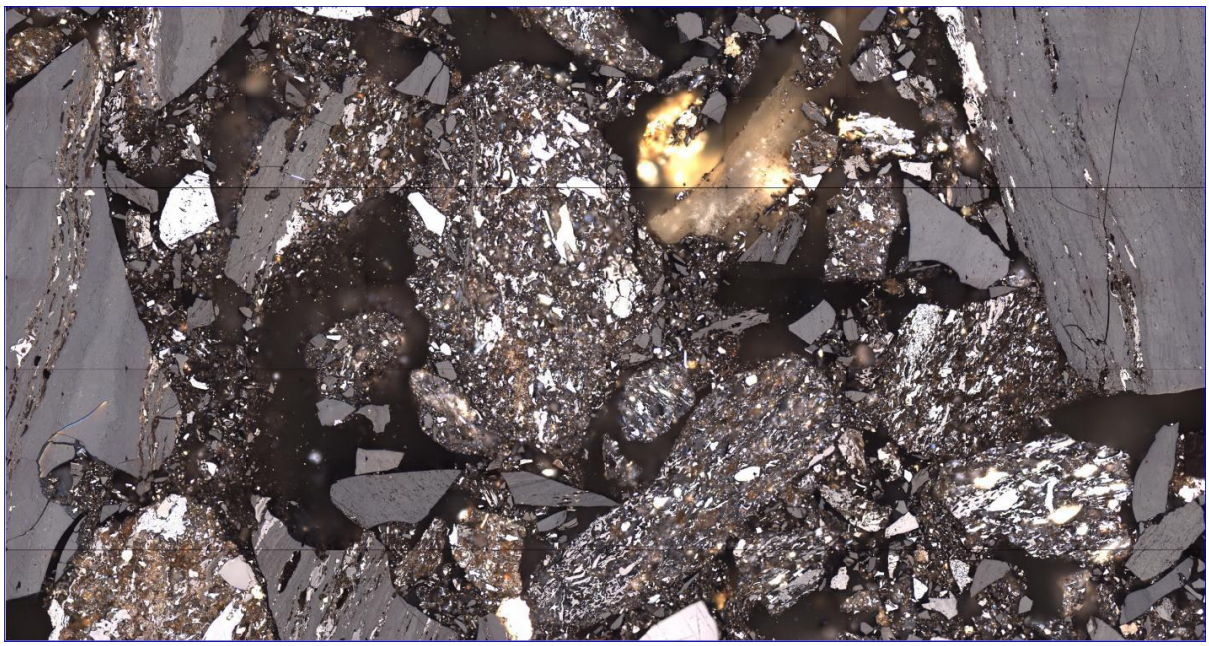

Figure A.6. Scanned overview of vitrinite rich sample

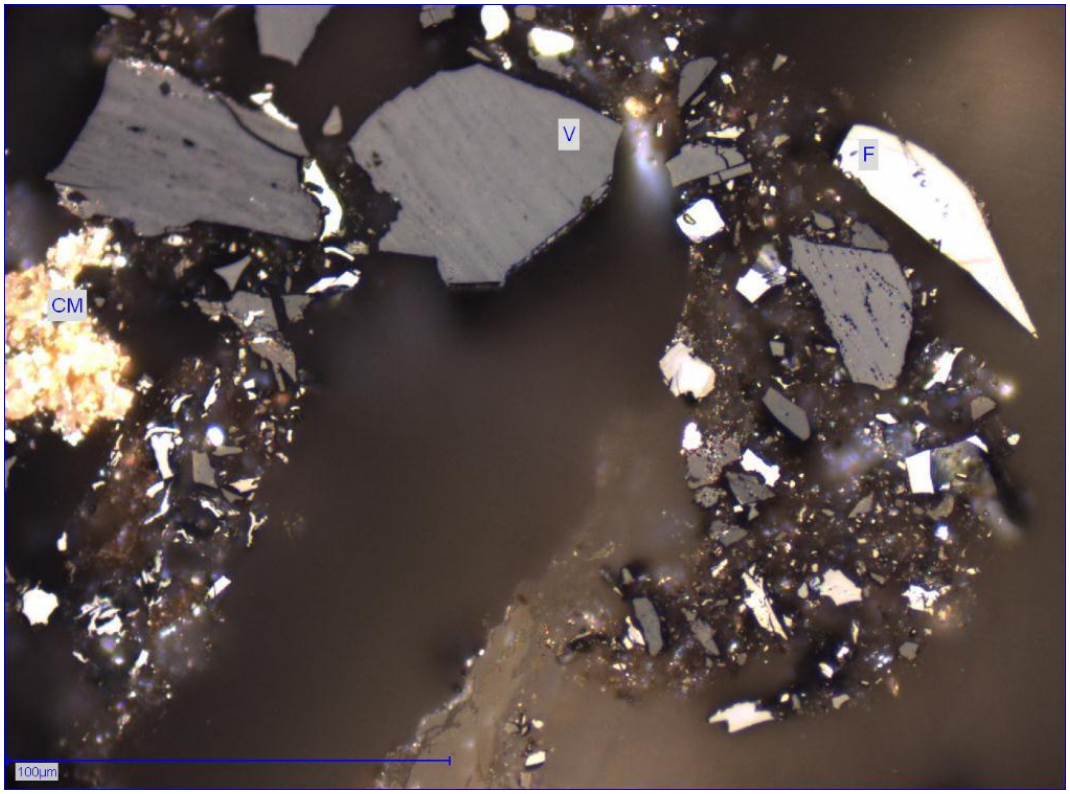

Figure A.7. Particles of vitrinite (V), Fusinite (F) and carbonate minerals (CM)

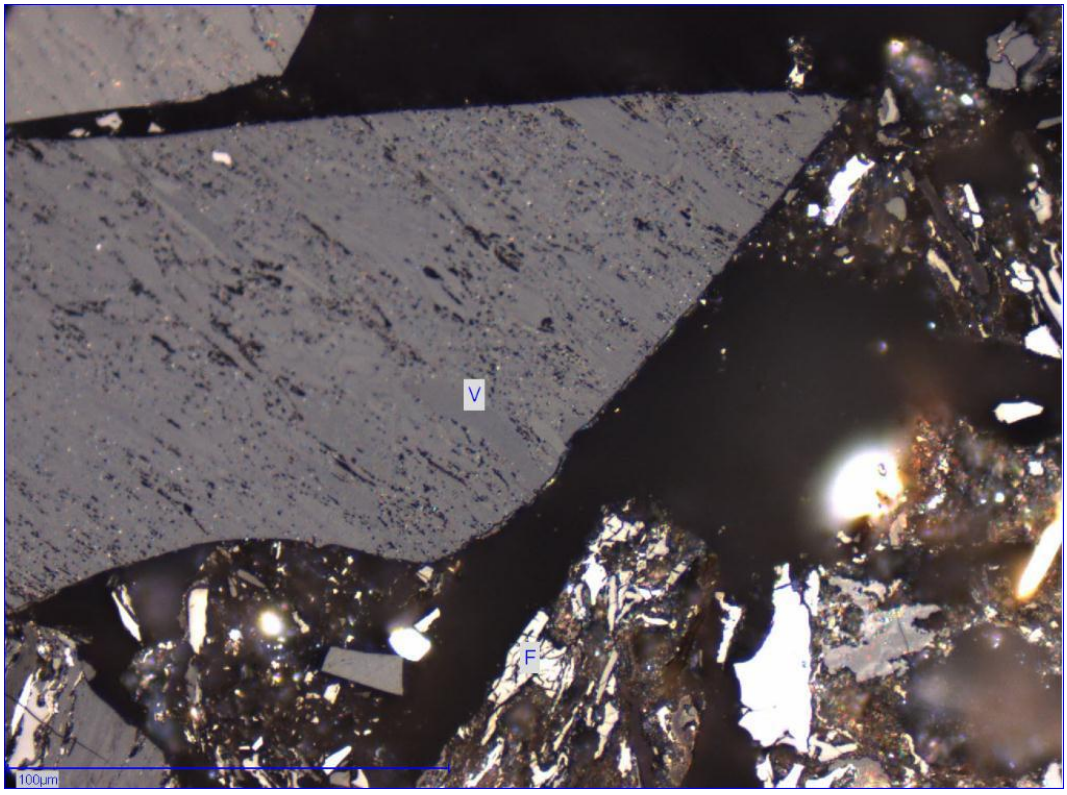

Figure A.8. Particles of Vitrinite (V) and fusinite (F)

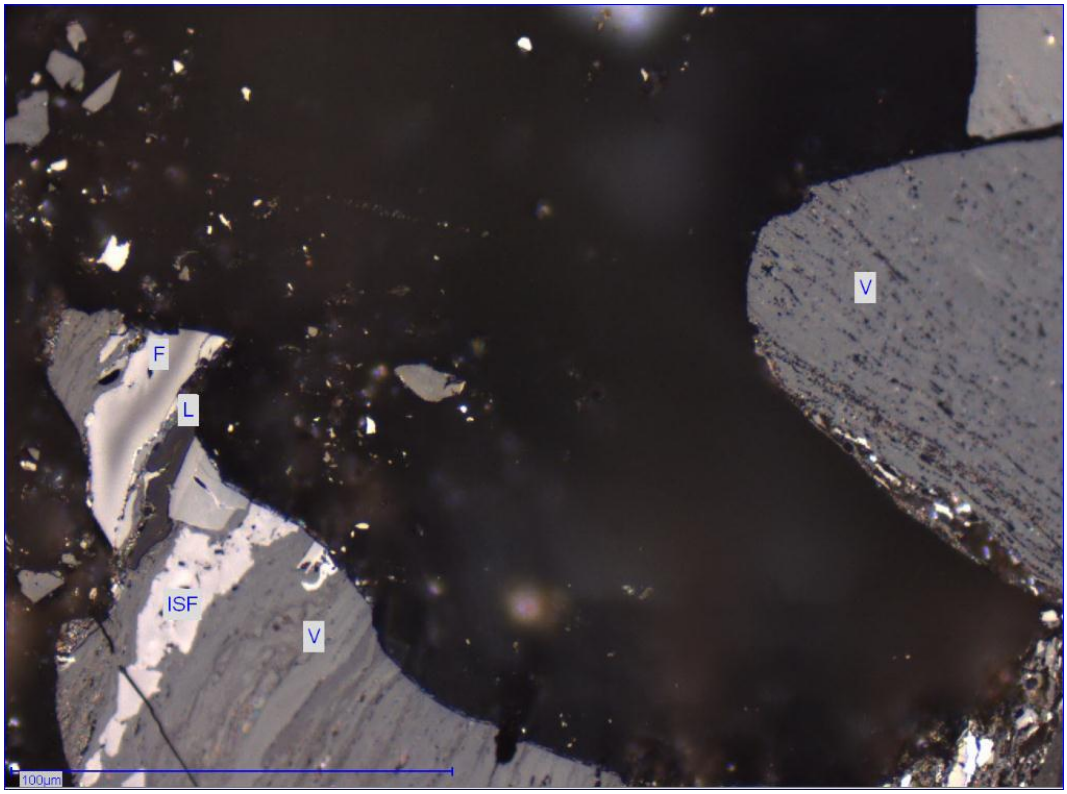

Figure A.9. Particles of vitrinite (V), semi fusinite (ISF), fusinite (F) and liptinite (L)

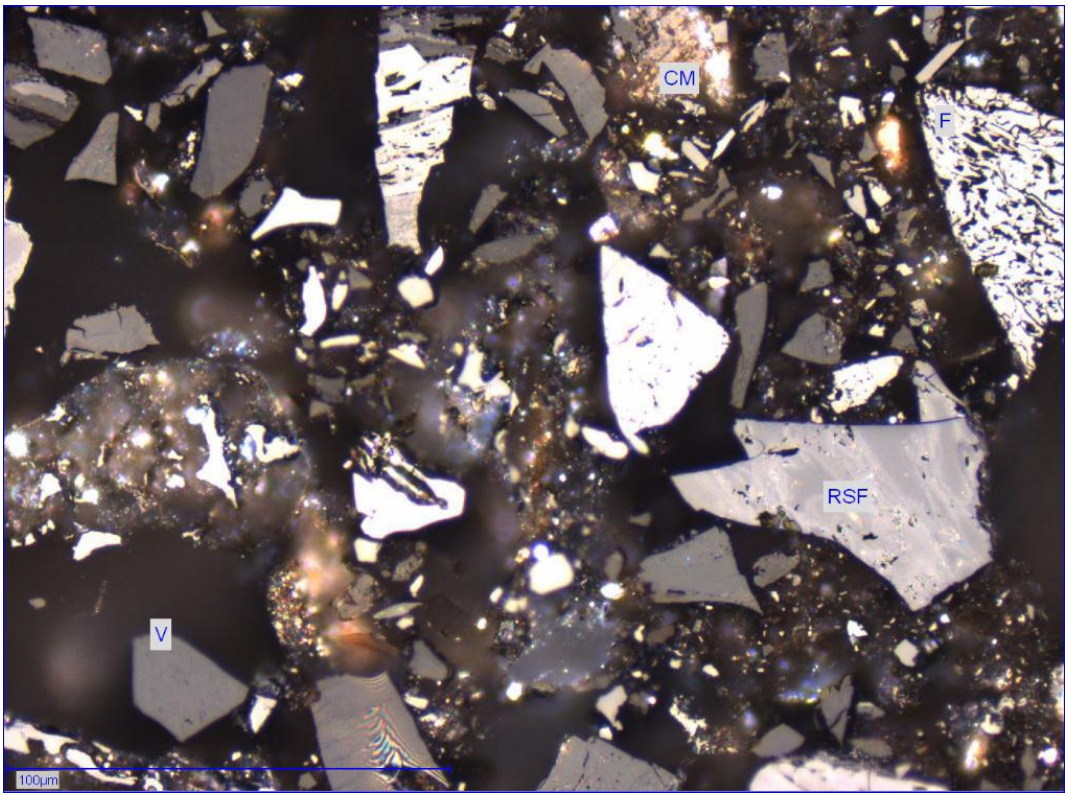

Figure A.10. Particles of vitrinite (V), reactive semi fusinite (RSF) and carbonate minerals

A.3. Procedures and standards

All the analysis was done at Bureau Veritas, Advanced Coal Technology. The procedures and standards that were followed are given below.

- **Sample preparation**

ACT-TPM-001 based on ISO 13909-4: 2001

- **Moisture content (%)**

ACT-TPM-010 based on SANS 5925: 2007

- **Ash content (%)**

ACT-TPM-011 based on ISO 1171: 2010

- **Volatile matter content (%)**

ACT-TPM-012 based on ISO 562: 2010

- **Total sulphur via IR spectroscopy (%)**

ACT-TPM-013 based on ISO 19579: 2006

- **Gross calorific value (MJ/kg)**

ACT-TPM-014 based on ISO 1928: 2009

- **Screen analysis (mm)**

ACT-TPM-003 based on SABS ISO 1953 – 1994 (Not SANAS Accredited)

- **Petrographic analyses of bituminous coal and anthracite**

ACT-TPM-026 based on ISO 7404: 1994 Part 1 to 5 (Not SANAS Accredited)

APPENDIX B

Appendix B contains the following experimental results:

- B.1. Inertinite rich coal samples: desorption isotherms
- B.2. Inertinite rich coal samples: filter cakes dried at static conditions
- B.3. Inertinite rich coal samples: comparison between static bed and fluidised bed
- B.4. Inertinite rich coal samples: filter cakes dried in the fluidised bed
- B.5. Inertinite rich coal samples: Non-ideal fluidised conditions
- B.6. Inertinite rich coal samples: repeatability tests
- B.7. Inertinite rich coal samples: model fit
- B.8. Vitrinite rich coal samples: desorption isotherm
- B.9. Vitrinite rich coal samples: filter cakes dried at static conditions
- B.10. Vitrinite rich coal samples: comparison between static bed and fluidised bed
- B.11. Vitrinite rich coal samples: filter cakes dried in the fluidised bed

B.1. Inertinite rich coal samples: desorption isotherms

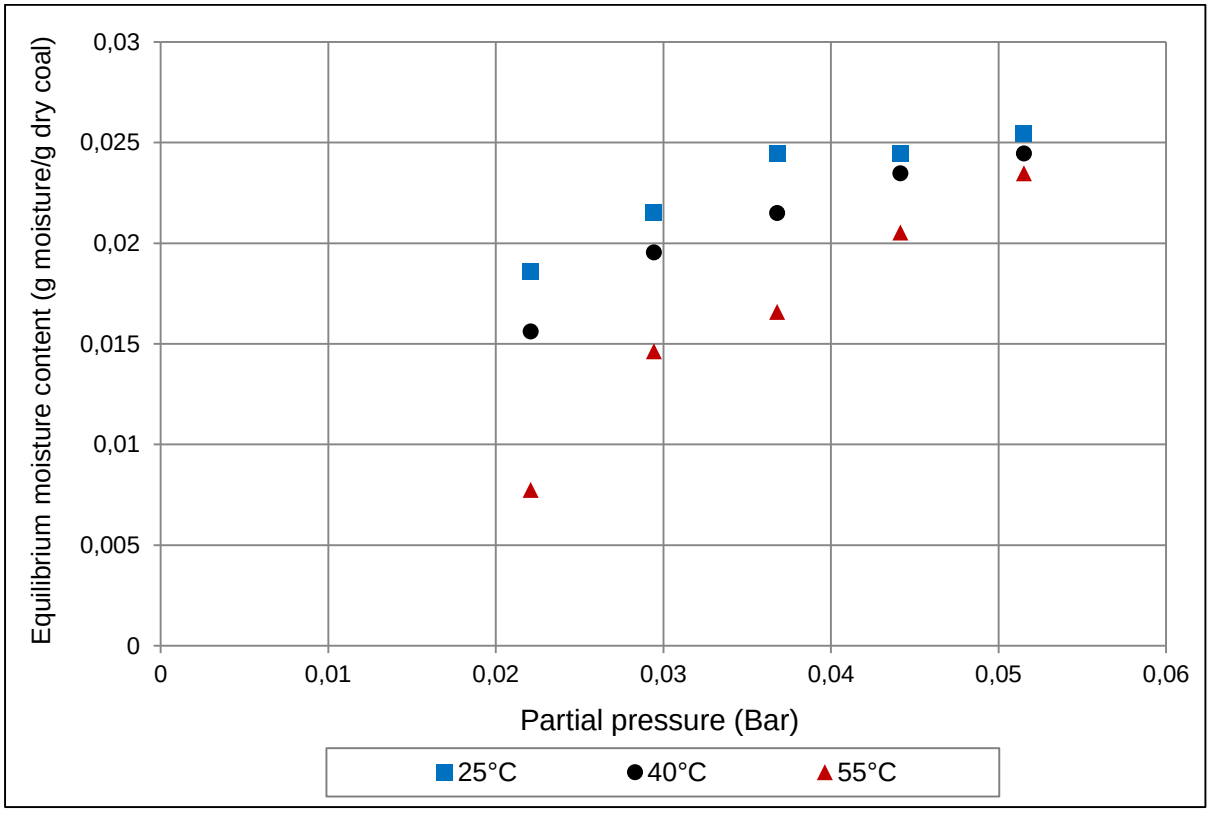

Figure B.1. Desorption isotherm at 25°C, 40°C and 55°C and a humidity range of 70% to 30%

B.2. Inertinite rich coal samples: filter cakes dried at static conditions

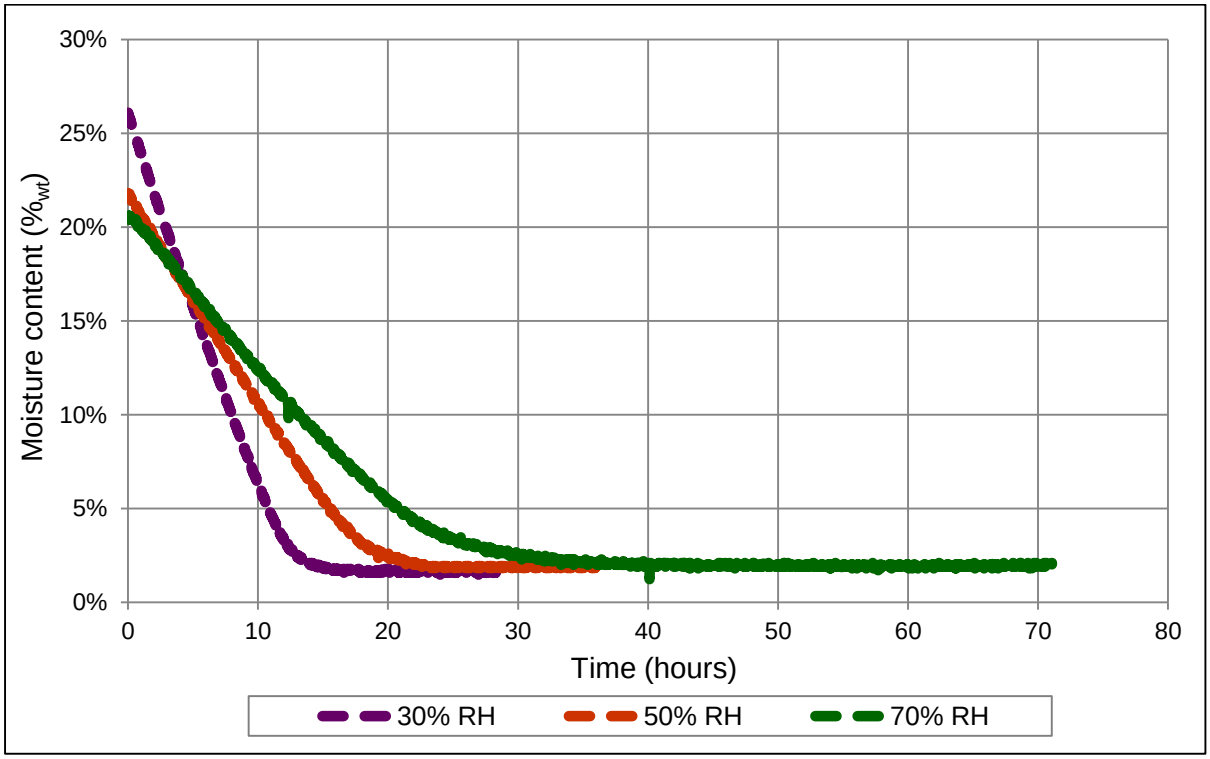

Figure B.2. Static bed drying of filter cakes at 25°C and various relative humidity conditions

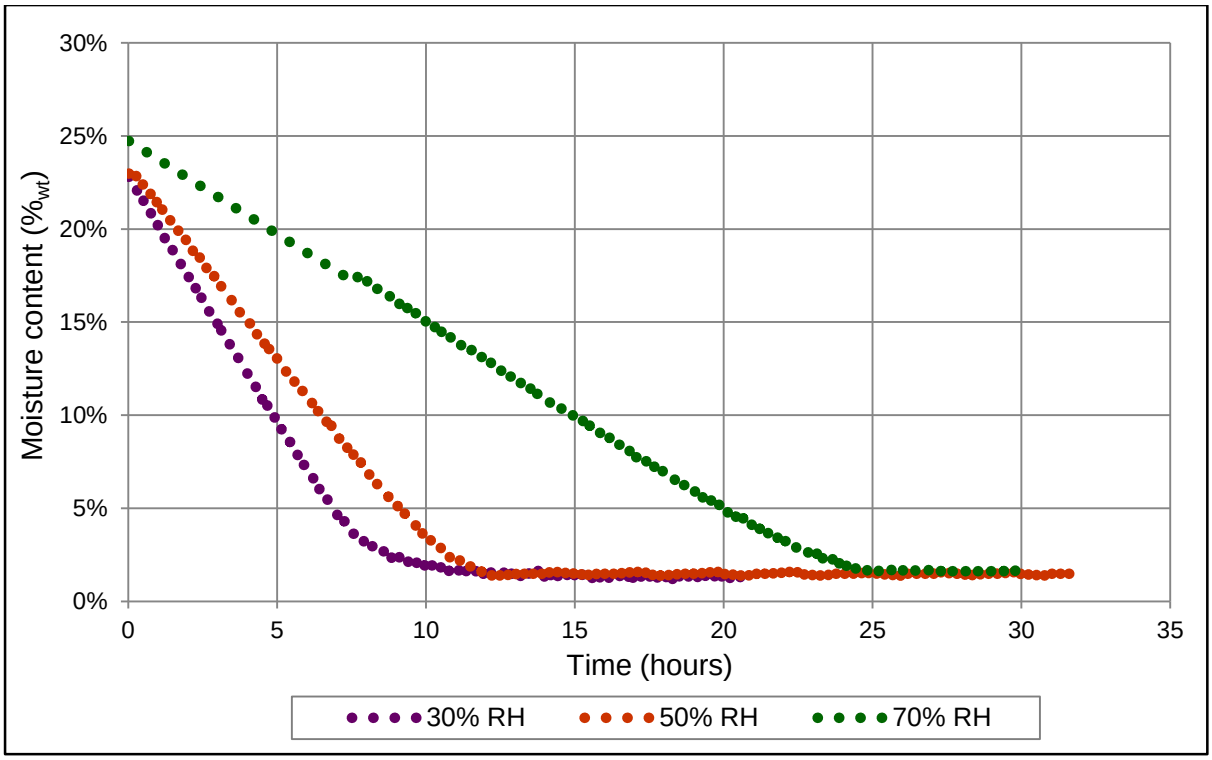

Figure B.3. Static bed drying of filter cakes at 40°C and various relative humidity conditions

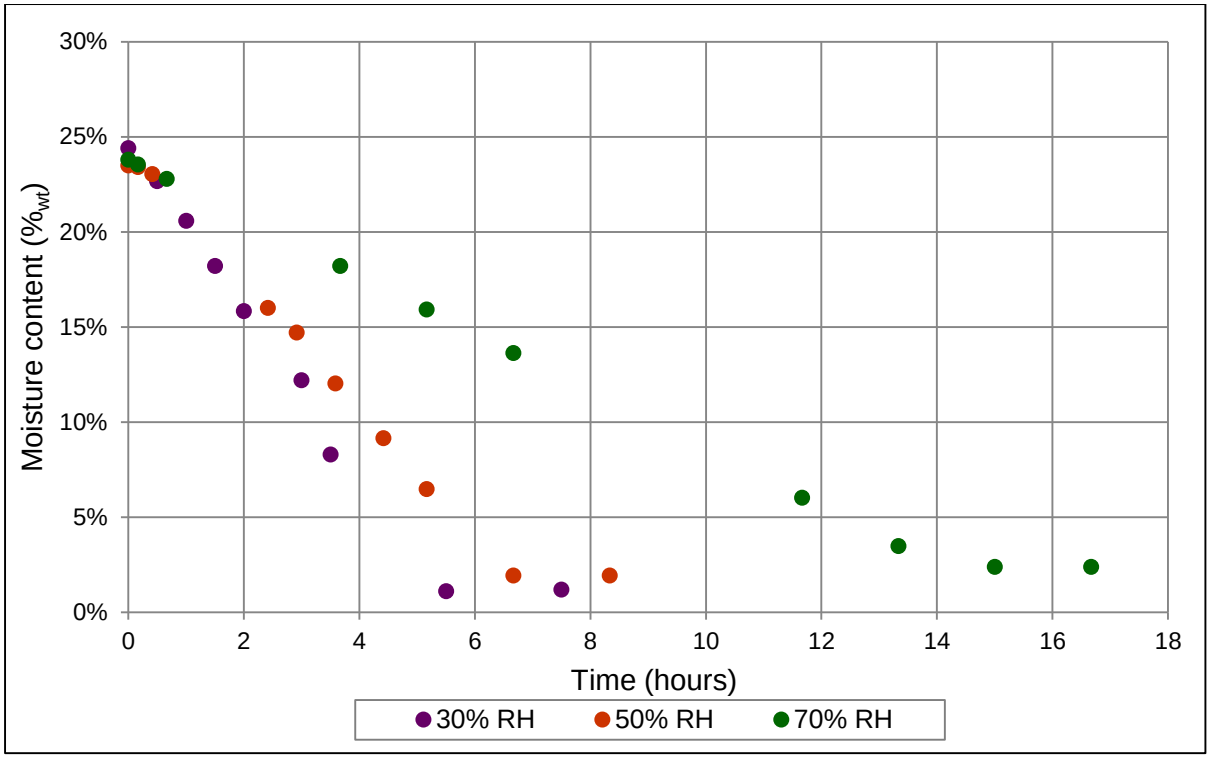

Figure B.4. Static bed drying of filter cakes at 55°C and various relative humidity conditions

B.3. Inertinite rich coal samples: comparison between static bed and fluidised bed

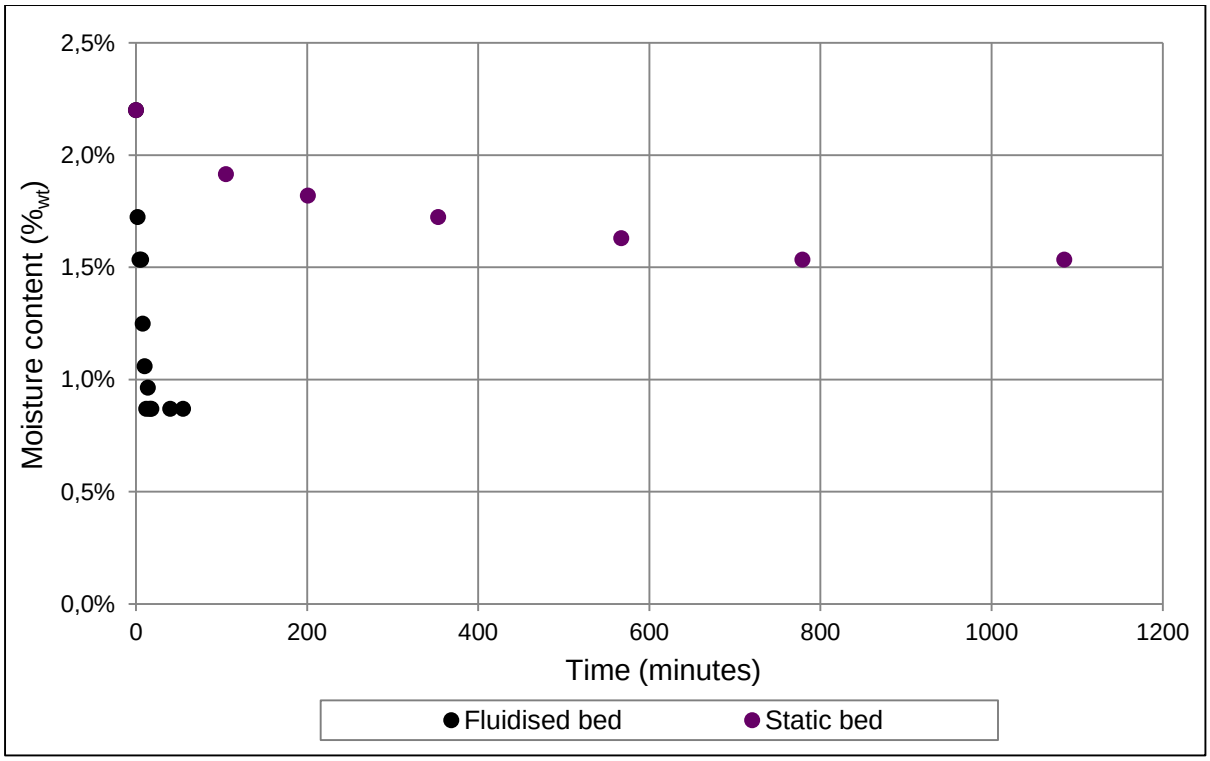

Figure B.5. Comparison between static and fluidised bed to reduce equilibrium moisture content at 25°C and 30% RH

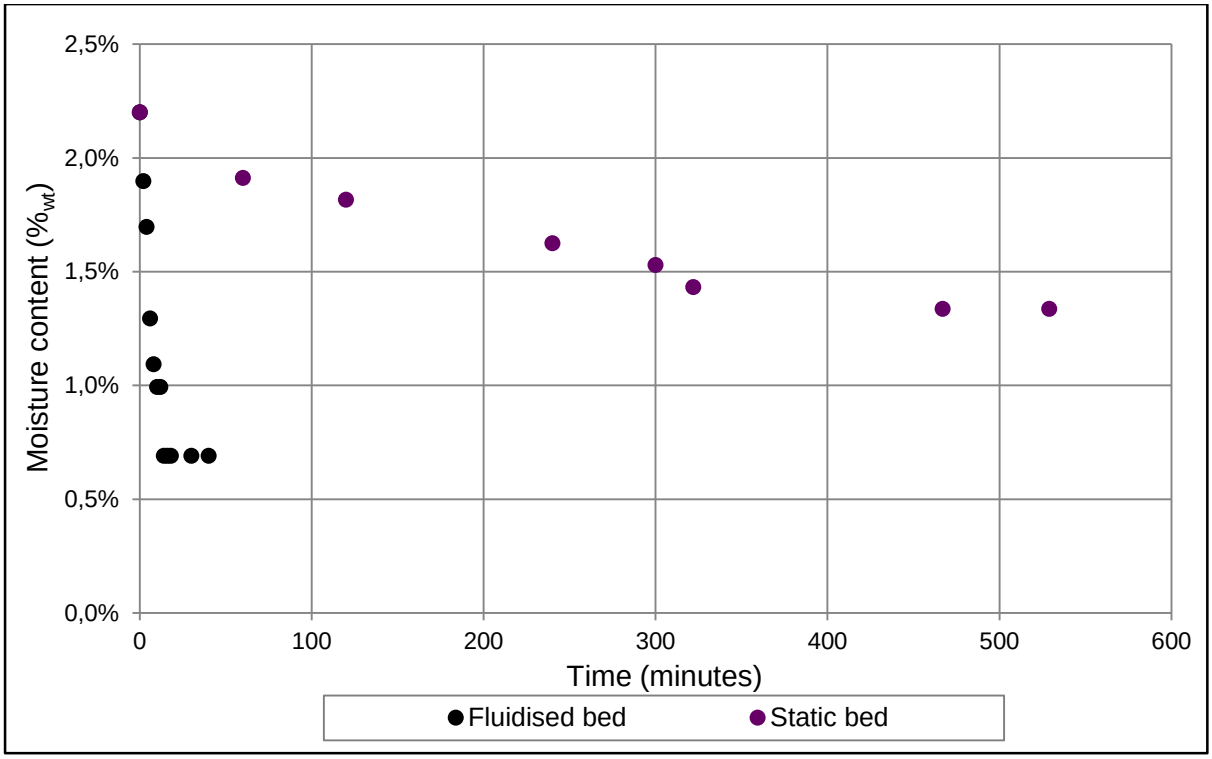

Figure B.6. Comparison between static and fluidised bed to reduce equilibrium moisture content at 40°C and 30% RH

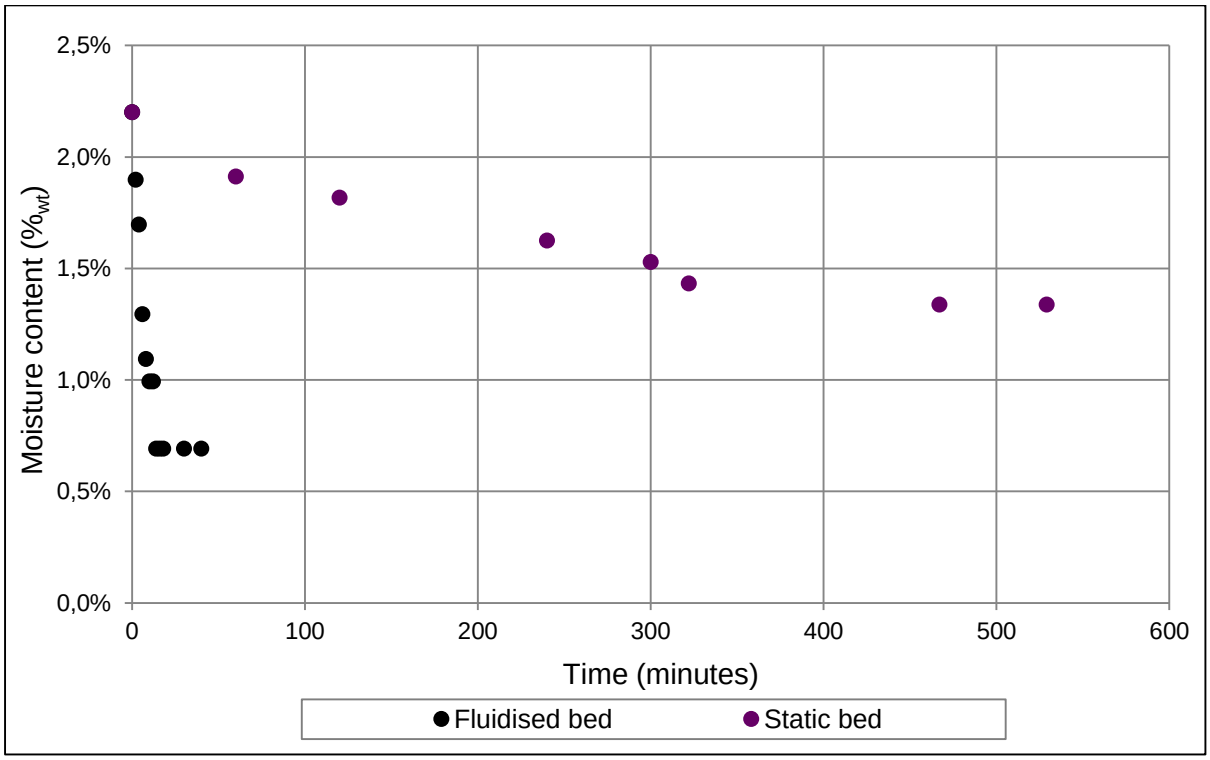

Figure B.7. Comparison between static and fluidised bed to reduce equilibrium moisture content at 55°C and 30% RH

B.4. Inertinite rich coal samples: filter cakes dried at static conditions

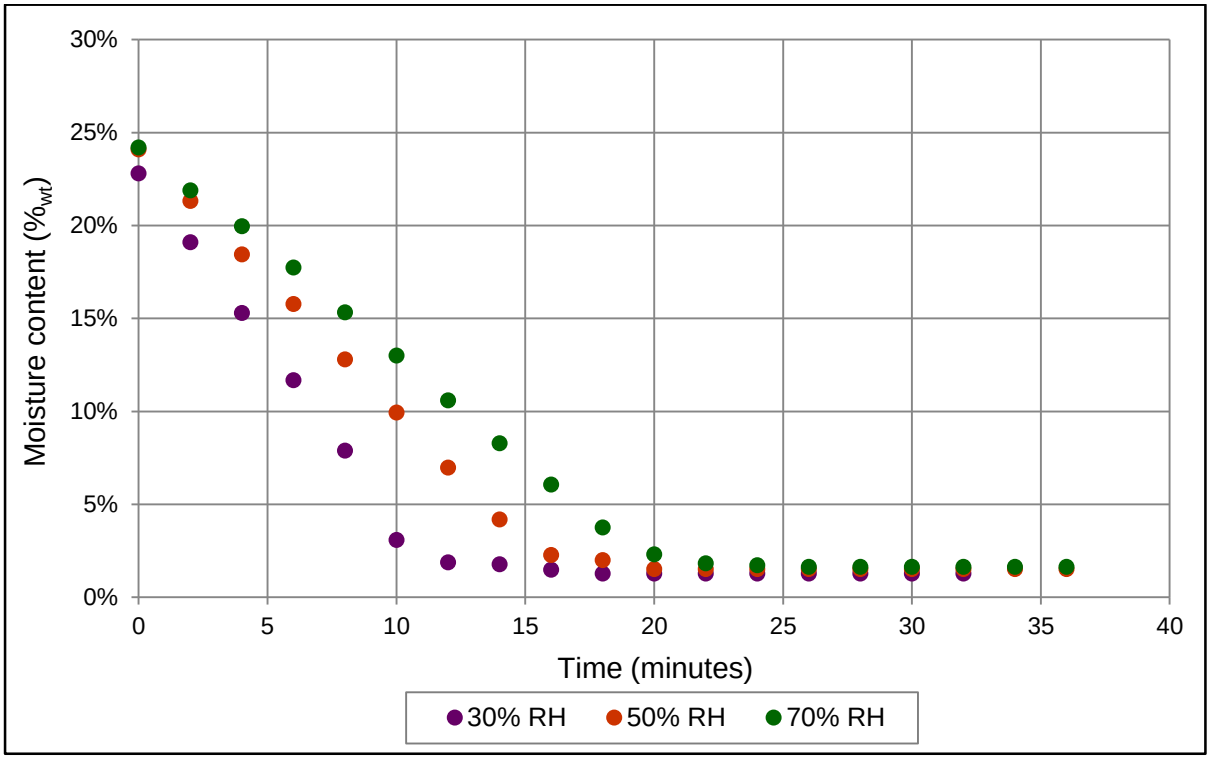

Figure B.8. Drying of filter cakes in a fluidised bed at 25°C and various relative humidity conditions

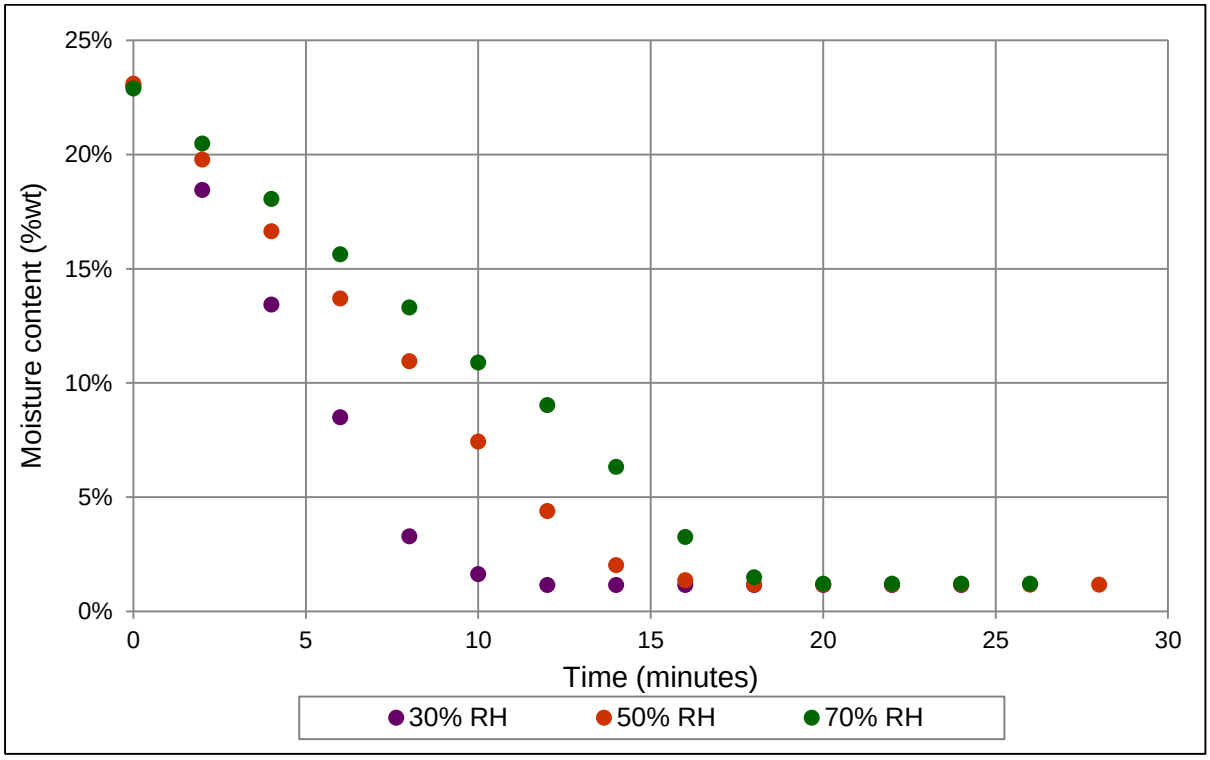

Figure B.9. Drying of filter cakes in a fluidised bed at 40°C and various relative humidity conditions

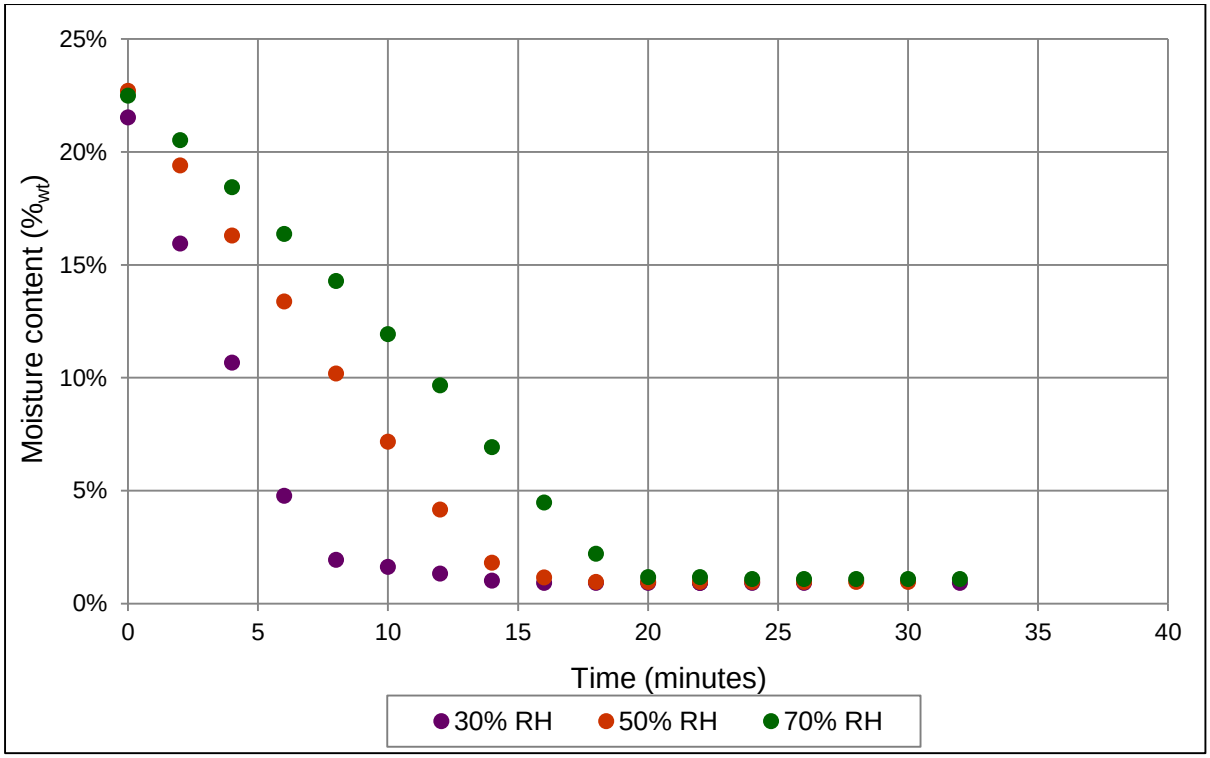

Figure B.10. Drying of filter cakes in a fluidised bed at 55°C and various relative humidity conditions

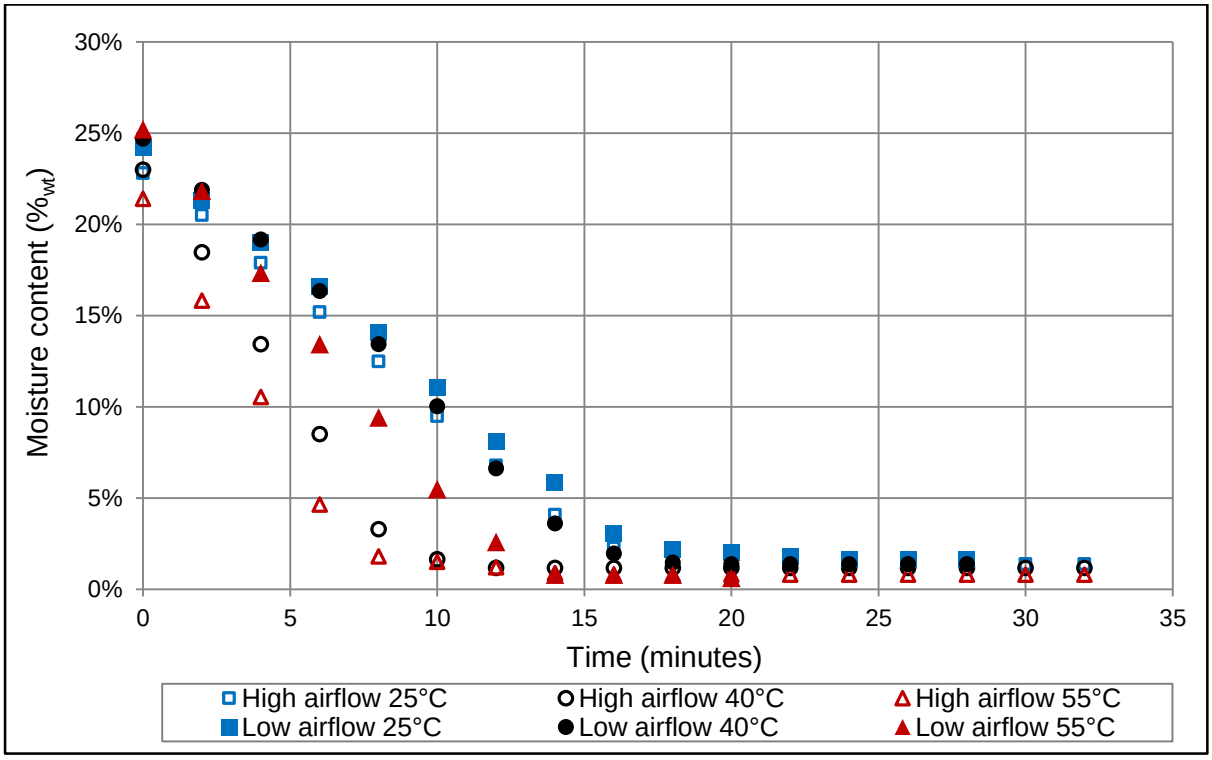

Figure B.11. Drying of filter cakes at low and high airflow in a fluidised bed at 25°C, 40°C and 55°C and 30% RH

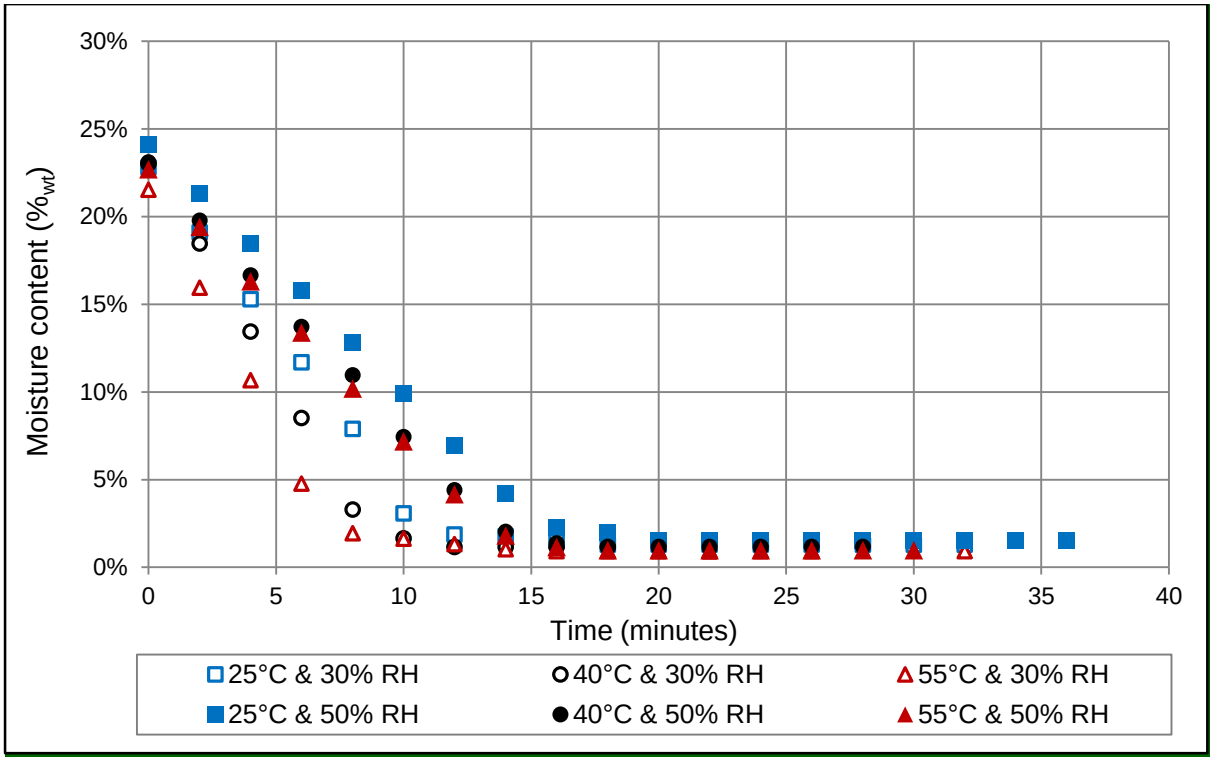

Figure B.12. Drying of filter cakes in a fluidised bed at 25°C, 40°C and 55°C and 30 and 50% RH

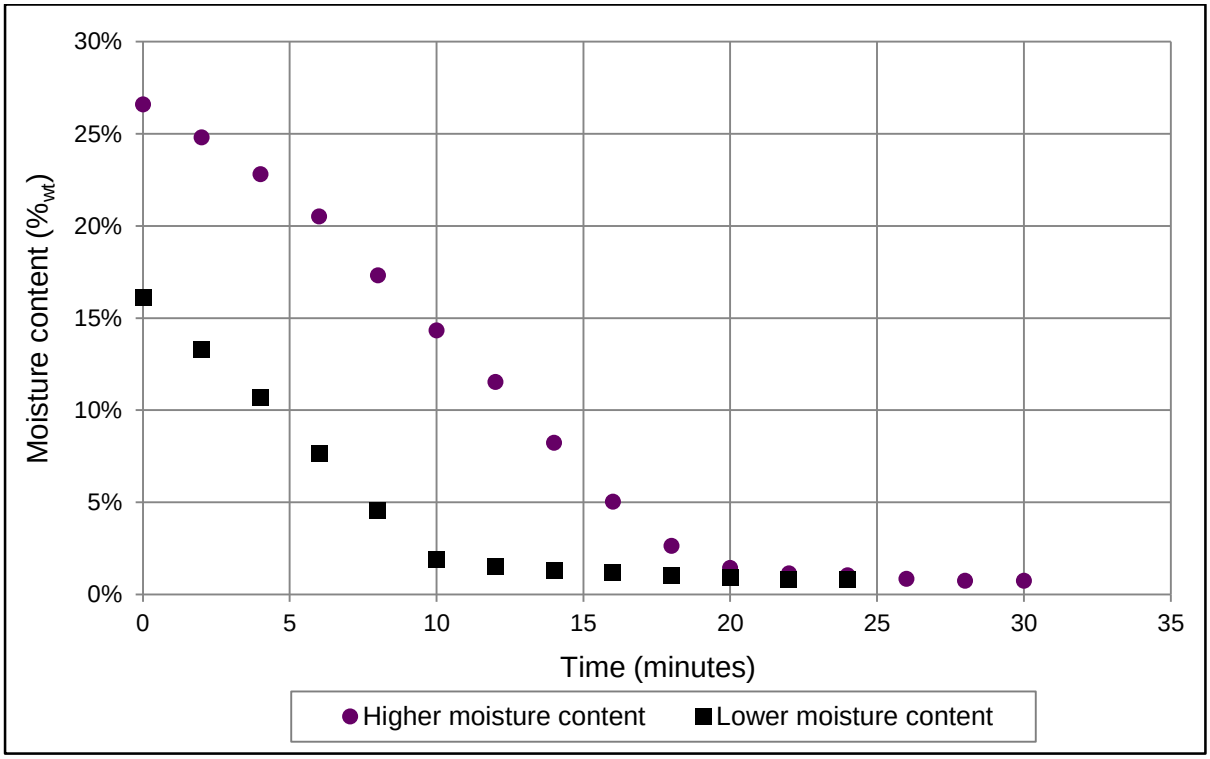

Figure B.13. Drying of 15%$_{wt}$ and 25%$_{wt}$ filter cakes in a fluidised bed at 55°C and 50% RH

B.5. Inertinite rich coal samples: non-ideal fluidised conditions

Filter cakes of 100g and a moisture content of about 25%$_{wt}$ each were broken up and dried in a fluidised bed with warm air at 55°C at a relative humidity of 50%. Some wet particles of the one test run got stuck on the side of the fluidised bed cylinder as can be seen in Figure 4.13. When observing the drying curves in Figure 4.14. it was clear the both test samples had similar drying rates. The test sample without any wall effect had a drying rate of 0.0135 $\frac{\%\, moisture}{min}$ and the test sample with wall effect had a drying rate of 0.0137 $\frac{\%\, moisture}{min}$.

Furthermore it was also noted during the experimental work that the airflow wasn't able to sufficiently dry the particles that got stuck to the side of the fluidised bed cylinder. Those particles remained moist and cleaved to the wall during the course of the experimental run. The test run was stopped when the moisture content continued to remain constant for several minutes. The final moisture content of the test sample with the wall effect was 3.19%$_{wt}$ higher compared to the other test sample without the wall effect. This moisture content will however vary from test run to test run, according to the amount of wet particles stuck on the wall of the vessel.

Figure B.14. Particles sticking to the side of the fluidised bed cylinder

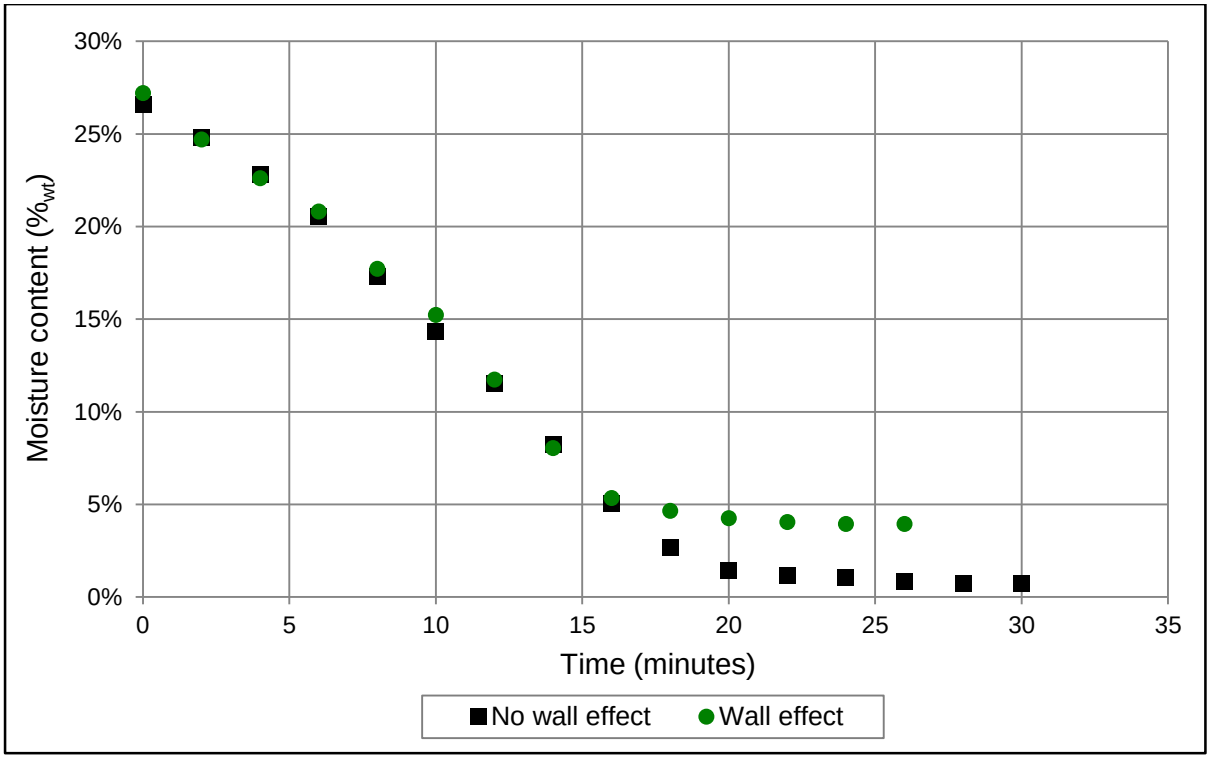

Figure B.15. Drying of filter cakes, with and without wall effect, in a fluidised bed at 55°C and 50% RH

B.6. Inertinite rich coal samples: repeatability tests

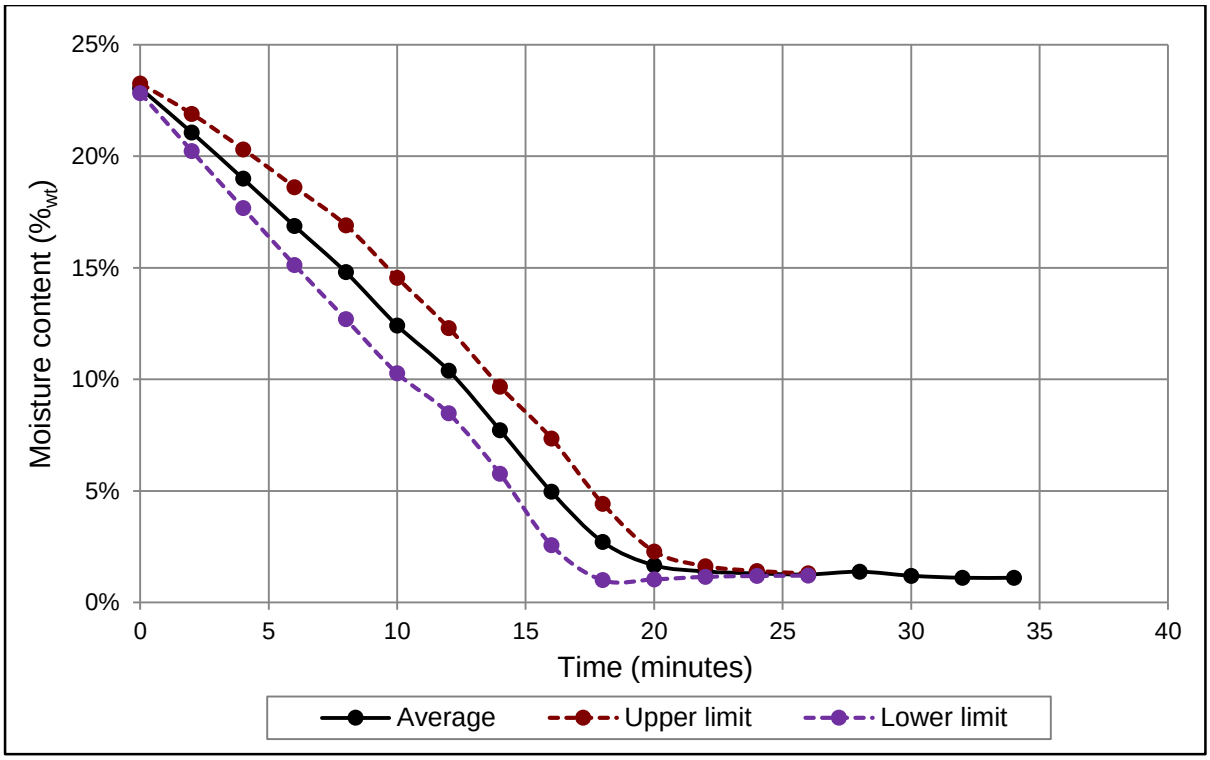

Figure B.16. Average and standard deviation of repeats done at 40°C and 70% RH

Table B.1. Calculated average and standard deviation at 40°C and 70% RH

Time (min)	Experiment 1 ($\%_{wt}$)	Experiment 2 ($\%_{wt}$)	Average ($\%_{wt}$)	Standard deviation ($\%_{wt}$)
0	22.90%	23.20%	23.05%	0.21%
2	20.48%	21.65%	21.07%	0.83%
4	18.06%	19.93%	19.00%	1.32%
6	15.64%	18.11%	16.88%	1.74%
8	13.32%	16.29%	14.80%	2.10%
10	10.90%	13.93%	12.41%	2.14%
12	9.04%	11.75%	10.39%	1.91%
14	6.34%	9.11%	7.73%	1.96%
16	3.27%	6.65%	4.96%	2.39%
18	1.50%	3.93%	2.72%	1.71%
20	1.23%	2.11%	1.67%	0.62%
22	1.23%	1.56%	1.39%	0.24%
24	1.23%	1.38%	1.30%	0.11%
26	1.23%	1.29%	1.26%	0.05%

Table B.2. Calculated average and standard deviation at 55°C and 50% RH

Time (min)	Experiment 1 (%wt)	Experiment 2 (%wt)	Average (%wt)	Standard deviation (%wt)
0	16.14%	16.70%	16.42%	0.20%
2	13.27%	15.06%	14.16%	0.63%
4	10.69%	10.03%	10.36%	0.23%
6	7.62%	4.43%	6.03%	1.13%
8	4.56%	1.72%	3.14%	1.00%
10	1.88%	1.43%	1.66%	0.16%
12	1.50%	1.14%	1.32%	0.13%
14	1.31%	0.85%	1.08%	0.16%
16	1.21%	0.76%	0.98%	0.16%
18	1.02%	0.76%	0.89%	0.09%
20	0.92%	0.76%	0.84%	0.06%

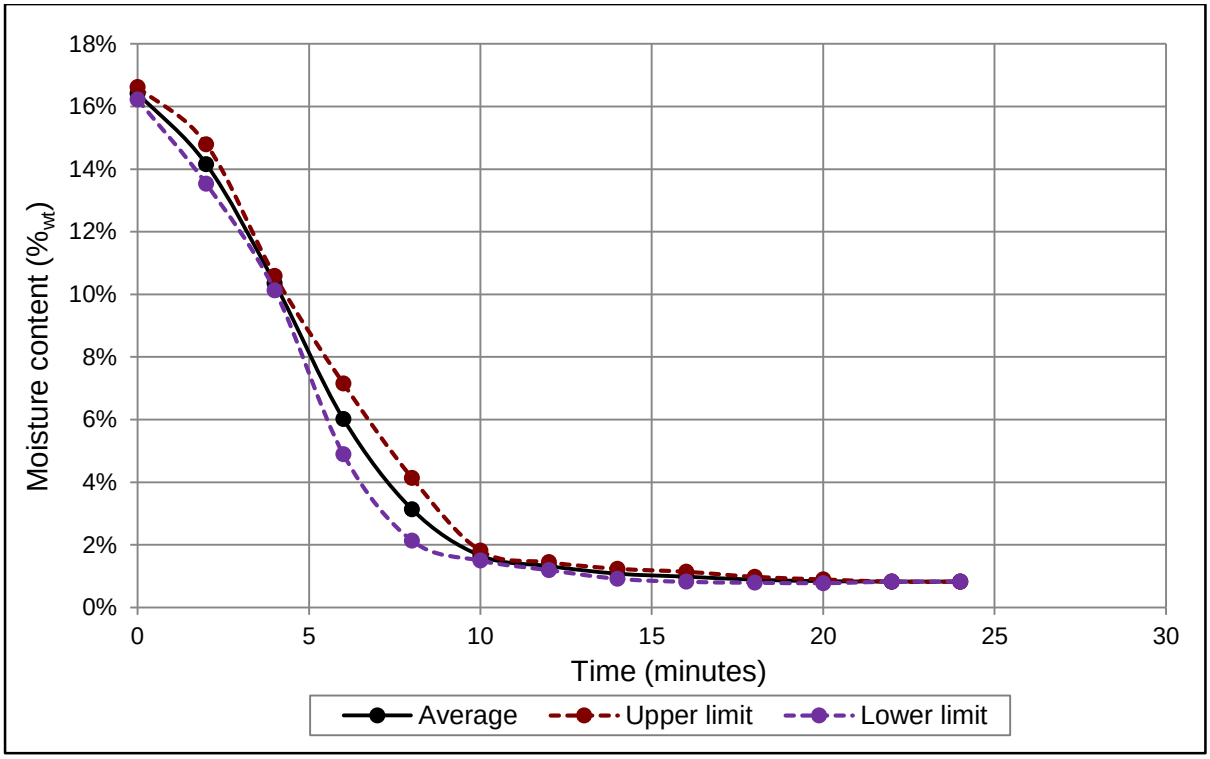

Figure B.17. Average and standard deviation of repeats done at 55°C and 50% RH

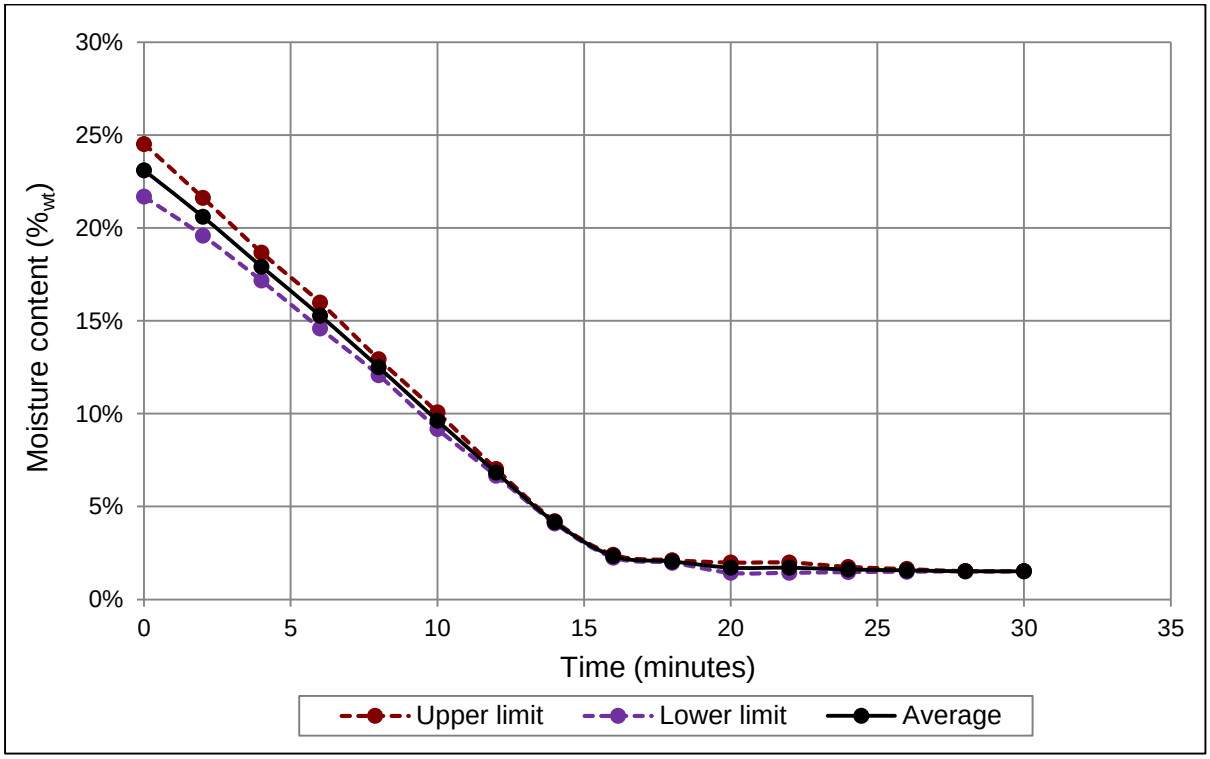

Figure B.18. Average and standard deviation of repeats done at 25°C and 50% RH

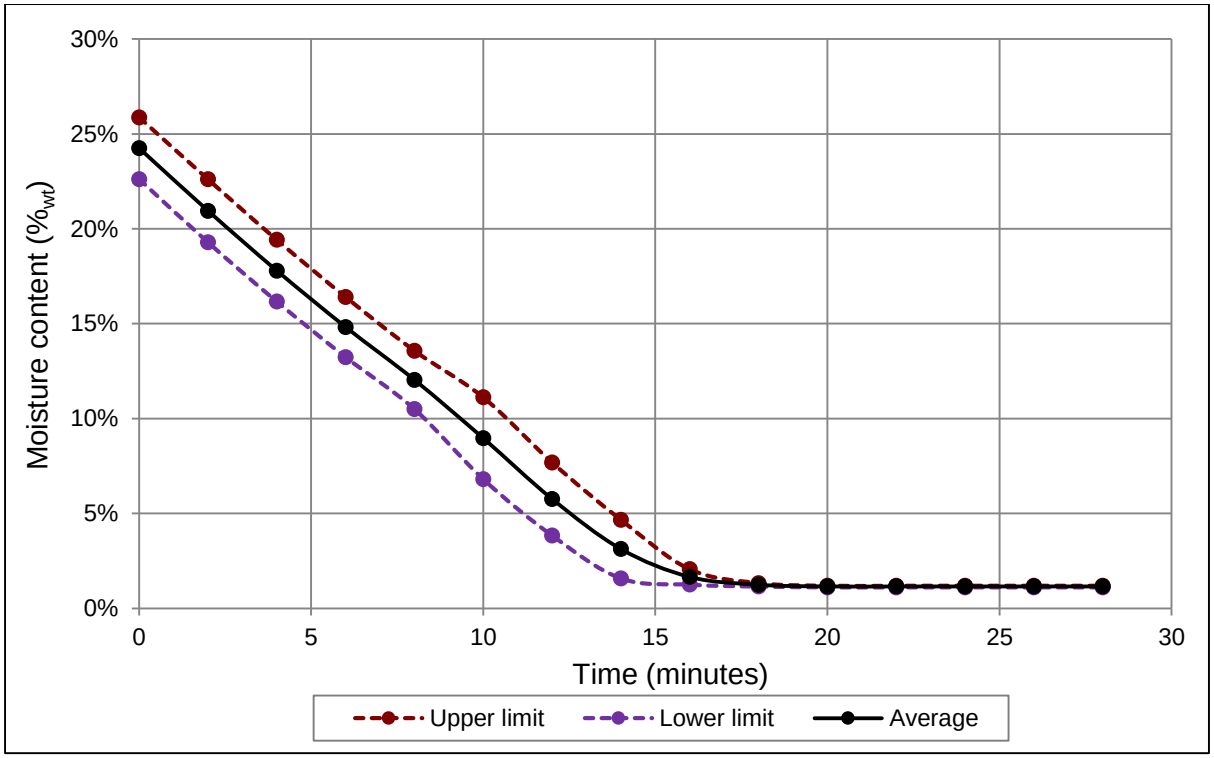

Figure B.19. Average and standard deviation of repeats done at 40°C and 50% RH

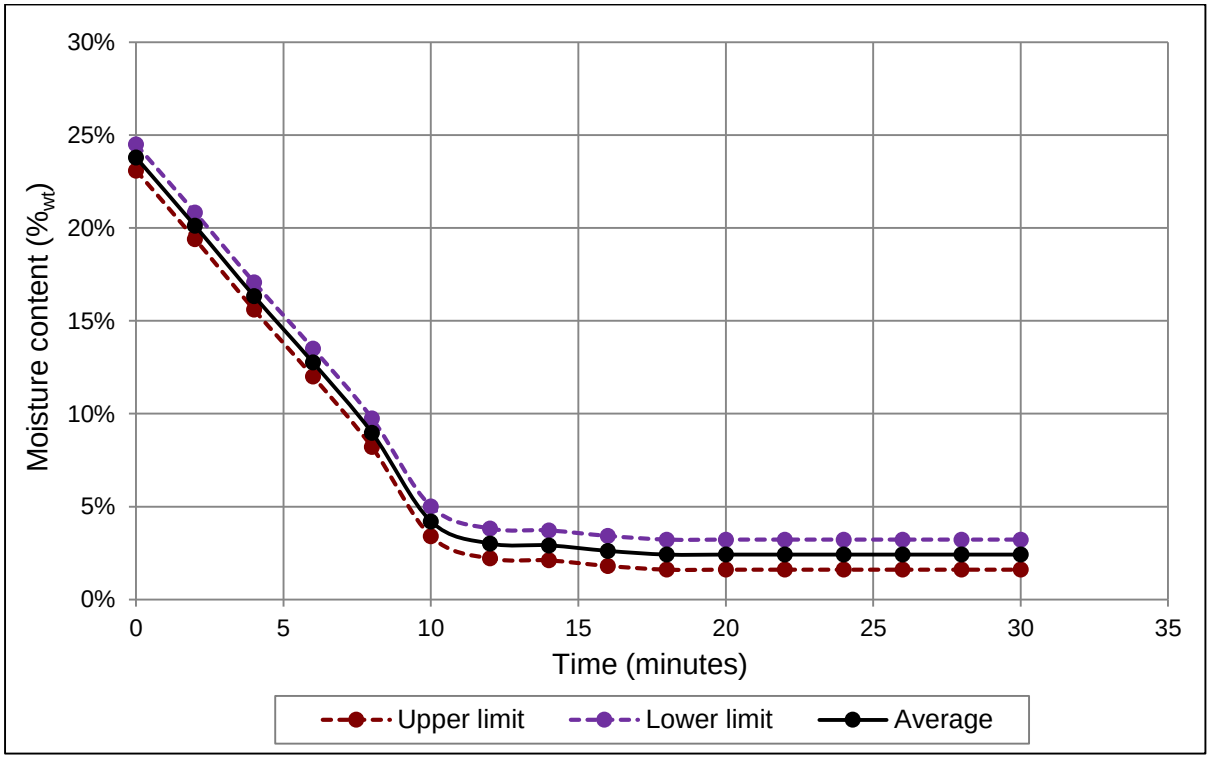

Figure B.20. Average and standard deviation of repeats done at 25°C and 30% RH

B.7. Inertinite rich coal samples: model fit

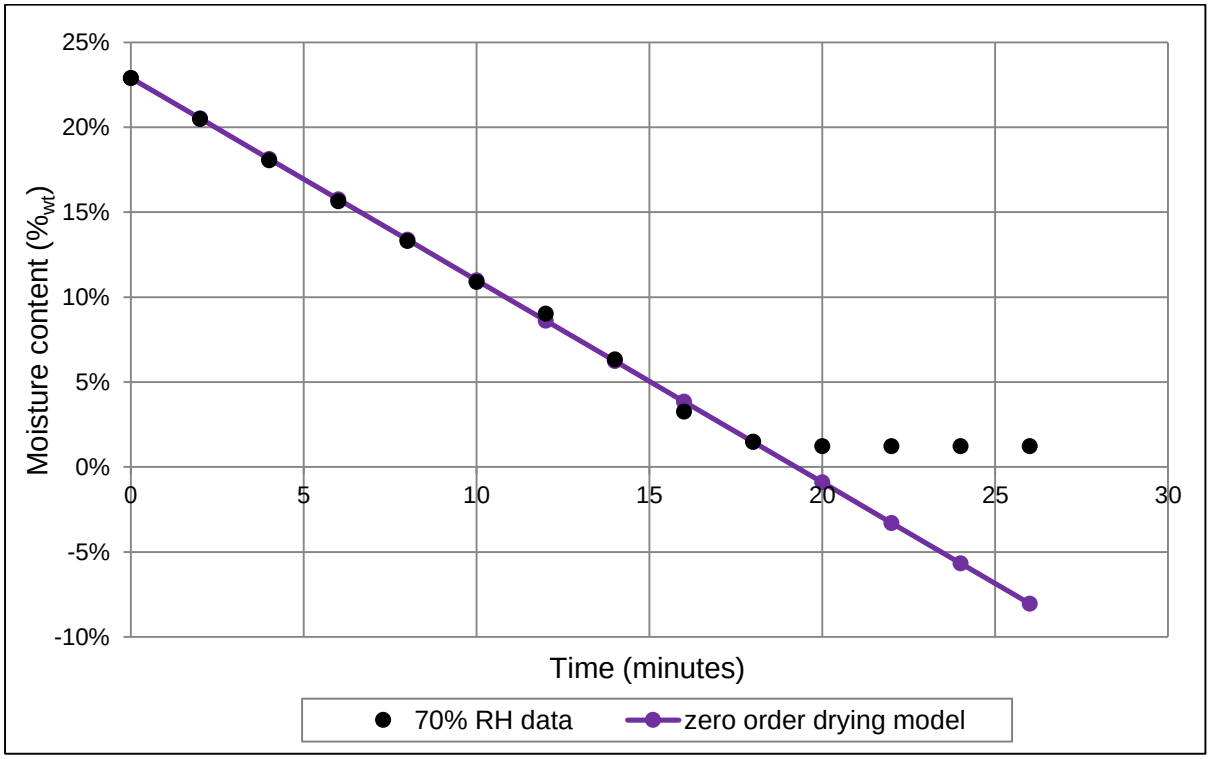

Figure B.21. Comparison between drying models and experimental data; 40°C and 70% RH

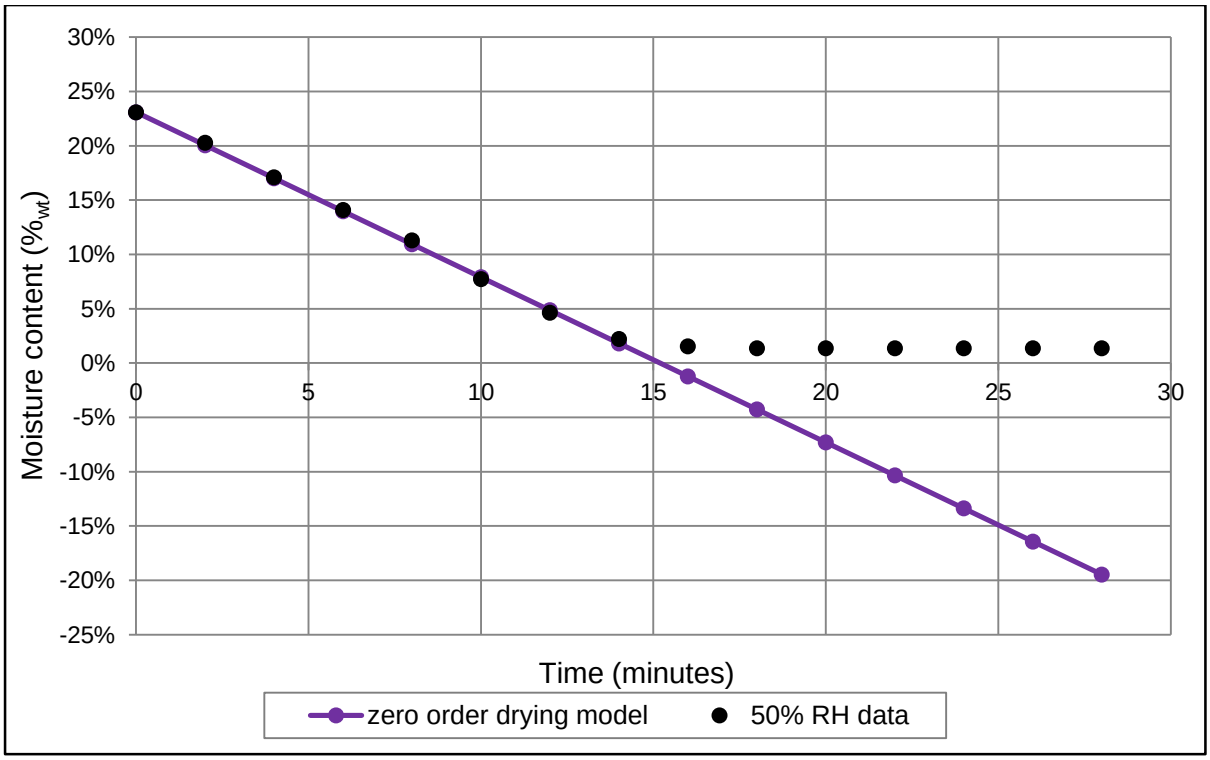

Figure B.22. Comparison between drying models and experimental data; 40°C and 50% RH

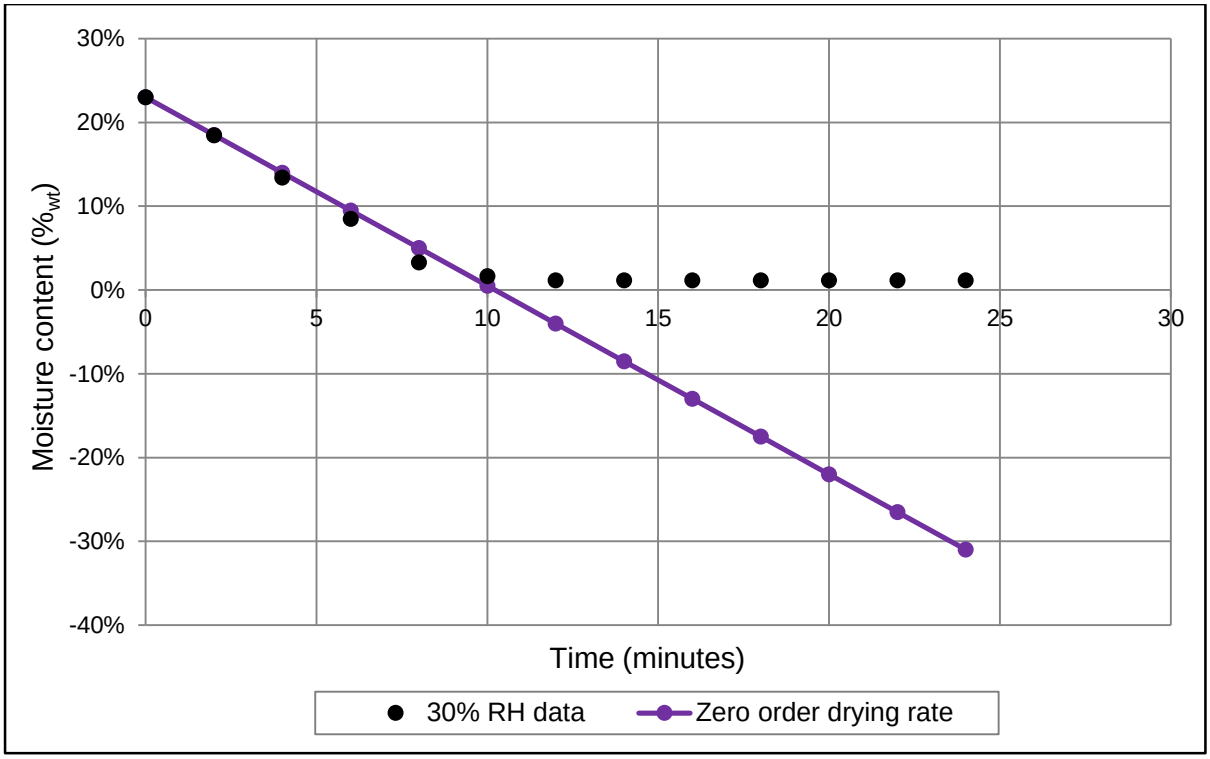

Figure B.23. Comparison between drying models and experimental data; 40°C and 30% RH

B.8. Vitrinite rich coal samples: desorption isotherms

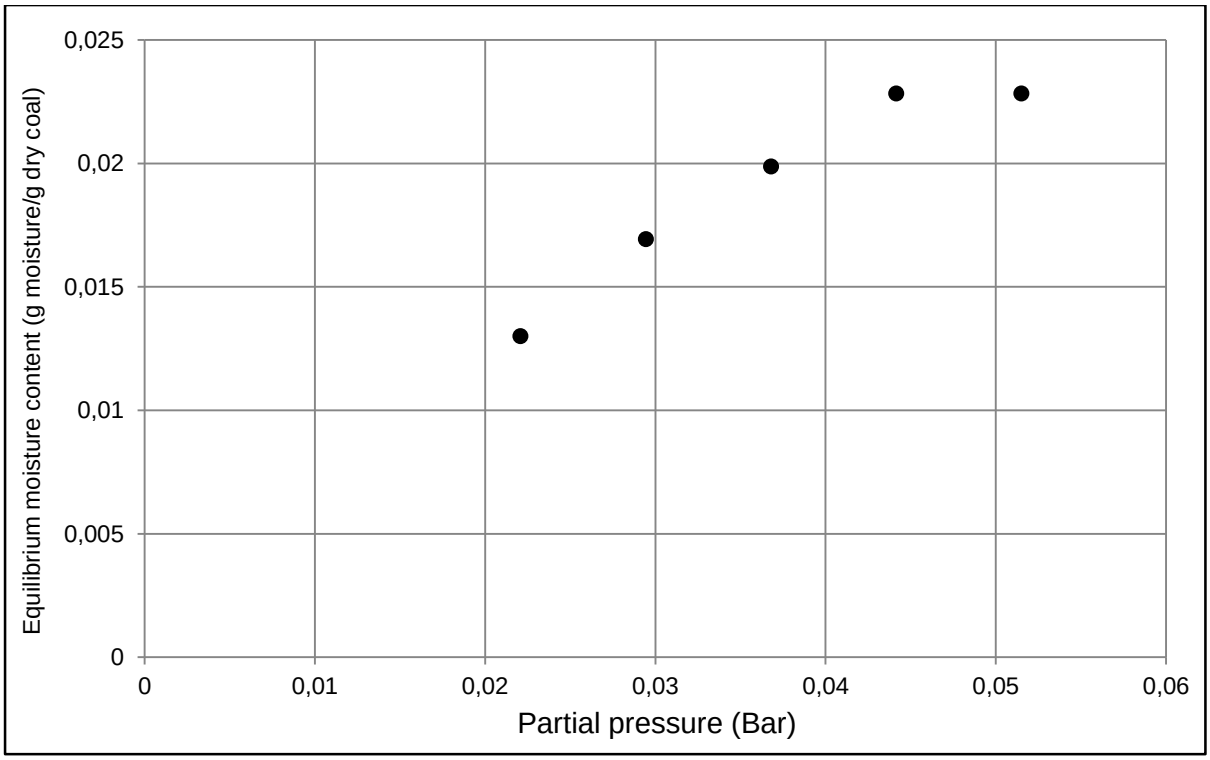

Figure B.24. Desorption isotherm at 40°C and a humidity range of 70% to 30%

B.9. Vitrinite rich coal samples: filter cakes dried at static conditions

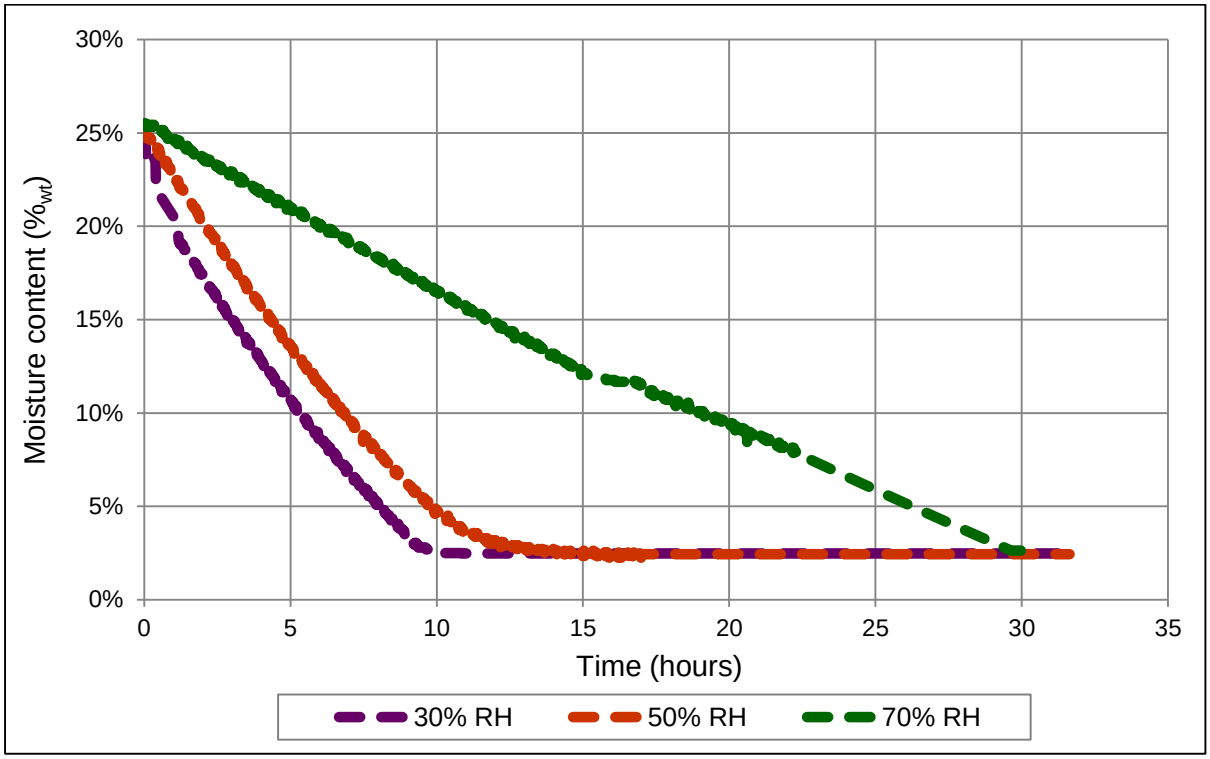

Figure B.25. Static bed drying of filter cakes at 40°C and various relative humidity conditions

B.10. Vitrinite rich coal samples: comparison between static bed and fluidised bed

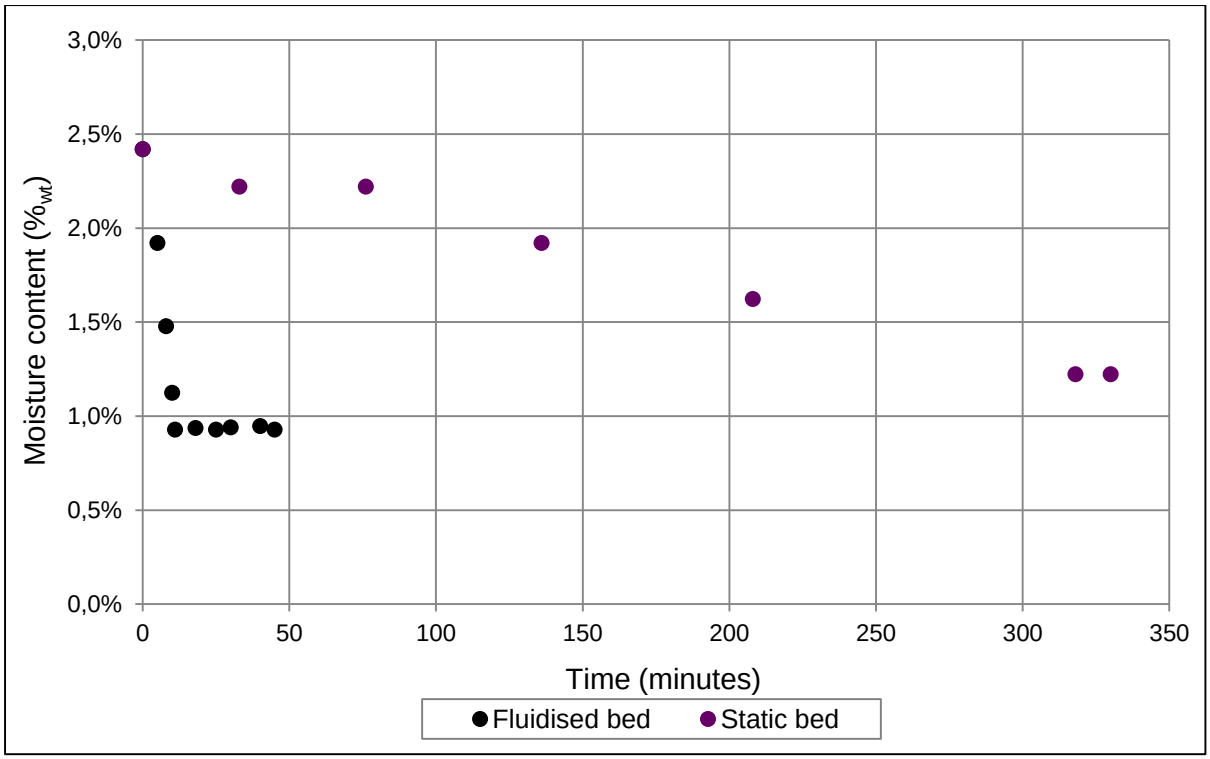

Figure B.26. Comparison between static and fluidised bed to reduce equilibrium moisture content at 40°C and 30% RH

B.11. Vitrinite rich coal samples: filter cakes dried in the fluidised bed

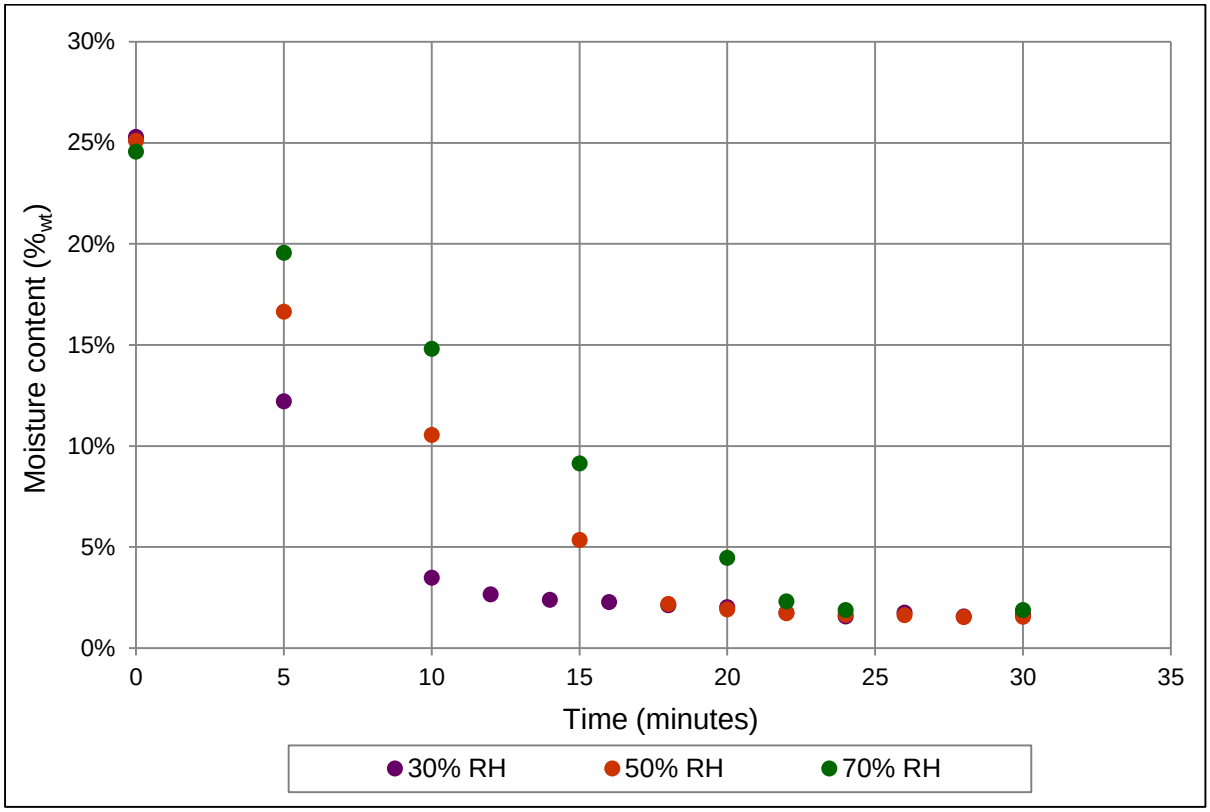

Figure B.27. Drying of filter cakes in a fluidised bed at 40°C and various relative humidity conditions